WADD TECHNICAL REPORT TR 60-889

INVESTIGATION OF INTERMETALLIC COMPOUNDS FOR VERY HIGH TEMPERATURE APPLICATIONS

Jonathan Booker
Robert M. Paine
A. James Stonehouse

The Brush Beryllium Company

APRIL 1961

AERONAUTICAL SYSTEMS DIVISION

NOTICES

When Government drawings, specifications, or other data are used for any purpose other than in connection with a definitely related Government procurement operation, the United States Government thereby incurs no responsibility nor any obligation whatsoever; and the fact that the Government may have formulated, furnished, or in any way supplied the said drawings specifications, or other data, is not to be regarded by implication or otherwise as in any manner licensing the holder or any other person or corporation, or conveying any rights or permission to manufacture, use, or sell any patented invention that may in any way be related thereto.

Qualified requesters may obtain copies of this report from the Armed Services Technical Information Agency, (ASTIA), Arlington Hall Station, Arlington 12, Virginia.

This report has been released to the Office of Technical Services, U. S. Department of Commerce, Washington 25, D. C., for sale to the general public.

Copies of WADD Technical Reports and Technical Notes should not be returned to the Wright Air Development Division unless return is required by security considerations, contractual obligations, or notice on a specific document.

WADD TECHNICAL REPORT TR 60-889

INVESTIGATION OF INTERMETALLIC COMPOUNDS FOR VERY HIGH TEMPERATURE APPLICATIONS

Jonathan Booker
Robert M. Paine
A. James Stonehouse

The Brush Beryllium Company

APRIL 1961

MATERIALS LABORATORY
CONTRACT AF 33(616)-6540
PROJECT No. 7350

AERONAUTICAL SYSTEMS DIVISION
AIR FORCE SYSTEMS COMMAND
UNITED STATES AIR FORCE
WRIGHT-PATTERSON AIR FORCE BASE, OHIO

McGregor & Werner, Inc., Dayton, O.
400 - October 1961 - 5-118 & 119

FOREWORD

This report was prepared by The Brush Beryllium Company under Contract No. AF 33(616)-6540. The contract was initiated under Project No. 7350, "Ceramic and Cermet Materials, Task No. 73500, "Ceramic and Cermet Materials Development." The work was administered under the Materials Central, Directorate of Advanced Systems Technology, Wright Air Development Division, with Lt. T. Lippart as the project engineer.

This report covers work conducted from 1 May, 1959, to 31 October, 1960.

The program was carried out under the direction of W. W. Beaver, Vice President, Research and Development for The Brush Beryllium Company. The authors wish to acknowledge the valuable assistance of J. Carrabine and D. Fetsko in the thermal property measurement work and J. Hurd and D. Schwegler in the mechanical property measurement area.

ABSTRACT

Intermetallic beryllides from the systems tantalum-beryllium, tungsten-beryllium, and hafnium-beryllium along with the disilicides of tungsten, tantalum, and molybdenum, were screened for compounds capable of serving as structural materials at temperatures above 2500°F. The compounds studied were $TaBe_{12}$, Ta_2Be_{17}, Hf_2Be_{21}, $MoSi_2$, $TaSi_2$, and WSi_2. The preparation, fabrication, oxidation resistance, and thermal-shock resistance are discussed. Values are given for the transverse-rupture strengths, impact resistance, mean-linear coefficients of thermal expansion, enthalpy, specific heat, and thermal conductivity.

An investigation of the rates of oxidation of intermetallic beryllides was initiated. The oxidation of $TaBe_{12}$, Hf_2Be_{21}, $ZrBe_{13}$, and Ta_2Be_{17} in the range 2300° to 2750°F was found to obey an exponential rate law which was cubic or a higher power rate law. In most cases, the cubic rate law applied. The products of the oxidation of $ZrBe_{13}$ at 2500°F were identified as Zr_2Be_{17} and BeO. Tentative activation energies for a cubic rate process were calculated for $TaBe_{12}$ and Hf_2Be_{21}.

PUBLICATION REVIEW

This report has been reviewed and is approved.

FOR THE COMMANDER:

W. G. RAMKE
Chief, Ceramics and Graphite Branch
Metals and Ceramics Laboratory
Materials Central

TABLE OF CONTENTS

TABLE OF CONTENTS (Continued)

LIST OF TABLES

LIST OF ILLUSTRATIONS

LIST OF ILLUSTRATIONS (Continued)

I. INTRODUCTION

Intermetallic compounds with high melting points and resistance to oxidation offer a great potential for structural service at temperatures beyond the range of present-day alloys. The primary aim of the investigation described in this report is the development of an intermetallic compound or compounds capable of serving as structural materials at temperatures of 2500°F and higher with an expected service life of up to ten hours. A material should be oxidation resistant, have good streagth at operating temperature, be resistant to thermal shock, and be capable of fabrication into useful hardware in order to be serviceable at the temperatures under consideration.

This investigation is an extension of previous work on the development of intermetallic compounds carried out under D.O. AF 33(616)56-12 during the period of 13 March, 1956, to 31 October, 1958. The work under the previous contract was initiated with a survey of metallic systems for oxidation resistant compounds at 2300°F and higher. An oxidation resistant material was arbitrarily defined as a material exhibiting no more than 2 mils penetration in 100 hours at temperature. The preliminary literature survey indicated about 95 binary intermetallic systems which contained or might be expected to contain compounds with sufficiently high melting points. Thirty-five systems were chosen for experimental work, these systems being primarily binaries between aluminum, silicon, beryllium, germanium, or zirconium and the transitional metals. A number of compounds of aluminum, beryllium, and silicon were found to meet the arbitrary requirements for oxidation resistance.

The second phase of the early work consisted of a survey of the properties of the materials identified in the initial effort. This property survey concentrated primarily upon mechanical strength at temperature and further definition of the oxidation resistance of the material. The aluminum compounds, most notably $NbAl_3$ and $TaAl_3$, were not characterized to a great extent, as their oxidation resistance degenerated at temperatures

---

Manuscript released by authors December, 1960 for publication as a WADD Technical Report.

above 2500° F. The specific end use which motivated the research was of such a nature that the high density silicides did not appear overly advantageous, resulting in concentration of the effort on the remaining class of compounds, the beryllides.

As a result of this effort, it was concluded that $ZrBe_{13}$, Nb_2Be_{17}, $NbBe_{12}$, Ta_2Be_{17}, and $TaBe_{12}$ were materials of considerable potential for long term use in the temperature range of 2300° to 2800° F on the basis of oxidation resistance, mechanical strength, and thermal conductivity. At this stage, the program was transferred to another governmental agency more directly concerned with the end use of the materials as originally conceived.

The present contract was initiated as a result of consideration of the problems likely to be encountered in designing aerodynamic surfaces for re-entry flight vehicles using currently available materials. Thus, the requirements of a suitable material were changed in that a service life of up to 10 hours was considered quite satisfactory. The operating temperature, however, was increased to 2500° F as a minimum with no maximum specified. The capability of the materials under examination for short time service at temperatures above 3000° F was to be examined.

Inasmuch as performance at as high a temperature as possible is very desirable, the investigation has centered around refractory metal beryllides and silicides. The work was initially divided into two phases: (1) the selection of not less than five nor more than ten compounds on the basis of previous experience, reappraisal of the literature, and theoretical considerations for experimental screening as high temperature materials, and (2) determination of mechanical and physical property data on the promising materials obtained in the screening effort. After the program was underway, additional effort was provided covering more fundamental studies on the oxidation mechanism operative with beryllides at high temperature as well as additional property determinations.

Initially, compounds from the Ta-Be, Hf-Be, W-Be, Mo-Si, Ta-Si, and W-Si systems were screened and surveyed. On the basis of preliminary results, the materials which were studied more extensively included Ta_2Be_{17}, $TaBe_{12}$, Hf_2Be_{21}, $TaSi_2$, and WSi_2. $ZrBe_{13}$ was included in the oxidation mechanism study because it was desirable to use this compound as a model.

II. PRELIMINARY SCREENING OF COMPOUNDS

A. Selection of Compounds

The literature search and experimental work performed under D. O. 33(616)56-12 was used as the primary reference source for the properties of a large number of intermetallic compounds. The results of the above work are summarized in WADC TR 59-29, Parts I and II. It was concluded from this work that the compounds most likely to show oxidation resistance at high temperatures would contain aluminum, beryllium, or silicon, but that intermetallic compounds of aluminum would not be expected to show adequate oxidation resistance above about 2500°F. The area of search for intermetallic compounds which would be oxidation resistant above 2500°F was thus narrowed to compounds between beryllium or silicon and the high melting or refractory metals.

The tantalum-beryllium, tungsten-beryllium, and hafnium-beryllium systems were selected as the beryllium-containing compounds, and the disilicides of molybdenum, tantalum, and tungsten were chosen as the silicon-containing compounds. Since the number of compounds were limited to a maximum of ten, the compounds chosen for the initial screening were:

$TaBe_{12}$	WBe_{12}
Ta_2Be_{17}	WBe_2
$TaBe_2$	$MoSi_2$
$HfBe_{13}$	$TaSi_2$
Hf_2Be_{17}	WSi_2

The tantalum-beryllium system had previously been thoroughly explored for compounds, and it was known that $TaBe_{12}$ and Ta_2Be_{17} possessed good oxidation resistance for 100 hours at temperatures up to 2800°F and at temperatures to 2500°F for $TaBe_2$. These compounds have exhibited tenacious oxide films during thermal cycling at these temperatures. $TaBe_{12}$ showed somewhat better oxidation resistance than the compounds containing less beryllium in the 100-hour tests; however, the higher melting point of Ta_2Be_{17} and the expected still higher melting point of $TaBe_2$ could cause these lower beryllides to be superior to $TaBe_{12}$ for short times. $TaBe_3$ was not included in the ten compounds but was held as an alternative compound to be substituted if results on the other tantalum-beryllium compounds so indicated.

The hafnium-beryllium and tungsten-beryllium systems have not been thoroughly investigated. These systems were selected primarily because it was thought that their respective compounds would have high melting points. The oxidation resistance of the hafnium beryllides was expected to resemble that of the zirconium beryllides, and the hafnium compounds selected were based on an analogy to the zirconium-beryllium system. The only compounds in either the hafnium-beryllium or tungsten-beryllium systems for which crystallographic data have been reported are WBe_2[1] and WBe_{12}. In previous work at The Brush Beryllium Company with the tungsten-beryllium system, a composition close to WBe_5 showed good oxidation resistance at 2300° F. This composition appeared to be more stable than WBe_{12}; that is, WBe_{12} lost beryllium rapidly when heated in a vacuum at high temperatures. Though the more beryllium-rich compound(s) may show superior oxidation resistance, it was thought that other compounds in this system should not be bypassed in the preliminary screening.

The silicides, $MoSi_2$, $TaSi_2$, and WSi_2, were chosen for initial screening experiments primarily for their high melting points. No information about the oxidation resistance of WSi_2 was found, but $MoSi_2$ has been shown to possess inherent high-temperature oxidation resistance. $MoSi_2$ has been studied extensively, and good oxidation resistance is reported at temperatures as high as 3100° F. Its major drawback is its brittleness and poor thermal shock resistance; however, it may be that these properties can be improved by suitable additions of a second phase, possibly an intermetallic compound. $TaSi_2$, which might be expected to possess greater thermal conductivity than other silicides (its electrical conductivity is much greater), may be more thermal-shock resistant than most silicides. Preliminary work under the previous contract indicated short time oxidation resistance for $TaSi_2$ at 2300° F, although at this particular temperature with the low density sample at hand, complete oxidation occurred in 100 hours. For these reasons, and because of its high melting point, $TaSi_2$ was included in the initial work on the present project. In the case of all three silicon systems, it was thought that the disilicide would have the greatest oxidation resistance, and hence the greatest chance of passing the initial screening tests.

Other silicides, although of potential interest, did not appear as promising as those of tantalum and tungsten. The silicides of chromium, most notably Cr_3Si, have shown oxidation resistance but have a relatively low melting point (Cr_3Si has the highest melting point, at 3190° F[1]). Similarly, the silicides of titanium, while oxidation resistant have a relatively low melting point. Zirconium-silicon compounds have not exhibited adequate oxidation resistance at relatively low temperatures (1830° F).[1] Similarly, $NbSi_2$ has failed to exhibit oxidation resistance at elevated temperatures.[15]

B. Preparation of Compounds and Phase Studies

All of the intermetallic compounds used in this investigation, with the exception of $MoSi_2$, have been prepared at The Brush Beryllium Company by solid-state reaction of the constituent metal powders. The $MoSi_2$ was purchased as a powder from Electro Metallurgical Company. The first preparations of these materials involved quantities of about 100 cc absolute volume, which was enough for initial identification and fabrication experiments.

The compounds in the tantalum-beryllium system to be prepared were $TaBe_{12}$, Ta_2Be_{17}, and $TaBe_2$. No difficulties were encountered in the preparation of $TaBe_{12}$ and Ta_2Be_{17}. These compounds had previously been prepared at The Brush Beryllium Company, and X-ray analyses of the initial preparations made for this investigation showed them to be essentially single-phase compositions. When the stoichiometric proportions corresponding to $TaBe_2$ were reacted, the resulting powder was shown by X-ray analysis to be a mixture of $TaBe_3$ and $TaBe_2$, with $TaBe_3$ the major phase. (These compounds were identified by analogy with the niobium-beryllium system.) Chemical analysis of the reacted powder indicated 9.19% beryllium content, whereas the theoretical values are 9.06% beryllium for $TaBe_2$ and 13.0% beryllium for $TaBe_3$. From the chemical analysis, it is clear that this powder contained tantalum and beryllium in the ratio of 1 to 2. There was no evidence of free tantalum in the X-ray pattern. This mixed-phase powder was vacuum hot pressed at 2780°F, and a sample from the resulting compact was submitted for X-ray and chemical analysis. The X-ray results showed a marked increase in the proportion of $TaBe_2$, which compound was now the major phase; however, $TaBe_3$ was still present in large amounts (approximately 30%). Chemical analysis gave 9.06% Be, compared with 9.19% Be in the original reacted powder.

Two other attempts were made to prepare single-phase $TaBe_2$, using the percentage of beryllium powder as a variable. Chemical analyses of the resulting powders gave 8.98 and 8.32% beryllium. X-ray patterns of all the reacted powders (including the powder discussed above) were similar enough to be called identical. These patterns showed a major phase of $TaBe_3$ and a minor phase of $TaBe_2$. The presence of $TaBe_3$ in large amounts in this material, even though the ratio of tantalum to beryllium was correct for $TaBe_2$, suggested incomplete reaction of the metal powders. To check this possibility, a mixture of the three reacted powders was heated to 2820°F in vacuum. (The original reaction temperature had been 2370°F.) X-ray analysis showed that the major phase in the resulting powder was $TaBe_2$, with $TaBe_3$ still present as a minor phase. Chemical analysis gave 9.02% Be. This

result indicates that the formation of $TaBe_2$ requires a higher temperature than is normally employed in the preparation of the majority of intermetallic compounds studied and that $TaBe_2$ probably could be prepared as a single-phase under the proper conditions of time and temperature. Efforts to prepare the single-phase compound were discontinued when it became evident that because of poor oxidation resistance this compound (mixture) would not be continued in the investigation.

Because of the persistence of $TaBe_3$ in the $TaBe_2$ preparations and because $TaBe_2$ was eliminated as a potential compound to be studied, $TaBe_3$ was prepared and screened as a possible high-temperature material. The preparation of this compound was straightforward and easily accomplished. Vacuum hot-pressing the reacted $TaBe_3$ at 3090° F did not change the X-ray diffraction pattern or the composition appreciably.

At the beginning of this investigation, the tungsten-beryllium system had not been studied extensively; however, WBe_2 and WBe_{12} had been reported[1]. Since the higher beryllides were expected to be the more oxidation resistant, and in order to verify the identity of the compounds in this system to be screened, the stoichiometric compositions, WBe_2, W_2Be_{17}, and WBe_{12}, were reacted. X-ray analysis showed the reaction product from the stoichiometric composition, WBe_2, to be single-phase WBe_2. The stoichiometric proportions for W_2Be_{17} gave a mixture of WBe_2 and WBe_{12} upon reaction, with WBe_{12} as major phase. This is a good indication that there is no W_2Be_{17} compound in the tungsten-beryllium system, for the M_2Be_{17} compound is readily formed in other systems in which it is known to exist. (The molybdenum-beryllium system also shows no M_2Be_{17} compound.)

Reaction of the WBe_{12} composition produced an essentially single-phase powder with the expected MBe_{12} compound structure. In one preparation of WBe_{12}, a minor unidentified phase was detected by X-ray diffraction. Since the structure of this phase was identical to a compound in the molybdenum-beryllium system tentatively assigned the formula "$MoBe_{16}$", the compositions WBe_{16}, WBe_{17}, WBe_{18}, WBe_{19}, and WBe_{20} were reacted in order to verify the existence of such a compound in the tungsten-beryllium system. X-ray analyses of these reacted powders indicated that this new phase approximated the composition WBe_{22}. Since some beryllium is lost during reaction of the metal powders (a fact which is substantiated by chemical analysis), the stoichiometric compositions corresponding to WBe_{22}, WBe_{23}, and WBe_{24}, were next reacted. While a single-phase composition was not obtained, the percentage of WBe_{12} was very small in all three of the compositions, reaching a minimum in the WBe_{23} composition. Chemical analyses of

these reacted powders gave 51.0%, 52.0%, and 53.9% beryllium, respectively; whereas the stoichiometric percentages of beryllium in WBe_{22}, WBe_{23}, and WBe_{24}, would be 51.89%, 53.00%, and 54.05%, respectively. These analyses revealed that the composition which X-ray analysis indicated to be richest in the beryllium-rich compound corresponded to WBe_{22}. This phase, therefore, has been assigned tentatively the formula WBe_{22}. WBe_{22} had not been reported in the literature and was not one of the compounds originally selected for screening; however, since it was observed in the course of this investigation and represented a possible high temperature compound, its identification and characterization was pursued. WBe_{22} has a face-centered cubic structure ($a = 11.64\text{Å}$) with an X-ray density of 3.23 g/cc.

The compounds chosen for preliminary screening from the hafnium-beryllium system were $HfBe_{13}$ and Hf_2Be_{17}, assuming an analogy with the zirconium-beryllium system. The compound $HfBe_{12}$ also had been reported tentatively[2]. It was included in the initial investigations here primarily to verify its existence. Hafnium and beryllium powders were mixed in the stoichiometric proportions of $HfBe_{13}$, $HfBe_{12}$, and Hf_2Be_{17}, and reacted at 2370°F. Only the Hf_2Be_{17} compound was obtained as an essentially single-phase composition, according to X-ray analysis, whereas a mixture of phases was obtained in the cases of $HfBe_{12}$ and $HfBe_{13}$. The three reacted powders were vacuum hot pressed to provide dense test specimens and in the case of the $HfBe_{12}$ and $HfBe_{13}$ compositions to achieve single-phase preparations through homogenization and additional reaction of the constituents. Chemical and X-ray analyses of the hot-pressed materials showed that there was no change in the Hf_2Be_{17} compound after hot pressing. On the other hand, the pressing of the $HfBe_{12}$ composition showed an essentially single-phase structure and the pressing of the $HfBe_{13}$ composition showed the same structure as the major phase with a small amount of $HfBe_{13}$ present. Another reacted composition which had been mixed as $HfBe_{12.5}$ showed the same phase as did $HfBe_{12}$ and $HfBe_{13}$ as a result of hot pressing. The percentage of beryllium determined by chemical analysis for the reacted and hot-pressed composition, $HfBe_{12}$, $HfBe_{12.5}$, and $HfBe_{13}$ are tabulated below:

Pressing Number	Original Composition	% Beryllium		
		Stoichiometric	Reacted Powder	Hot-Pressed Material
282	$HfBe_{12}$	37.72	36.3	34.4
322	$HfBe_{12.5}$	38.7	36.6	34.3
286	$HfBe_{13}$	39.63	39.2	34.2

These results show that the same hot-pressed composition is obtained for all three starting compositions, which indicates that this particular composition is the more stable one. This stable phase is not structurally isomorphous with MBe_{12} compounds and, as the tabulation shows, is composed of approximately 34.3% beryllium and 65.7% hafnium. The empirical formula calculated from these percentages is $HfBe_{10.3}$. The density of Hf_2Be_{21} calculated by rule of mixture is 4.25 g/cc. The powder density of Pressing No. 282 is 4.26 g/cc, that for 286 is 4.30 g/cc, and for 322 is 4.26 g/cc. The compound tentatively was assumed to be Hf_2Be_{21}.

As a further check on the stability of this compound, samples of pressings 282 and 286 were annealed in vacuum for three hours at 2730°F. There was no significant change in the analyses (chemical and X-ray) after the annealing run, thus substantiating the stability of the composition Hf_2Be_{21}.

In an effort to prepare single-phase Hf_2Be_{21} directly from the element powders, the stoichiometric proportions of this compound plus 1% excess beryllium (to allow for beryllium loss) were mixed and reacted. A mixed-phase powder, containing Hf_2Be_{21} as a major phase (estimated 80%) with $HfBe_{13}$ and Hf_2Be_{17} as minor phases, was obtained. The reacted powder contained 34.1% beryllium. In a later attempt to prepare this compound, the percentage of beryllium powder was increased slightly. A mixed-phase powder again was obtained containing the same compounds as in the first attempt but with an increase in the amount of $HfBe_{13}$ present. This reacted powder contained 35.0% beryllium. A shortage of hafnium powder prevented further attempts to prepare the single-phase compound through direct reaction of the metal powders.

Though the compound $HfBe_{13}$ is apparently unstable at the temperatures of consideration in this investigation, the existence of the compound has been verified. $HfBe_{13}$ has a face-centered cubic structure with $a_0 = 10.00$ Å and is isomorphous with $ZrBe_{13}$. The X-ray density is 3.93 g/cc. Hf_2Be_{17} is isomorphous with Nb_2Be_{17}, Ta_2Be_{17}, and Zr_2Be_{17}. The hexagonal cell has $a = 7.48$ Å and $c = 10.93$ Å. The X-ray density is 4.78 g/cc. The structure of Hf_2Be_{21} has not been established, but the powder pattern of this phase is given in Appendix I.

The compounds, $TaSi_2$ and WSi_2, were obtained as essentially single-phase preparations by solid-state reaction of the constituent elements at 2370°F. X-ray diffraction analysis of the $MoSi_2$ which was received from the Electro Metallurgical Company showed this material to be essentially single-phase $MoSi_2$.

C. Fabrication of Test Specimens

The intermetallic compounds chosen for investigation under this contract were prepared as powders and were fabricated into suitable test specimens. Fabrication of these intermetallic powders was accomplished in a vacuum hot-pressing operation, using techniques previously developed for intermetallic compounds of beryllium. While there were general similarities in the procedure for hot-pressing of various materials, some experimentation was necessary to establish the proper conditions for densification of each compound. A maximum of 2000 psi had been established as the pressure which may be used reliably with the type and shape of large graphite die employed. Accordingly, this was the maximum pressure used in normal hot-pressing operations. The pressings were made under vacuum and with bare graphite tooling, where possible. In some instances, the material reacted with the bare graphite tooling during the pressing operation. When this occurred, the particular material was isolated from the graphite tooling in subsequent pressings by die liners, mold washes, etc.

Fabrication data for all of the pressings made during the course of this investigation are given in Table I. The immersion density of the as-pressed compact is given in column 6, and the absolute density is given in column 7. The absolute density is obtained by measurement of the powder density of a portion of the pressed compact. The pressings for a given intermetallic system are grouped, as are the pressings for a particular compound within the system, to facilitate reference to the table while certain aspects of the fabrication of a given compound are being discussed.

The conditions for the fabrication of $TaBe_{12}$ and Ta_2Be_{17} were established from previous work at The Brush Beryllium Company. On the whole good densities were obtained for these pressings. as is seen in Table I.

Only one attempt to fabricate $TaBe_2$ was made. This pressing apparently proceeded very well while compaction was being measured during the pressing cycle; however it did not attain the expected density. Further attempts to fabricate this compound did not seem warranted in view of the poor oxidation resistance of the fabricated material so no further pressings were made.

Several attempts were made to fabricate $TaBe_3$ before a sufficiently dense piece was obtained. It will be observed that the temperature required for fabrication of full-density $TaBe_3$ was higher than that for the

TABLE I
PREPARATION OF TEST SPECIMENS BY HOT-PRESSING

Pressing No.	Material	Pressing Size[a]	Maximum Temp. (°F)	Maximum Pressure (psi)	Density Immersion (g/cc)	Density Absolute (g/cc)	% of Absolute
220	$TaBe_{12}$	1	2780	2000	4.18	4.18	100.
222	$TaBe_{12}$	1	2780	2000	4.15	4.18	99.2
277	$TaBe_{12}$	1	2825	2000	3.86	4.22	92.3
308	$TaBe_{12}$	1	2775	2000	4.25	4.26	100.
350	$TaBe_{12}$	2	2825	2000	4.32	4.29	100.
227	Ta_2Be_{17}	1	2685	2000	4.76	4.80	99.2
276	Ta_2Be_{17}	1	2825	2000	4.51	4.98	94.0
309	Ta_2Be_{17}	1	2785	2000	4.96	4.97	99.8
318	Ta_2Be_{17}	2	2825	2000	4.88	5.09	95.9
352	Ta_2Be_{17}	2	2825	2000	5.01	4.99	100.
374	Ta_2Be_{17}	3	2825	2000	4.90	4.95	99.0
426	Ta_2Be_{17}	1	2825	2000	4.95	4.95	100.
228	$TaBe_3$	1	2780	1600	8.38	8.95	93.6
274	$TaBe_3$	1	2825	2000	7.07	8.18	86.4
280	$TaBe_3$	4	2930	2000	7.56	8.23	91.9
283	$TaBe_3$	4	2825	2500	7.48	8.20	91.2
298	$TaBe_3$	4	3090	2000	8.19	8.19	100.
271	WBe_{12}	1	2595	1500	4.32	4.44	97.3
252	WBe_2	1	2750	2000		Very Porous	
262	WBe_2	5	3010	2000	9.20	10.2	90.2
265	WBe_2	1	3180	2000	9.80	10.2	96.1
296	WBe_2	6	3225	2000	7.57	10.2	74.2
366	WBe_{12}	7	2270	2000	2.20	--	--
372	WBe_{12}	7	2390	2000	3.23	3.20	100
221	Hf_2Be_{17}	4	2825	2000	4.11	4.66	88.2
282[b]	Hf_2Be_{11}	4	2825	2000	4.27	4.26	100.
286[c]	Hf_2Be_{11}	4	2625	2000	4.07	4.30	94.7
322	Hf_2Be_{11}	2	2825	2000	4.08	4.26	95.8
358	Hf_2Be_{11}	2	2825	2000	4.24	4.48	94.6
361	Hf_2Be_{11}	2	2825	2000	4.36	4.34	100.
375	Hf_2Be_{11}	1	2825	2000	4.41	4.42	100.
237	$MoSi_2$	5	2780	2000	5.82	6.19	94.0
285	$MoSi_2$	1	2955	2000		Severe Graphite Reaction	
292	$MoSi_2$	1	2825	2000	6.04	6.19	97.6
293	$MoSi_2$	1	2730	2000	6.11	6.20	98.7
295	$MoSi_2$	1	2775	2000	5.7	6.19	92.0
305	$MoSi_2$	1	2760	2000	5.99	6.20	96.6
321	$MoSi_2$	1[d]	2710	2000	6.05	6.19	97.7
242	$TaSi_2$	5	2680	2000	8.55	8.88	96.3
278	$TaSi_2$	1	3000	2000	9.08	9.08	100.
299	$TaSi_2$	1	2955	2000	8.85	8.96	98.8
301	$TaSi_2$	1	2955	2000	8.91	9.04	98.6
302	$TaSi_2$	5	2940	2000	8.80	8.99	97.9
313	$TaSi_2$	2	2910	2000	8.65	8.84	97.9
338	$TaSi_2$	2	2910	2000	8.84	8.92	99.1
376	$TaSi_2$	2	2910	2000	8.85	8.87	99.8
248	WSi_2	5	2710	2000	8.91	9.60	93.0
283	WSi_2	5	2910	2000	8.16	9.46	96.9
290	WSi_2	1	3000	2000	8.99	9.62	93.5
294	WSi_2	1	3000	2000	9.89	9.84	100
300	WSi_2	1	3000	2000	9.59	9.70	98.8
306	WSi_2	1	2940	1800	9.58	9.68	99.0
141	WSi_2	8	1000	2000	9.61	--	--
147	WSi_2	8[d]	1000	2000	9.64	9.64	100.
163	WSi_2	9	1000	2000	9.66	--	--
146	WSi_2	9	3000	2000	9.11	--	--
149	WSi_2	9[d]	1000	2000	9.41	9.61	97.9

[a] Pressing size
1 2 1/2 x 1 1/2 x 11/16 inches
2 2 1/2 x 1 1/2 x 1 1/4 inches
3 2 inch diameter x 1 inch
4 2 inch diameter x 1/2 inch
5 2 inch diameter x 2 inches
6 2 13/16 inch diameter x 1 1/2 inch
7 2 inch diameter x 3/4 inch
8 2 13/16 inch diameter x 2 1/4 inches
9 2 7/8 inch diameter x 2 1/2 inches

[b] Material originally pressed from $HfBe_{11}$ composition

[c] Material originally pressed from $HfBe_{13}$ composition

[d] Pressed with molybdenum liner

other compounds in the tantalum-beryllium system. Chemical analysis of each of the fabricated compacts revealed that the compound was stable at the temperatures of fabrication.

No difficulty was experienced in fabricating WBe_{12} to good density at the relatively low temperature of 2595° F.

In the case of WBe_2, a full-density specimen has not been fabricated. It is apparent from the table that a higher temperature is needed for the fabrication of WBe_2 than for any other compound fabricated in this investigation. The failure to achieve full density in Pressing No. 296 was ascribed to mechanical difficulties, i. e., sticking of the punches. Since relatively good density was obtained in Pressing No. 265 which was used for the initial test specimen and since WBe_2 had been eliminated as a compound to be continued in this investigation, the fabrication of a full-density compact was not of utmost importance. Therefore, no further fabrication work was done on WBe_2.

WBe_{22} was not one of the compounds originally chosen for investigation. This compound was observed in the survey of the tungsten-beryllium system, and it was thought that the identification and characterization of this compound was of interest to this contract, since this compound is a possible high-temperature material. It was expected that the fabrication of WBe_{22} would be effected at a lower temperature than is needed for compounds containing less beryllium, and it will be observed that a full density compact was obtained at 2390° F. The pressing was cracked, but nevertheless, test specimens were obtained for beryllium assay, structural identification, and oxidation tests.

The fabrication of hafnium beryllides proceeded without great difficulty. Only the two compounds, Hf_2Be_{17} and Hf_2Be_{21}, were fabricated per se, since the higher beryllide compositions, $HfBe_{12}$ and $HfBe_{13}$, were unstable at the pressing temperature and lost beryllium until the stable composition, Hf_2Be_{21}, was reached.

The principal problem encountered in the fabrication of $MoSi_2$ and WSi_2 was reaction of these compounds with the graphite tooling. The first pressings of these materials were small cylindrical specimens, and while there was bonding between the pressed compacts and the graphite punches, the two could be separated without harming the intermetallic specimens. These pressings were low in density, and it was decided to raise the temperature of fabrication in order to obtain greater densities.

When fabrication of a 3 1/2- x 2 1/2- x 11/16-inch block of $MoSi_2$ was attempted at a higher temperature, the bond between the pressing and the graphite caused the pressing to crack on cooling. This apparently occurred as a result of stresses which were built up on cooling, which in turn were caused by differences in thermal expansion between graphite and the silicide. The large surface area and the relative thinness of the rectangular pressings made these pieces more vulnerable to such failure (compared with cylindrical pressings). This effect was not observed in the first rectangular pressing of WSi_2 (Pressing No. 290); however, it did occur in later pressings. The reaction of the $MoSi_2$ or the WSi_2 with the graphite, in itself, did not appear to be severe (very little pitting and sharp interfaces were observed), but the bonding was, nevertheless, very tight. In an effort to minimize the reaction of these silicides with the graphite, the pressing temperature was lowered. Compacts with good density were obtained at the lower temperatures; however, reaction with the graphite was still severe enough to cause the specimen to break on cooling, and some of the desired test pieces could not be made. The reaction with the graphite tooling was eliminated by lining the die and facing the punches with 3- or 10-mil molybdenum foil. Compacts of good density have been obtained in this way; however, there are indications that the thin foil interferes with densification because of a tendency to flow or crumble under the conditions of temperature and pressure required for fabrication. A thicker foil may eliminate this problem.

In the fabrication of the cylindrical WSi_2 pressings (343, 353, and 360), it was necessary to face only the punches with molybdenum foil. Pressings No. 343 and 360, as well as the rectangular Pressing No. 369, were not full-density pressings. These three pressings were annealed in hydrogen at 3000° F with the hope of obtaining further densification. Density of all these compacts increased slightly as a result of the annealing treatment. H. P. 343 increased from 9.16 to 9.30 g/cc, H. P. 360 increased from 9.33 to 9.43 g/cc, and H. P. 369 increased from 9.41 to 9.48 g/cc. Thermal conductivity specimens were machined from Pressings No. 343, 353, and 360. Powder densities were not measured for these pressings since it is necessary to crush the compact to make this measurement.

The fabrication of $TaSi_2$ proceeded without the complication of severe reaction with the graphite tooling in all cases except H. P. 376. The intermetallic powder used in this pressing was from the same lot as had been used for previous $TaSi_2$ pressings, and there were no changes in the conditions of fabrication. It would be premature to alter the conditions of fabrication of this compound because of the results from this

one pressing; however, if this behavior recurs, it may be necessary to employ molybdenum sheet die liners in the fabrication of $TaSi_2$ in the same fashion as is required for the fabrication of $MoSi_2$ and WSi_2.

D. Oxidation Tests for Screening Purposes

The compounds selected for investigation under this contract were to be screened using oxidation resistance and ability to withstand nominal thermal shock as the criteria on which continuation of evaluation of a compound would be based. The preliminary investigation of both of these properties were incorporated in one test. The test was carried out in a tubular Globar furnace in laboratory air at 2900° F. Test samples were 1/2 x 1/2 x 1/4 inch. Three heating cycles and three cooling cycles for a total of ten hours at temperature were used in these tests. No attempt was made to preheat the samples before introduction into the furnace, and the samples were air-quenched upon removal from the furnace. A maximum of two mils penetration in ten hours was arbitrarily established as the maximum allowable oxidation for a useful compound. The penetration data were obtained from micrometer measurements of the machined specimen before oxidation and after abrasion of the scale to bright metal with removal of pits after the oxidation run. Penetration data obtained in this manner gives the maximum penetration (depth of deepest pit), which is usually greater than the penetration calculated from weight-change data. Appreciable amounts of unoxidized metal are removed in this procedure, expecially when deep pits are encountered.

The data resulting from the oxidation tests are summarized in Table II. The density values recorded in the third column of Table II are based on the immersion densities of the specimens and the powder densities of the crushed pressings.

H. P. 228, which is designated $TaBe_2$, was actually a mixed-phase product containing about 30% $TaBe_3$ (by X-ray analysis). This specimen was, for all practical purposes, completely oxidized. From this test, it might be anticipated that acceptable oxidation resistance would probably not be found in this portion of the tantalum-beryllium system. To check this further, however, $TaBe_3$ was tested. This compound was prepared as an essentially single-phase material.

Samples from four different pressings of $TaBe_3$ were tested. As shown in Table II, Pressings No. 274, 280, and 283 were all of low density. Severe spalling of the oxide scale (along with pieces of underlying metal) occurred on cooling the specimens from H. P. 274 and H. P. 283 after one hour, and the tests were discontinued. H. P. 280 was completely

TABLE II

SCREENING OXIDATION TESTS

(Laboratory Air; 2900°F)

Pressing No.	Material	% of Absolute Density	Weight Gain (mg/cm^2) 1 Hr	5 Hr	10 Hr	Maximum Mils Penetration in 10 Hours[b]
228	$TaBe_2$	93.6	24.4	130	333	--
274	$TaBe_3$	86.4	33.4	Discontinued after 1 hour		
280	$TaBe_3$	91.9	30.9	Complete oxidation in 5 hours		
283	$TaBe_3$	91.2	31.0	Discontinued after 1 hour		
298	$TaBe_3$	100.	12.8	59	350	--
227	Ta_2Be_{17}	98.8	2.6	8.4	16.5	1.6
222	$TaBe_{12}$	98.9	1.9	3.9	5.9	1.2
237	$MoSi_2$	94.9	0.7	0.8	1.0	0.75
237	$MoSi_2$	95.2	1.4	1.7	1.9	1.0
242	$TaSi_2$	96.3	0.8	1.4	1.2	0.75
248	WSi_2	92.4	(-0.43)	(-0.49)	(-0.35)	0.85
253	WSi_2	98.7	(-0.49)	(-0.35)	(-0.25)	0.75
253	WSi_2	98.7	(-0.42)	(-0.44)	(-0.35)	0.80
265	WBe_2	96.1	-55	-409	-765	39
271	WBe_{12}	97.3	Partial melting (1 hour)			
271	WBe_{12}	97.3	Partial melting (1 hour)			
372	WBe_{22}	100.	Complete oxidation in 1 hour			
281	Hf_2Be_{17}	88.2	7.8	10.2	14.3	2.8
282	Hf_2Be_{21}[c]	100.	6.4	9.8	10.6	2.05
286	Hf_2Be_{21}[d]	94.7	1.46	3.72	4.80	1.4

[a] Calculations based upon powder densities as absolute.

[b] Mils penetration obtained by micrometer measurements before the test and after removal of the scale and pits from the oxidized specimen.

[c] Material pressed from $HfBe_{12}$ composition (as-reacted).

[d] Material pressed from $HfBe_{13}$ composition (as-reacted).

oxidized after 5 hours at temperature. On the other hand, the specimen from the full-density H. P. 298 showed much less weight gain per unit area than the lower density specimens for comparable periods of exposure. After 10 hours at temperature, a small pea-sized kernel of metal still existed in the center of this full-density specimen. In this respect, this sample behaved like H. P. 228, the mixed-phase $TaBe_2$-$TaBe_3$ composition. The weight-gain data clearly indicate that the lower beryllides of tantalum do not possess sufficient oxidation resistance to be continued in this program.

There was a net weight loss for WSi_2 upon oxidation, while the weight gain for $MoSi_2$ and $TaSi_2$ was not sufficient to account for the measured penetration data obtained from micrometer measurements. The weight-gain data in these instances can only be regarded as an indication of the extent of oxidation, for if oxidation were severe, the weight losses should be relatively large. Since the measured penetration for these silicides was quite low, only comparisons of a semi-quantitative nature may be drawn from the measured penetration data when the limitations of this procedure at low penetration levels are considered. At any rate, the data indicate that these silicides are sufficiently oxidation-resistant at this temperature to warrant further investigation. In addition, there was no evidence of deterioration (spalling, cracking, etc.) during the tests which might indicate a lack of thermal shock resistance in these compounds.

The oxidation of WBe_2 proceeded very rapidly. As shown by the measured penetration, the oxidation was too great for this material to be included in further work on this project. The scale was adherent and did not spall from thermal shock. There was evidence of vapor coming from the sample upon introduction into the hot furnace (a white smoke was visible).

In the case of WBe_{12}, the samples appeared to have melted after one hour at 2900° F. They had flattened out and contained numerous large pores. The total weight of the two samples showed a slight gain in weight over the weight of the combined samples before oxidation. (The combined weight of the samples had to be used because the samples were fused together after one hour at temperature.) X-ray analysis of the samples after oxidation revealed the presence of WBe_{12}, with lesser amounts of WBe_2 and the more beryllium-rich phase WBe_{22}. Despite the fact that the samples of WBe_{12} were not completely oxidized after one hour of exposure at temperature, the failure to hold their shape was sufficient cause to discontinue testing this material under the present program. Although WBe_{22} was not one of the primary compounds for screening, a cursory examination showed that it oxidized completely in 1 hour at 2900° F.

The hafnium-beryllium compounds tested showed satisfactory oxidation resistance at 2900° F. Pressings 282 and 286 resulted from different starting materials (282 from a $HfBe_{12}$ composition and 286 from a $HfBe_{13}$ composition); however, chemical and X-ray analyses plus powder density determinations showed that the same major phase (Hf_2Be_{21}) was present in both fabricated pieces as a result of hot pressing. Considering the weight-gain data and the relatively low density of the test specimen, the results for pressing 286 were very good. The maximum measured penetration shown for this pressing was considerably higher than that calculated from the weight change; however, the measuring technique whereby the oxide scale is ground away prior to micrometer measurement is not very accurate at low penetration levels. The Hf_2Be_{17} specimen showed the greatest penetration among these hafnium beryllide specimens, but also had the greatest porosity. Because of the wide variation in porosity, a definite conclusion as to the relative oxidation resistance of the hafnium beryllides could not be drawn. Even though the results of these preliminary oxidation tests must be considered tentative, they do indicate that the hafnium beryllides are at least equivalent, and perhaps superior, to the zirconium beryllides in oxidation resistance.

For the purposes of brevity and easy reference, comparative data for all the compounds tested in this program are given in Table III. On the basis of preliminary oxidation resistance and qualitative resistance to thermal shock, the compounds, $TaBe_{12}$, Ta_2Be_{17}, Hf_2Be_{21}, Hf_2Be_{17}, $MoSi_2$, $TaSi_2$, and WSi_2 were eligible for further investigation under this contract. However, to reduce the number of compounds and to limit costs, only one hafnium beryllide, Hf_2Be_{21}, was included in further investigations. As a further means to aid in determining which of the remaining compounds would prove most promising, the low-temperature oxidation resistance of these compounds was examined.

A rectangular specimen of each compound was placed in a cold (room temperature) furnace through which untreated compressed air was flowing at a controlled rate. The furnace was slowly brought to 1100° F and allowed to remain at this temperature overnight (15 hours). The next day the temperature was raised slowly to 2000° F and kept at this temperature for 19 hours. Then the furnace was cooled to 1250° F, the power was turned off, and the samples were removed at room temperature. Data received from this test are recorded in Table IV. The lack of low temperature oxidation resistance of $MoSi_2$ was verified by this test. It will be observed that average and calculated penetration data are in good agreement except in the case of $MoSi_2$. The discrepancy in these values for $MoSi_2$ is undoubtedly due to the lack of formation of a protective film and to the volatility of molybdic oxide at these temperatures. From the

TABLE III

SUMMARY OF OXIDATION TESTING

Pressing No.	Material	Mils Penetration[a] 10 Hours at 2900°F
228	$TaBe_2$	Complete oxidation
298	$TaBe_3$	Complete oxidation
227	Ta_2Be_{17}	1.6
222	$TaBe_{12}$	1.2
237	$MoSi_2$	0.75
242	$TaSi_2$	0.75
253	WSi_2	0.75
265	WBe_2	39.0
271	WBe_{12}	Sample failure
372	WBe_{22}	Complete oxidation
281	Hf_2Be_{17}	2.8
286	Hf_2Be_{21}	1.4

[a]Mils penetration was obtained from micrometer measurements first on the machined piece before oxidation and then upon removal of scale and pits to bright metal after oxidation. The values are for maximum penetration.

TABLE IV

SUMMARY OF DATA FROM LOW-TEMPERATURE OXIDATION TEST

Compound	Pressing No.	% of Absolute Density	Weight Gain (mg/cm^2)	Mils Penetration		
				Avg.	Max.	Calc.
$TaBe_{12}$	39	98.8	1.22	0.1	0.9	0.1
Ta_2Be_{17}	178	97.4	0.85	N. D.[a]	2.2	0.09
Hf_2Be_{21}	282	100	0.93	0.1	0.2	0.09
$MoSi_2$	293	98.7	2.96	3.55	4.05	0.36
$TaSi_2$	301	98.8	1.59	0.2	0.45	0.16
WSi_2	294	100	0.53	N. D.	0.15	0.06

[a] N. D. - not detectable

appearance of the oxidized $MoSi_2$ specimen, which underwent the most severe attack of all the samples tested, the measured penetration more aptly describes the extent of oxidation of this material.

After the test, a gray, crystalline, adherent deposit covered the surfaces of all the samples except $MoSi_2$ and WSi_2. The surface of the $MoSi_2$ was covered with a buff-colored, flaky deposit, while the WSi_2 sample was only tarnished with an irridescent film. WSi_2 appeared to be far more resistant to oxidation than any of the other materials under the conditions of this test. As a result of this test, it was decided to limit the further testing of $MoSi_2$.

The appearance of the samples before (top) and after (bottom) the test is shown in Figure 1. All the samples had a polished metallic luster before the test, although this does not show clearly in the photograph.

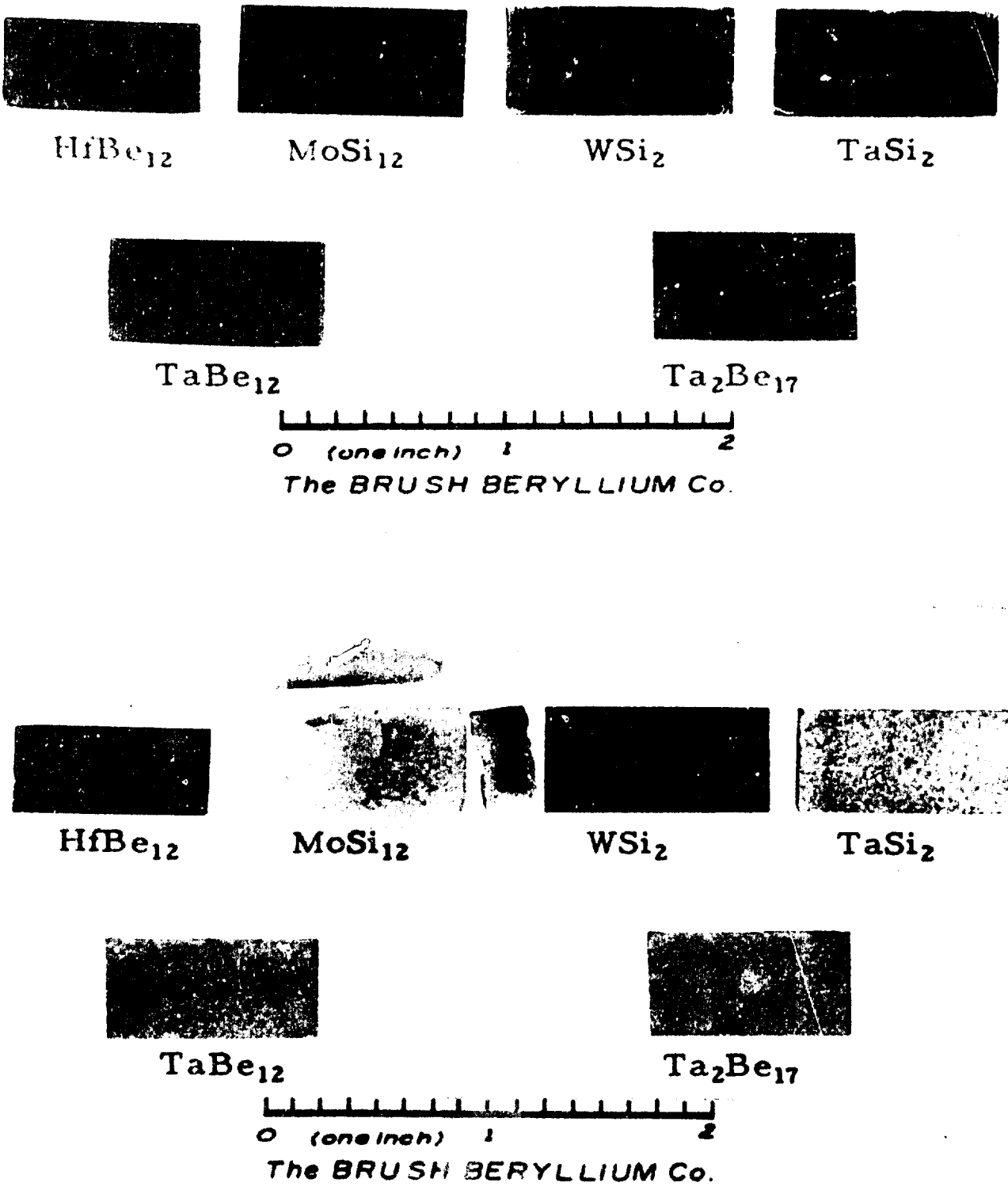

Fig. 1 - Appearance of Samples Before (Top) and After (Bottom) Low-Temperature Oxidation Tests (2000°F)

III. PROPERTY MEASUREMENT PROGRAM

A. Oxidation Resistance

Since resistance to oxidation at high temperature was a prime prerequisite to the successful development of intermetallic materials under this program, data on the maximum service temperature with respect to oxidation resistance were gathered as described in this section. Since it was known that $TaBe_{12}$ and Ta_2Be_{17} exhibited less than 2 mils penetration in 100 hours at 2800°F,[1] testing under this program (in which the desired life at maximum temperature was limited to ten hours) was conducted with a minimum temperature of 2900°F. After preliminary screening at 2900°F, as described in the previous section, the work next described was undertaken to determine the oxidation characteristics of the materials up to 3500°F or to destruction of the material, whichever was the lower temperature.

1. Equipment and Method

Resistance heating, with the sample serving as resistor, was used as the method for heating the specimens. The equipment used to obtain the desired temperatures is shown in Figure 2, and a diagram of the principal circuitry is shown in Figure 3. The power requirements were met by an 8-KVA saturable core reactor. The output from this unit was fed into an 8-KVA step-down transformer (10:1) which, in turn, supplied the necessary current to the water-cooled copper contacts in which the sample to be heated was placed. The output power of the saturable core reactor was controlled by a Brown magnetic amplifier. The temperature was measured by a Brown small-target, total radiation unit which focused on a 1/8-inch-diameter target area. The system was controlled by a Brown strip-chart, recording-control potentiometer with Electr-o-volt control, which featured a compensating rheostat to adjust for non-black-body conditions.

A switch located on the panel of the Electr-o-volt control unit allowed for automatic or manual operation of the equipment. Full power (~740 amperes, 10.8 volts) was applied to the sample at start-up when automatic operation was used. Under manual operation, the power supplied to the sample could be controlled. A current-limiter inserted between the 10:1 stepdown transformer and the magnetic amplifier was an additional aid to current control. Normally, manual control was used to raise the specimen to the desired temperature, and automatic control was used to maintain that temperature.

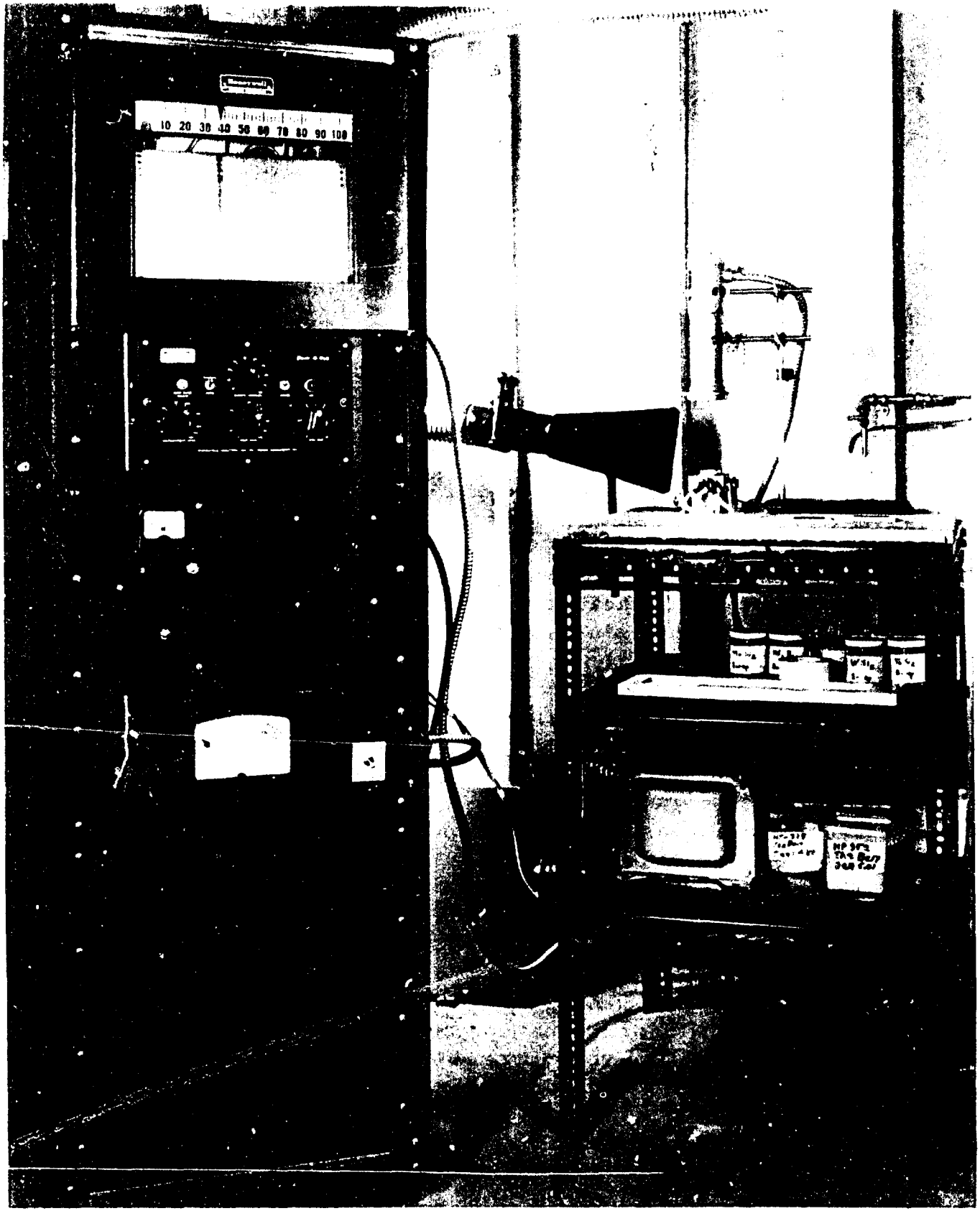

Fig. 2 - High Temperature Oxidation Apparatus

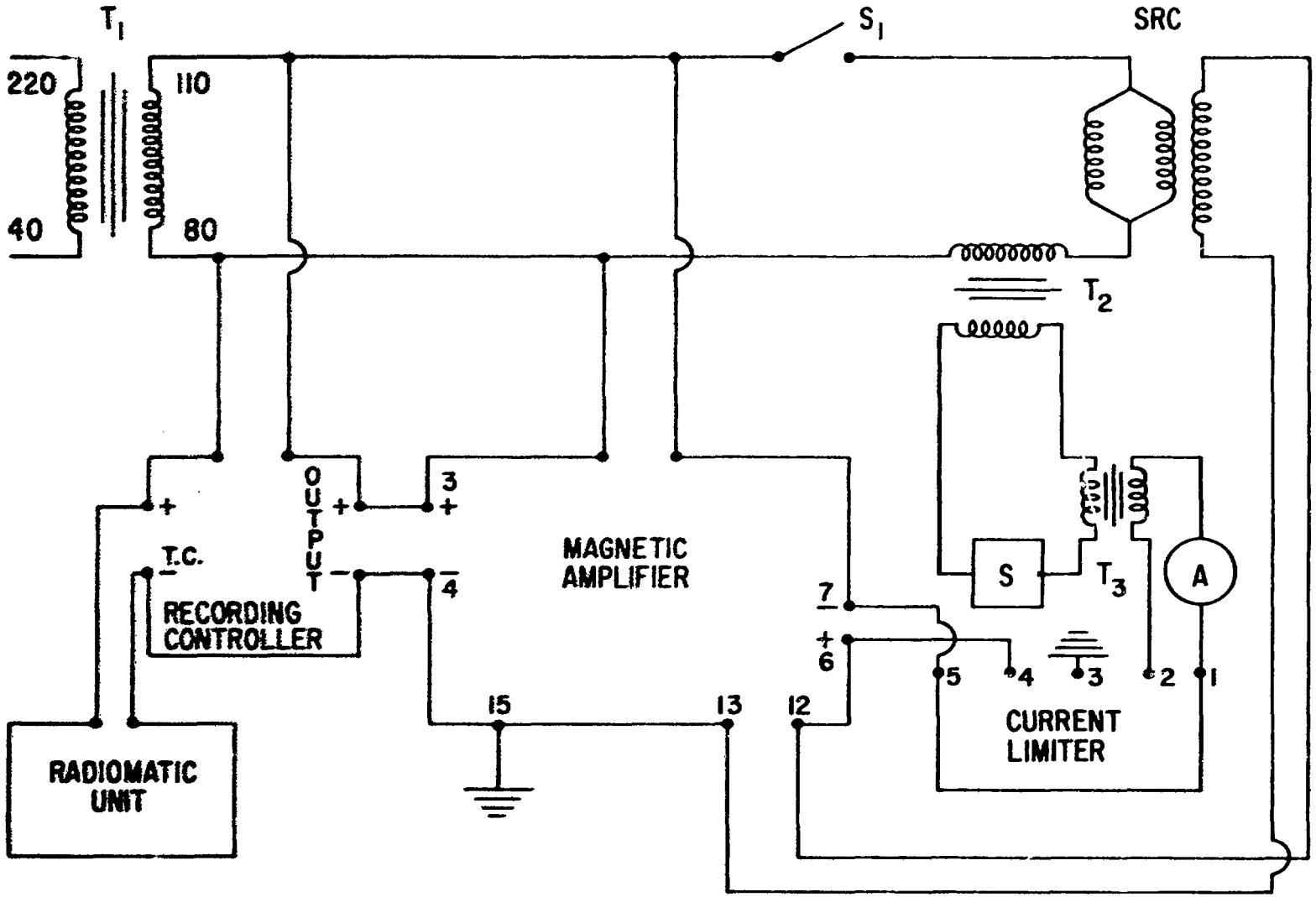

Fig. 3 - Diagram of High Temperature Oxidation Apparatus

The recorded temperature was checked frequently against the temperature readings obtained with an optical pyrometer. The optical pyrometer was used to calibrate the response of the total radiation pyrometer. Assuming the optical pyrometer readings as correct, the recorded temperature could be made to agree with the optical pyrometer readings by proper adjustment of the compensating rheostat incorporated in the control equipment. After an initial adjustment of the compensating rheostat, good correlation of temperature between the two measuring instruments was obtained when the emission characteristics of the surface of the sample remained uniform.

Initial experiments were conducted using an intermetallic specimen 3 inches long, 1/2 inch wide, and 1/8 inch thick with the width of a 1 1/2-inch section at the center reduced to 1/4 inch. The transfer of heat from the center section to the ends was very rapid, creating a very severe thermal gradient at the water-cooled copper contacts, which resulted in specimen failure (due to cracking) at this point. A 1/2-inch section at the center of the specimen was reduced further to 0.160 inch. This modification in the sample design concentrated the hot zone and provided a sufficient length of intermetallic between the hot and cold portions of the sample to eliminate the severe thermal gradient. Some additional difficulties such as arcing of the contacts were encountered, but were essentially eliminated by improved sample mounting techniques.

Figure 4 is a close-up illustration of the sample mounted in the water-cooled sample holders. The double reduction in the width of the sample, to concentrate the hot zone in the center of the specimen, is clearly visible. The total radiation pyrometer was sighted at the center of the reduced section.

2. High Temperature Oxidation Testing of Beryllides

As a result of the preliminary screening tests at 2900° F described previously (Section II-D), the beryllium-containing compounds selected for further study included: $TaBe_{12}$, Ta_2Be_{17}, Hf_2Be_{21}, and Hf_2Be_{17}. In the case of the hafnium compounds, the preliminary testing failed to indicate decisive superiority of either compound ($HfBe_{13}$ was indicated as being thermally unstable decomposing to Hf_2Be_{21} under hot pressing conditions). Primarily due to the cost of hafnium metal, as well as the total number of compounds under consideration, it was decided to limit further work to one hafnium compound. The compound, Hf_2Be_{21}, was chosen on the basis of somewhat better results than those for Hf_2Be_{17} in the screening tests.

Fig. 4 - Sample and Sample Mounting

The silicon carbide element furnace used for screening operations is operable to 3000° F by virtue of its tubular element. Data were therefore taken on the beryllides at 3000° F with this unit, as summarized in Table V.

As can be seen by the results of this test, 3000° F apparently represents the top use temperature for these compounds as prepared to date. Individual samples of each of the compounds, $TaBe_{12}$, Ta_2Be_{17}, and Hf_2Be_{21}, underwent catastrophic oxidation in this test; other samples exhibited a degree of resistance, but in no instance was a 2 mil penetration limit in ten hours achieved. The differences in oxidation resistance between these various preparations at this temperature were probably due to minor impurity variations, which become significant as the limiting temperature for oxidation resistance is reached. It may be concluded from this test that all four compounds may be useful at 3000° F where service life of short periods is involved, e.g., five hours. Impurity control efforts would seem necessary for reliability of performance to be achieved at this temperature.

The resistance heating equipment for oxidation testing at 3000° to 3500° F was generally not operated successfully with beryllide specimens in this temperature range. This was primarily due to the formation of non-uniform scale on the surface of the specimen, resulting in (1) variable emission characteristics and severe temperature differences between the surface scale and the intermetallic bar and (2) relatively low oxidation resistance of the materials above 3000° F. As the oxide scale formed, the total radiation received by the radiamatic unit decreased, so that more power was required for maintaining the set temperature as read by the instrument. With the scale temperature at the control temperature of 3000° or 3200° F, the actual specimen temperature was considerably higher, resulting in rapid failure due to oxidation and/or melting. Due to the non-uniformity of scale formation, satisfactory corrections for this phenomenon were not possible. At lower temperatures, e.g., 2900° F, the equipment performed nicely with beryllides, but conventional furnacing is more suitable for these temperatures.

Numerous attempts were made to obtain oxidation data on both Ta_2Be_{17} and $TaBe_{12}$ with this equipment. In all cases, the samples consistently failed at an outside scale temperature of 3000° F after a time at temperature on the order of 5 minutes. The failures appeared to be the result of both oxidation and melting (a result of a lack of control of the internal temperature, as described above). These results, however, do reaffirm the results of the 3000° F tests described in Table V, leading to the conclusion that 3000° F would be the top service temperature for the compounds.

TABLE V

OXIDATION TESTS FOR BERYLLIDES IN GLO-BAR TYPE FURNACE

(Laboratory Air; 3000°F)

Pressing No.	Material	% of Absolute Density	Weight Gain (mg/cm^2) 1 Hr	5 Hr	10 Hr	Mils Penetration 10 Hours[a] Avg.	Max.	Calc.
222	$TaBe_{12}$	97.8	11.3	25.4	36.6	3.1	5.5	3.7
308	$TaBe_{12}$	99.1	5.4	17.9	162.5	Not measurable		16.3
227	Ta_2Be_{17}	98.7	155	258	328	Not measurable		33
309	Ta_2Be_{17}	99.6	7.9	15.2	33.0	1.9	3.2	3.3
282	Hf_2Be_{21}	100	13.7	36.1	59.2	--	--	7.2
286	Hf_2Be_{21}	100	13.1	32.5	59.1	--	--	7.3
322	Hf_2Be_{21}	97.7	50.8	94.0	123.2	Not measurable		16
281	Hf_2Be_{17}	88.5	9.7	21	32	5.2	6.8	4

[a]Mils penetration obtained by micrometer measurements before the test and (1) after removing the oxide scale to bright metal for "average" penetration and (2) after removing the deepest pits for "maximum" penetration. "Calculated" penetration based on weight gain, assuming uniform stoichiometric oxidation.

Similar difficulties were encountered with Hf_2Be_{21} samples. With two samples, a small semicircular depression developed in the center of each specimen upon heat-up. For the first sample, the temperature of the depression averaged 3220° F, while the temperature of the scale around the depression averaged 3000° F. This sample was at temperature for one hour. The second sample was at temperature for 2 hours and 5 minutes before failure occurred. Again the temperature of the depression averaged 3220° F, but the scale temperature averaged somewhat lower (2950° F). Examination of the samples after the run showed that failure was due to either complete oxidation at the point of the depression or melting at this point.

A third sample of Hf_2Be_{21} was raised to 3200° F and held there for twenty minutes; then the temperature was raised to 3750° F over a five-minute period. For twenty minutes, which was the duration of the test, the temperature averaged 3750° F with frequent oscillations between 3700° and 3800° F. The sample was completely oxidized in the test region, indicating that perhaps the resultant oxide had become conductive at this high temperature. Another specimen was raised to 3400° F and held there. At the end of thirty-five minutes, severe oscillations in temperature began, and after forty minutes, the temperature was oscillating between 3310° and 3490° F. The sample failed after a total of forty-two minutes with a final temperature surge to 3800° F. Again the sample was completely oxidized in the test region.

In order to ascertain the possible usefulness of this compound at 3100° F for very short times, a sample of Hf_2Be_{21} was raised to this temperature in the equipment. The sample was at temperature for five minutes when a crack developed at one of the cold ends and the test was ended. A characteristic brown scale covered the hot zone, and the sample dimensions had changed. (The hot zone was slightly caved in on all sides.) Penetration data could not be obtained; however, the sample was broken at the center of the hot zone for examination. A void about 3/32 inch in diameter was observed in the center of the specimen. The scale from the hot zone was composed of HfO_2, BeO and Hf_2Be_{17}, as determined by X-ray analysis. The scale was removed to some extent and X-ray analysis showed major amounts of both Hf_2Be_{21} and Hf_2Be_{17}. The fractured surface was identified as predominately Hf_2Be_{17}. It was concluded from these observations of the sample that the extent of deformation and oxidation in the short time of the test were such that Hf_2Be_{21} would not be serviceable as a structural material at 3100° F.

3. High Temperature Oxidation Testing of Silicides

The results of preliminary screening tests conducted at 2900° F (Section II-D) indicated that further investigation of all of the silicides tested, $MoSi_2$, $TaSi_2$, and WSi_2, was warranted. The oxidation resistance of these materials was examined at 3000° F in a tubular silicon carbide element furnace as well as in the resistance heating equipment (sample serving as resistor).

The results of the tests made in the silicon carbide element furnace at 3000° F are tabulated in Table VI. At the conclusion of these tests, all of the samples were covered with a smooth, transparent, vitreous coating. It will be observed that WSi_2 showed a net weight gain at this temperature, whereas a net weight loss had been observed in the 2900° F tests. The results show the silicides to possess excellent oxidation resistance at 3000° F.

Tests were also made at 3000° F and above, using the resistance heating equipment. In general, temperatures could be controlled much more satisfactorily when testing the silicides in this equipment than when testing the beryllides (see preceding section). The transparent scale which formed on most of the silicide specimens apparently had a much smaller effect on the emission characteristics of these materials than was true in the case of the beryllides.

The initial tests at 3000° F were made to appraise the equipment; therefore, the tests were of short duration. The transparent coating was slightly pitted in the cases of $MoSi_2$ and WSi_2. No further tests were made on $MoSi_2$ because the low-temperature oxidation test (Section II-D) indicated poor oxidation resistance of this compound below 2000° F.

In the initial tests on $TaSi_2$, a sample from H. P. 335 was tested at 3185° F for about 1 1/2 hours. Temperature fluctuations up to 3275° F were frequent during this test because of fluctuations in the supply voltage. A very smooth transparent scale covered the hot zone of the sample. Figure 5 is a photograph of this sample after the test. From appearance, the final dimensions were very close to the original dimensions. Further attempts to measure the oxidation resistance or to find the maximum temperature of service for $TaSi_2$ by testing samples from H. P. 338 were unsuccessful. While there were no overt differences between H. P. 338 and H. P. 335, the oxidation products were different for samples from the two pressings. A clear, vitreous scale covered

TABLE VI

OXIDATION TEST DATA FOR SILICIDES

(Glo-Bar-Type Furnace; 3000° F)

Pressing No.	Material	% of Absolute Density	Weight Gain (mg/cm^2) 1 Hr	5 Hr	10 Hr	Mils Penetration 10 Hours[a] Avg.	Max.	Calc.
294	WSi_2	98.8	0.2	1.7	1.9	0.5	1.3	0.2
299	$TaSi_2$	99.8	0.9	1.6	2.4	0.1	0.2	0.3
323	$MoSi_2$	97.3	1.3	2.5	3.4	N. D.[b]	N. D.[b]	0.3

[a]Mils penetration obtained by micrometer measurements before the test and (1) after removing the oxide scale to bright metal for "average" penetration and (2) after deepest pits removed for "maximum" penetration. "Calculated" penetration based on weight gain, assuming uniform stoichiometric oxidation.

[b]Not detectable - Dimensions of sample after scale removal same as for unoxidized sample.

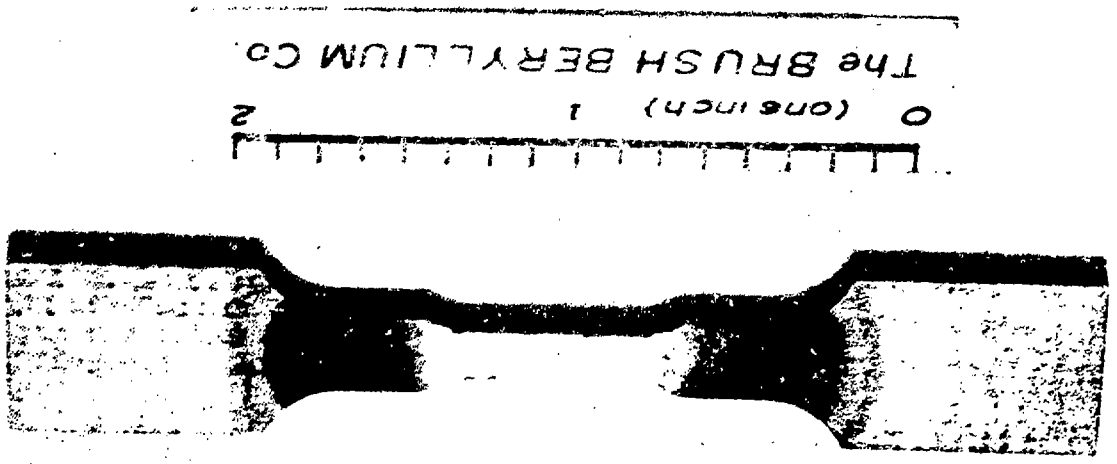

Fig. 5 - $TaSi_2$ After 1 1/2 Hours at 3185°F

the hot zone when samples from H. P. 335 were oxidized. On the other hand, when samples from H. P. 338 were oxidized, a chalk-white scale first formed, which was glazed by the vitreous coating subsequently formed. In addition, the scale which formed on samples from H. P. 338 had a tendency to spall upon cooling. Temperature control was also more difficult to maintain; however, one sample was raised to 3500° F and remained at this temperature for five minutes before failure occurred. (The sample burned through at the hot zone with subsequent loss of continuity.) $TaSi_2$ has a higher melting point than has WSi_2 (4350° and 3960° F, respectively), and, since the scale on the $TaSi_2$ specimen was not pitted at 3185° F, it is reasonable to expect a higher service temperature from $TaSi_2$. The oxidation resistance of this material should be examined further.

A sample of WSi_2 was oxidized in this equipment for 10 hours at 3000° F. The run was made in two parts - 2 1/2 hours the first day and 7 1/2 hours the following day. Temperature control was good; however, there were infrequent current surges which caused momentary temperature fluctuations. At the end of the run, there was a thin vitreous coating on the sample center section, which exhibited a rough appearance throughout the hottest portion. This roughness is probably the result of decomposition products escaping through the glassy film during the course of the oxidation. The formation and breaking of bubbles was clearly visible during the test. The sample as it appeared at the conclusion of the test is shown in Figure 6. A yellow and white scale had built up at the extreme ends of the hot zone. This sample was cut and mounted in bakelite so that one of the oxidized surfaces was exposed. The scale was removed from the exposed surface, which allowed viewing of a cross-section of the sample, showing an outer or oxide layer, the intermetallic, and the other outer surface layer. The average grain size increased from 18 microns near the edge of the hot zone to 46 microns in the hot zone. Figure 7 is a photograph of an area, showing the difference in grain size. The width of the observed surface before oxidation was 0.1608 inch as measured with a micrometer. The width of the specimen after oxidation was measured as 0.1642 inch by optical measurements on a polished cross section of the oxidized portion of the specimen. The increase in dimensions was presumably due to a swelling of the sample. The scale was not clearly visible when the sample was viewed at 100X, owing to its extremely small thickness.

An electron micrograph of the mounted sample is shown as Figure 8. The bakelite mounting is at the bottom of the picture, where there is a separation between the plastic and the sample. The upper portion shows the sample from the oxidized surface inward. No special significance should be attached to the contour of the surface, since during the metallographic polishing, the edges of the sample were somewhat

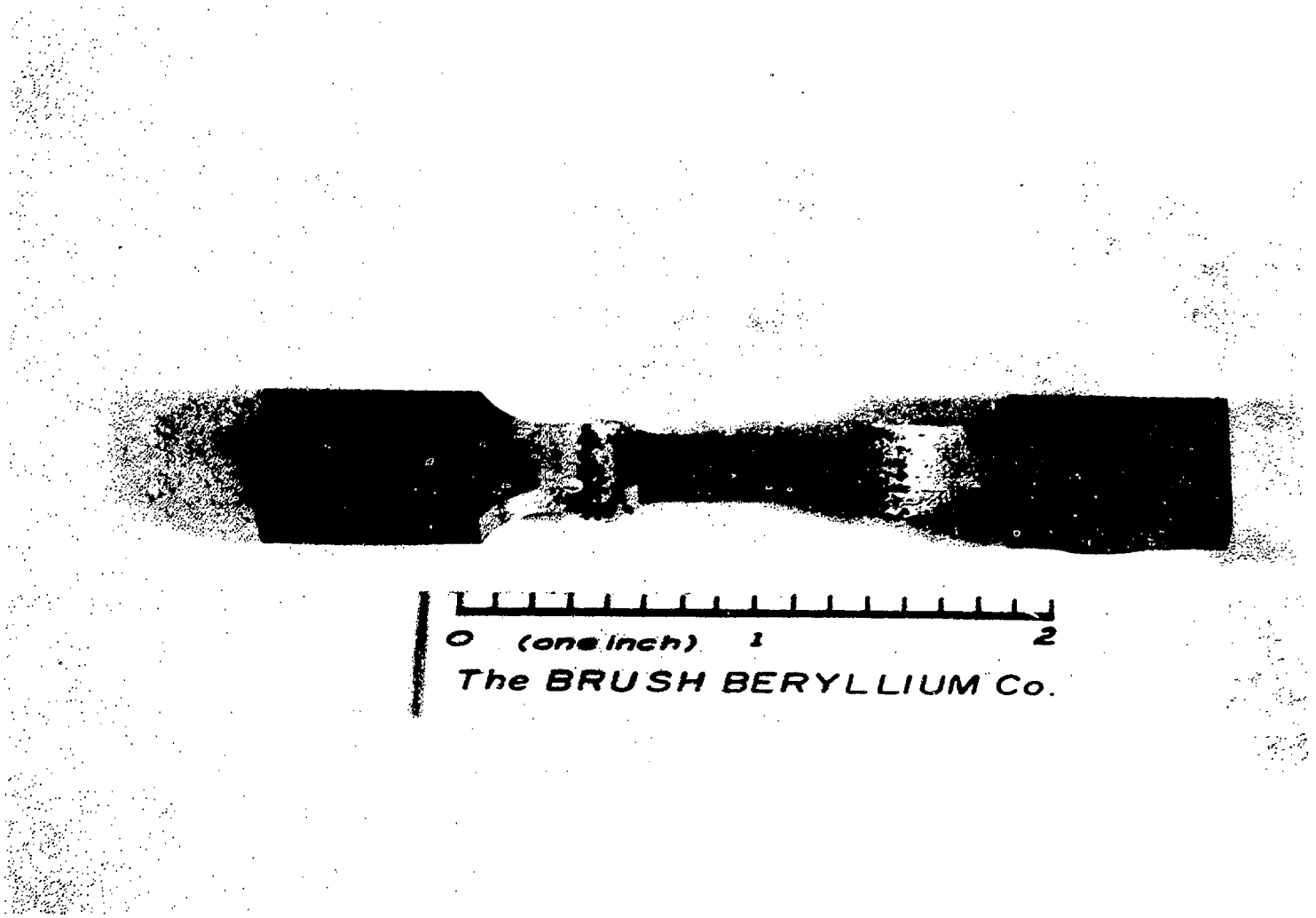

Fig. 6 - WSi_2 After 10 Hours Oxidation at 3000°F

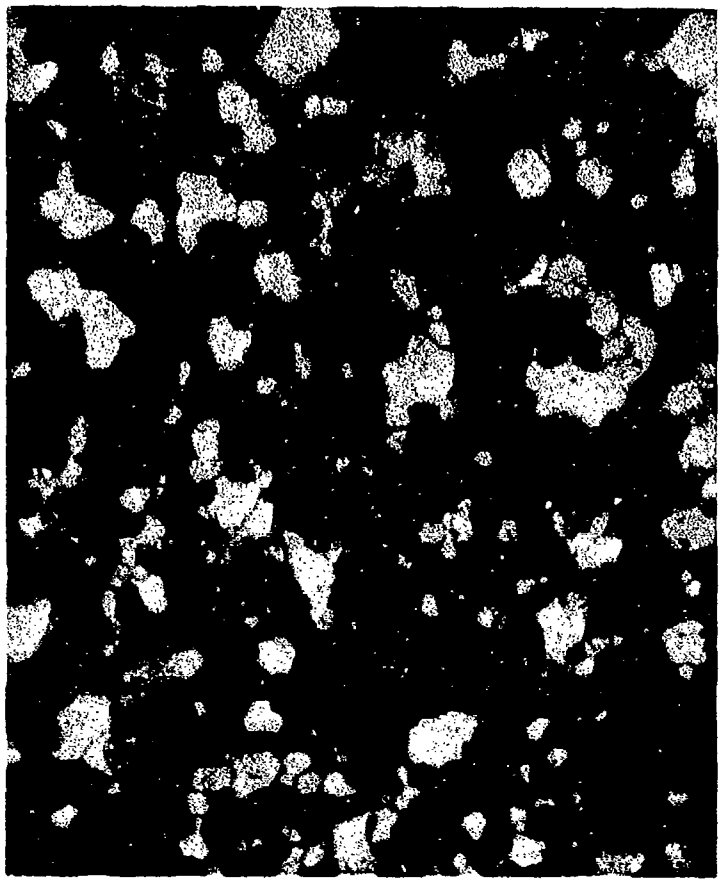

Fig. 7 - WSi_2 after 10-Hour Oxidation at 3000°F Showing Increase in Grain Size Toward "Hot" Zone, Polarized Light, 100X before Reproduction

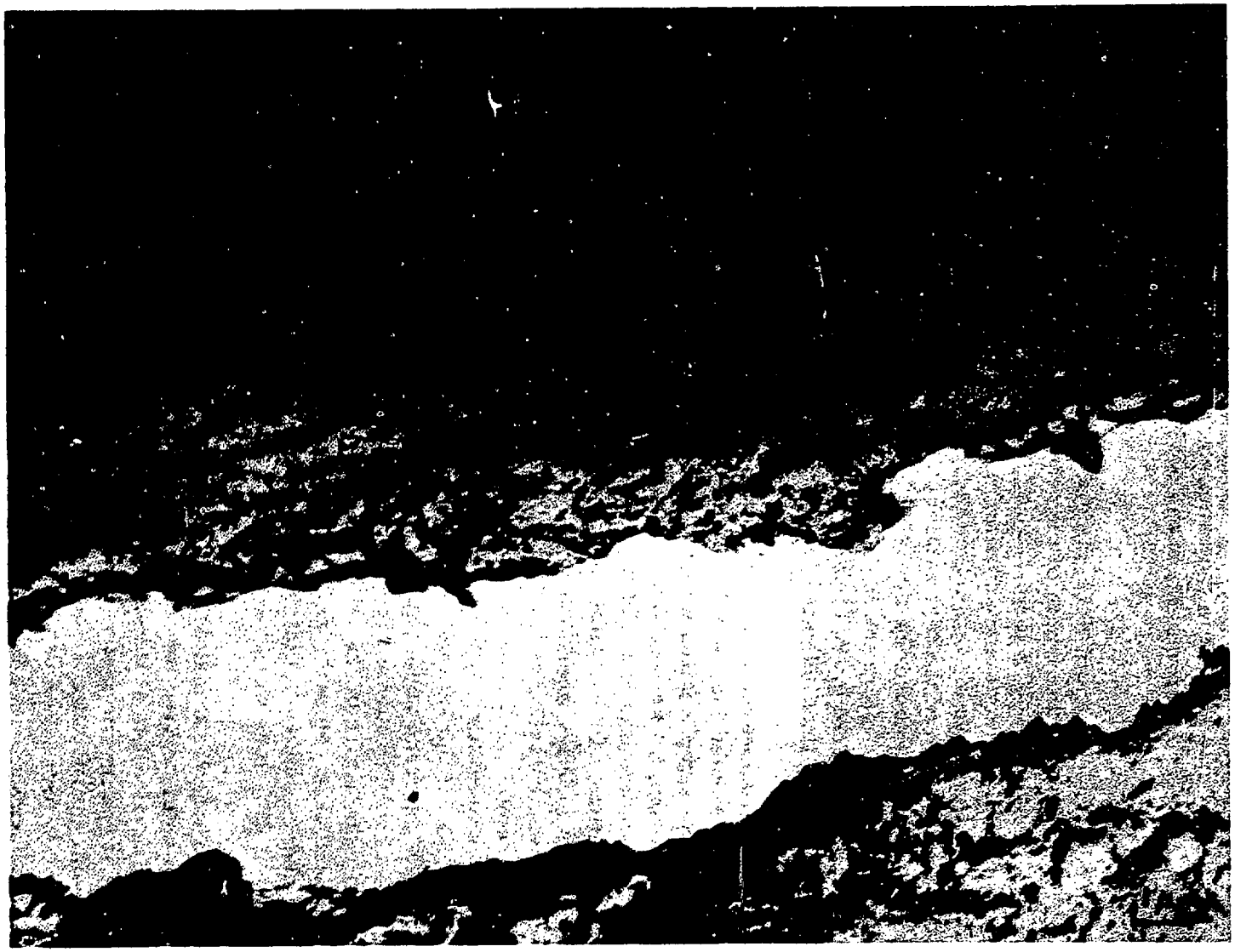

Fig. 8 - Electron Micrograph of WSi_2 - Cross Section of Oxidized Specimen 830X Before Reproduction

rounded. The oxide layer does not show on the micrograph. Figure 9 shows a portion of the same area at a higher magnification, and Figure 10 is a micrograph of an area within the sample. These electron micrographs were taken from chrome-shadowed positive carbon replicas of the WSi_2 sample.

In order to avoid the cycling experienced in the 3000° F test, it was decided to reduce the length of the test for future runs. Samples of WSi_2 were tested at 3100° F for 6 1/2 hours and at 3200° F for 6 hours. The samples had much the same appearance as did the 3000° F sample except that the roughness of the surface increased with increased temperature. The dimensions of the test section of the samples were determined in the same manner as those for the 3000° F sample. The 3100° F sample measured 0.1880 inch before the test and 0.1886 inch after the test; the 3200° F sample measured 0.1933 inch before and 0.1894 inch after. About 2 mils penetration is thus indicated for WSi_2 after 6 hours at 3200° F.

WSi_2 appeared to withstand the 3200° F test so well that the next test was scheduled for 3400° F. In the first attempt to reach this temperature, the sample failed at 3340° F, while failure occurred at 3330° F in the second attempt. Failure was due to apparent melting in each case. The test temperature was lowered to 3300° F, and two samples were tested at this temperature. One sample was at temperature for 27 minutes and the other for 12 minutes when failure occurred. The rough surface (formed as a result of volatilization through the glassy coating) was more pronounced than at lower temperatures, as would be expected. For both samples, failure was due to melting in the center of the specimen. As in the case of the beryllides, if the sample was not allowed to expand due to jamming of the contacts, a crack could occur. This crack would represent a high resistance and would cause a rapid temperature surge which would melt the sample. The nature of the failure rendered attempts to measure the extent of penetration impractical; however, visual examination indicated that the thickness and width dimensions a short distance (about 1/16 inch) from the point of failure were unchanged.

These tests indicate that WSi_2 has sufficient oxidation resistance to be of service for 6 hours at 3200° F, and has promise of a much longer service life at this temperature. At 3300° F and above, the life of the test specimens was very short; however, this may have resulted from mechanical difficulties. Additional tests should be made at these temperatures to properly evaluate the maximum temperature of service of this compound.

Fig. 9 - Electron Micrograph of WSi_2 - Cross Section of Oxidized Specimen
2300X Before Reproduction

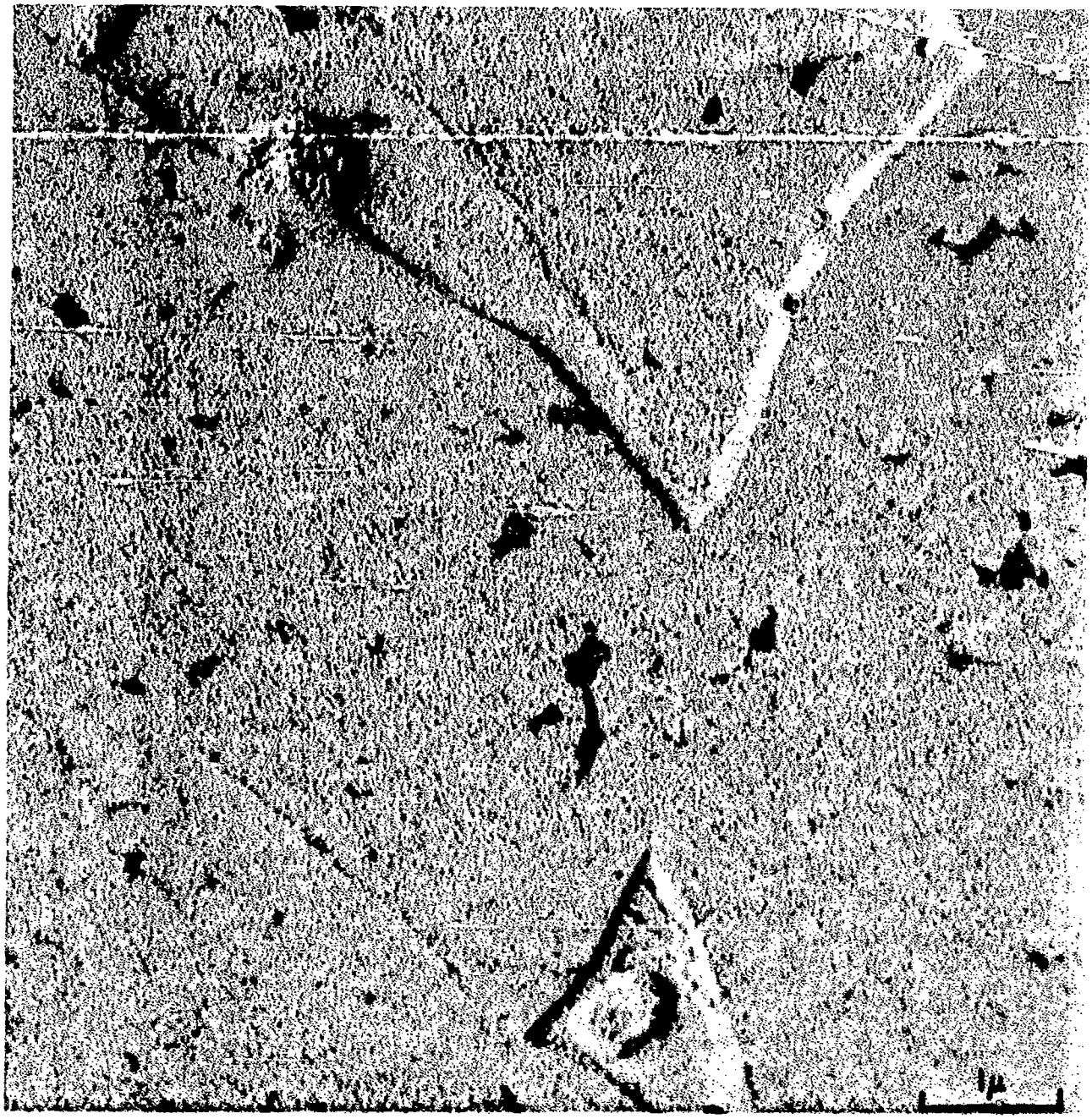

Fig. 10 - Electron Micrograph of Unoxidized WSi_2 2300X Before Reproduction

4. Oxidation of WSi_2 and $TaSi_2$ at 2300° and 2500° F

The buildup of deposits at the extremities of the hot zone (Figure 6) and the general appearance of the area between the hot zone and the contact ends of the oxidation specimens of $TaSi_2$ and WSi_2 suggested a redetermination of the oxidation resistance of these compounds at low temperatures. It was suspected that these materials would exhibit oxidation characteristics similar to what was observed for $MoSi_2$ (Section II-D) but at a somewhat higher temperature. The temperature range to be considered was between 2000° F and 2900° F, since the low-temperature oxidation had been checked to 2000° F and the preliminary oxidation measurements were made at 2900° F.

Tests have been made at 2500° F and 2300° F. The results of these tests are tabulated in Table VII. The samples were exposed to the indicated temperatures for a maximum of ten hours, using the 1-, 5-, and 10-hour cycling procedure. As can be seen in the table, both $TaSi_2$ and WSi_2 exhibited less than 2 mils measured penetration in 10 hours at 2500° F. The scales on the samples were adherent, and there was no evidence of spalling. At 2300° F all of the $TaSi_2$ specimens were covered with an intermixed brown and white adherent scale after 10 hours. Although the measured penetration was less than 2 mils at this temperature, it was considerably greater than at higher temperatures.

In the case of WSi_2, only one sample exhibited excessive oxidation. This sample from the low-density pressing H. P. 290 had patches of a mottled black and white scale on parts of its surface. The area covered by these patches was slightly raised in comparison with other areas of the surface. All of the other samples of WSi_2 possessed a dull gray adherent scale at the conclusion of the test. It is seen that the extent of penetration into these samples was very low.

Using two mils penetration in ten hours as a basis, these tests indicate that both $TaSi_2$ and WSi_2 possess satisfactory oxidation resistance at 2300° and 2500° F. However, at 2300° F, $TaSi_2$ is somewhat less oxidation resistant than is WSi_2. It may be inferred from these tests that WSi_2 will behave similarly to $TaSi_2$ at a temperature somewhat less than 2300° F. Before definite conclusions are drawn, these tests should be continued in the temperature range from 2100° to 2400° F.

TABLE VII

OXIDATION OF $TaSi_2$ AND WSi_2 AT 2300° AND 2500° F

Pressing No.	Material	% of Absolute Density	Weight Gain (mg/cm^2) 1 Hr	5 Hr	10 Hr	Temp. (°F)	Mils Penetration 10 Hr[a]
335	$TaSi_2$	98.1	0.11	0.49	0.77	2500	0.15
335	$TaSi_2$	96.9	0.34	0.98	2.10	2300	1.55
338	$TaSi_2$	98.2	0.44	1.43	3.13	2300	1.20
301	$TaSi_2$	99.4	0.42	1.50	3.14	2300	1.25
299	$TaSi_2$	99.8	2.54	4.66	5.85	2300	1.85
369	WSi_2	98.5	(-0.31)	(-0.35)	(-0.22)	2500	0.10
369	WSi_2	97.9	(-0.60)	(-0.55)	(-0.60)	2300	0.55
347	WSi_2	100.	(-1.38)	(-1.82)	(-2.06)	2300	0.90
294	WSi_2	98.6	(-0.55)	(-0.53)	(-0.50)	2300	0.55
290	WSi_2	94.3	(-2.07)	(-3.84)	(-7.23)	2300	7.0

[a]Mils penetration obtained by micrometer measurements before the test and after the deepest pits were removed from the sample after the test.

B. Mechanical Properties

1. Transverse-Rupture

a. Equipment and Procedures

The transverse rupture machine which was designed and built at The Brush Beryllium Company is a modification of a similar instrument devised by Stanley Mark, Jr., of the Carborundum Company of Niagara Falls, New York.[3] Figure 11 schematically shows the principal features of the machine.

The machine consists of a stress applicator, in this case a lever arm oriented in such a manner that when it is activated, it exerts a force on a pusher rod, which passes vertically downward through a furnace and presses against a heated test specimen. The specimen rests on two stationary anvils, resulting in single-point loading. Bending of the specimen is determined with the aid of a deflection-detection rod which protrudes from the bottom of the furnace (starting from the specimen and passing between the anvils) and is axially aligned with the pusher rod, but 180 degrees from it. The deflection rod is used to activate a Daytronic Model 300 Displacement Indicator which is connected to a Varian Associates Model G 11A Recorder. The machine in its present design is used for testing specimens of a rectangular cross section as simply supported, centrally loaded beams.

The stress applicator is a simple lever, water-loading system. Water flows into the can, which causes the pusher rod to press against the specimen with a force given by the product of the weight of water times the lever-arm ratio. The rate of water flow and the corresponding weight of the water can be determined quite accurately.

The pusher rod, the special anvil brick, and the deflection rod used are composed of KT silicon carbide and were supplied by the Carborundum Company. The pusher rod is 1 inch in diameter and 15 inches long. It is pointed to a knife edge on one end. The special brick which incorporates the anvils measures 9 x 4 x 1 1/4 inches. The special anvil features consist of two parallel semicircular ridges 2 1/2 inches apart and 1/4 inch high, which support the specimen. A hole in the center of this anvil brick allows the deflection rod to pass through it and contact the specimen. The specimen size used is 3 x 1/2 x 1/4 inches and the gauge length is 2 1/2 inches. The maximum capacity of the transverse-rupture machine at present is 750 pounds, corresponding to 90,000 psi which may be exerted on a specimen of the aforementioned size.

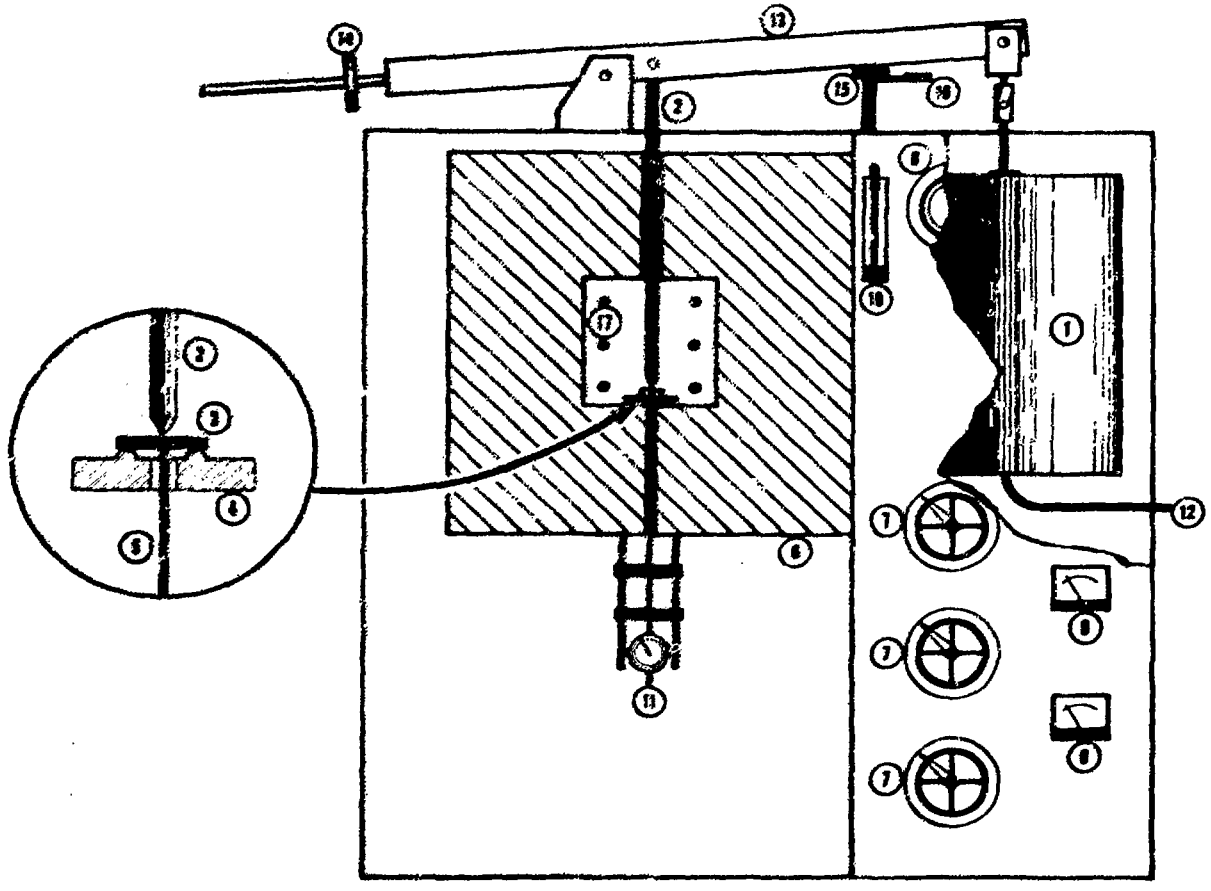

1. CAN
2. PUSHER ROD (SiC)
3. SPECIMEN
4. SPECIAL ANVIL BRICK (SiC)
5. DEFLECTION ROD (SiC)
6. FURNACE
7. FURNACE-CONTROL POWERSTATS
8. WATER FLOWMETER
9. AMMETERS
10. HYDRAULIC JACK FOR ADJUSTMENT OF BEAM CATCHER
11. DIAL EXTENSION INDICATOR
12. FLEXIBLE HOSE CONNECTION (WATER INLET & DRAIN)
13. LEVER ARM
14. LEVER ARM ADJUSTMENT (COUNTERBALANCE)
15. BEAM CATCHER
16. MICROSWITCH
17. GLOBAR HEATING ELEMENTS

Fig. 11 - Schematic of Transverse Rupture Machine

The furnace used is a silicon carbide element type, which is capable of reaching a temperature of 2750° F, and possibly higher for short periods of testing. Temperature control is effected through a platinum-platinum, 10% rhodium thermocouple in a porcelain well located about 2 1/2 inches from the specimen. From time to time the temperature is checked by optical pyrometer readings on the specimen itself.

In operation, the cold specimen is inserted in place on the two parallel anvils, the furnace having been previously brought up to the testing temperature. Actual loading is started after the specimen reaches the test temperature, usually after 5 to 10 minutes.

As the test proceeds, the specimen deflection is recorded on a strip chart. Upon rupture, the lever arm falls down on a catcher which reactivates a solenoid valve through a microswitch, shutting off the water flow. The ultimate load in gallons is converted to force in pounds on the specimen, which in turn gives the stress (psi) in the outermost "fibers" of the specimen by the equation:

$$S = \frac{3PL}{2bd^2}$$

where P = load on specimen in pounds
L = specimen span in inches
b = specimen width in inches
d = specimen thickness in inches

The proportional limit and modulus of elasticity are obtained from the stress-strain curve (recording) in the normal manner.

The results obtained with this equipment are probably accurate to within about 2 or 3% for the lower rupture strengths and approach 1% for the higher values (above 20,000 psi). Values for Young's modulus are much less accurate.

Preliminary investigations indicated that furnace bed deflection was not significant in the stress region normally used for calculating the elastic modulus. For larger loads, the bed deflections (obtained in calibration runs) were subtracted from the observed deflections.

b. Experimental Data and Discussion

The transverse-rupture test data are summarized in Table VIII. The rate of loading for all specimens was 120 lb/min, or 14,000 psi/min. Owing to the limited number of hot-pressed blocks of each compound available for mechanical testing, the data presented are only indicative of the strengths which can be obtained for a particular compound, and are not necessarily representative of the maximum strengths possible. Variations in density, grain size, and composition among the various fabricated pieces were frequent. Each of these variables can have an appreciable effect upon the mechanical properties of a material. Since it is not possible to determine the precise effect of each of these variables from the present data, additional testing should be carried out on the most promising materials.

The differences in absolute density of the Hf_2Be_{21} pressings resulted from the presence of different minor constituents. In H. P. 322, the minor phase present was $HfBe_{13}$, whereas Hf_2Be_{17} was the minor constituent present in H. P. 361. The differences in modulus-of-rupture values for these pressings, though not overly large, suggest that the presence of $HfBe_{13}$ as a minor constituent in H. P. 322 reduced the strength of this material, inasmuch as the grain size was relatively favorable and the density good. (The thermal instability of $HfBe_{13}$ has been discussed in a previous section.) Normally, it would be expected that the smaller grain size of H. P. 322 would exert a greater influence than would the density difference between the two pressings.

There is no direct correlation between a difference in grain size and the modulus-of-rupture values for $TaSi_2$. H. P. 335 had the smallest grain size (though a somewhat lower density also), yet its strength was commensurate with that of H. P. 301 which had the largest grains. The only apparent difference between H. P. 278 and H. P. 301 was grain size, so the lowered strength of H. P. 301 would seem to be the effect of large grains. With the strength of the small-grain-size H. P. 335 approximating the strength of H. P. 301 instead of that of H. P. 278, the grain-size effect is clouded and the indication is that some other factor is responsible for the observed differences in strength values for this material.

The difference in density (or in effect, porosity) would not normally be expected to cause such large differences in strength. The absolute, or powder, density of H. P. 278 was the highest of the three

TABLE VIII

SUMMARY OF TRANSVERSE-RUPTURE TEST DATA

Compound	Pressing No.	Sample Density (g/cc)	Sample Density % of Absolute	Grain Size (μ)	Test Temp. (°F)	Modulus of Rupture (10^3 psi)	Young's Modulus (10^6 psi)
Ta_2Be_{17}	318	4.91	98.6	18	2300	64.5	17
		4.88	98.0	18	2300	69.1	12
		4.91	98.6	18	2500	52.8	9
		4.90	98.4	18	2500	54.1	13
		4.90	98.4	18	2750	28.8	9
		4.91	98.6	18	2750	32.3	10
$TaBe_{12}$	149	4.07	96.0	12	2300	48.8	24
		4.07	96.0	12	2300	57.6	24
		4.07	96.0	12	2500	43.0	14
		4.07	96.0	12	2750	26.5	9
		4.07	96.0	12	2750	25.5	10
Hf_2Be_{21}	322	4.19	98.4	23	2300	21.8	17
		4.21	98.8	23	2500	14.9	4
		4.19	98.4	23	2500	17.9	5
		4.11	96.5	23	2750	1.7	--
		4.20	98.6	23	2750	2.3	--
Hf_2Be_{21}	361	4.33	99.8	35	2300	16.5	28
		4.35	100.	35	2500	23.0	15
		4.36	100.	35	2500	25.4	15
		4.36	100.	35	2750	17.1	9
		4.36	100.	35	2750	3.5	12
$MoSi_2$	305	6.07	98.1	33	2300	26.1	40
		5.94	96.0	33	2500	29.6	24
		6.06	97.9	33	2500	25.6	19
		6.04	97.6	33	2750	9.3	12
		6.02	97.3	33	2750	13.3	--
$TaSi_2$	278	8.85	97.5	28	2300	29.6	49
		8.94	98.5	28	2500	13.3	43
		8.95	98.6	28	2500	12.7	25
		8.66	95.4	28	2750	16.1	14
		8.88	97.8	28	2750	16.3	14
$TaSi_2$	301	9.02	99.8	55	2300	9.4	50
		8.95	98.7	55	2500	1.5	8
		8.81	97.2	55	2500	2.9	26
		8.95	98.6	55	2750	3.5	--
$TaSi_2$	115	8.68	95.6	23	2300	8.7	10
		8.70	95.8	23	2300	8.7	12
		8.68	95.6	23	2500	8.7	7
		8.69	95.7	23	2500	8.1	10
		8.71	95.9	23	2750	4.7	7
		8.73	96.1	23	2750	4.7	6
WSi_2	290	9.05	94.1	10	2300	46.8	40
		8.98	92.7	10	2300	44.5	17
		8.86	92.1	10	2500	40.4	16
		8.94	92.9	10	2500	47.5	13
		8.92	92.7	10	2750	30.4	--
		8.99	93.5	10	2750	36.4	--
WSi_2	147	9.70	100.	27	2300	57.5	39
		9.72	100.	27	2500	70.9	48
		9.75	100.	27	2500	68.5	--
		9.75	100.	27	2750	47.6	23
		9.75	100.	27	2750	44.5	11
WSi_2	169	9.51	99.2	51	2300	32.8	26
		9.64	100.	51	2300	34.3	19
		9.51	99.2	51	2500	12.2	19
		9.44	99.3	51	2500	20.7	26
		9.46	99.5	51	2750	26.7	24
		9.44	99.4	51	2750	21.7	15

pressings, being very close to the theoretical X-ray density for $TaSi_2$ (9.08 versus 9.10 g/cc). This may indicate that excess silicon in H. P. 301 and H. P. 305 was at least partially responsible for the low strength of these materials. This is particularly true for the small-grained H. P. 335, which had the lowest absolute density (8.84 g/cc).

In the case of WSi_2, there appears to be a definite correlation between strength and grain size. The low-density, small-grained H. P. 290 exhibits greater strength than the high-density large-grained H. P. 369. The strength of H. P. 369 samples is lower than that of H. P. 347 samples, and the only apparent difference between these pressings is grain size. The increased strength of H. P. 347 over H. P. 290 must be attributed to the density effect. The data obtained from these three pressings indicate that a high-density, small-grained material should possess excellent strength characteristics.

The data for $TaBe_{12}$ shown in Table VIII were obtained under another contract, and are typical values for this compound. Some of the modulus-of-rupture data for the beryllides are plotted in Figure 12. The plotted points for $TaBe_{12}$ and Ta_2Be_{17} are averaged values for each temperature taken for H. P. 149 and H. P. 318. Inasmuch as the data for Hf_2Be_{21} are quite inconsistent, an approximate strength versus temperature curve for this compound is represented, based upon the best values from both pressings. While the data at hand indicate that the strength of the tantalum beryllides is superior, it would be premature to conclude that Hf_2Be_{21} is a relatively low-strength material.

Some of the modulus-of-rupture data for the silicides are plotted in Figure 13. Again, average values have been plotted at each temperature for WSi_2, using the data from the strongest pressing of this material (H. P. 347). Data obtained from the other two pressings of this material suggest that WSi_2 is at least as strong at 2300° as it is at 2500° and that perhaps the single value obtained at 2300° for H. P. 347 is abnormally low. Plotting the data from the best pressing of $TaSi_2$ (H. P. 278) shows that the values obtained at 2500° are probably abnormally low, and these have been ignored in drawing the curve shown in Figure 13. The curve shown for $MoSi_2$ is a plot of the average values obtained from H. P. 305. Both powder density data and chemical assays indicate slight excesses of silicon over stoichiometry for most of the silicide pressings. This may be accounted for by allowances for the presence of some SiO_2, but it also could indicate that some of the low strengths were due to the presence of free silicon. For this reason, additional modulus-of-rupture data should be obtained for the promising silicides, and for $TaSi_2$ in particular.

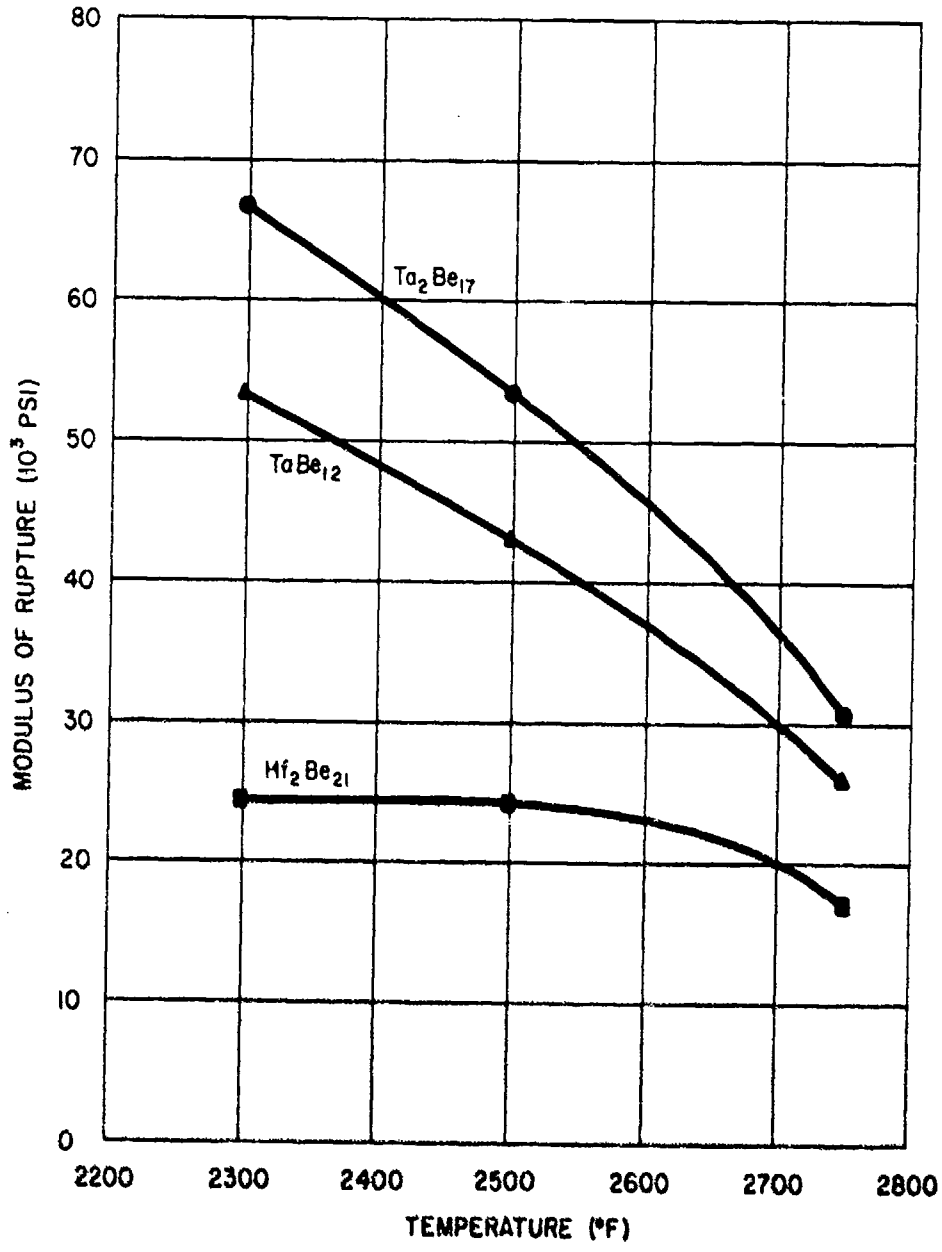

Fig. 12 - Strength of Various Beryllides

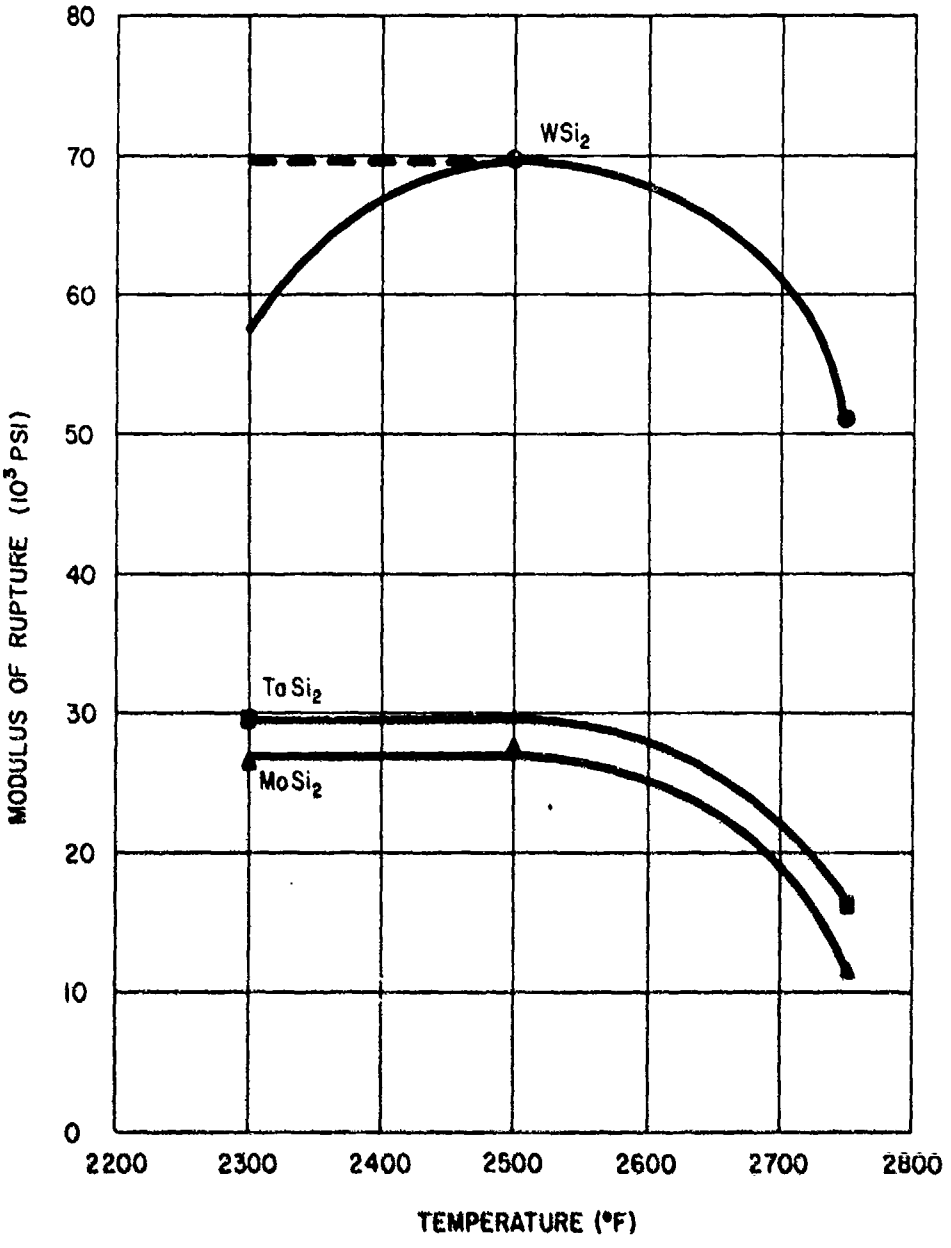

Fig. 13 - Strength of Various Silicides

2. Impact Resistance

The impact resistance of some of the compounds under investigation was measured at room temperature, 2500°, and 2750°F, using a type of test which is classified as a "simple beam test". In this type of test, the specimen is held as a simple horizontal beam and is broken by a single blow delivered midway between the specimen supports. An advantage of this type of test is that a value point is obtained for each specimen tested, as opposed to (for example) the drop impact method where several samples may be required for a single value point.

The testing apparatus was of the pendulum type, of rigid construction as contrasted with a simple pendulum, and was designed and built under Brush supervision. A graduated scale that indicated inch-pounds and fractions thereof allowed the impact energy to be read directly. The apparatus, the calibration of the apparatus, the procedure, and the specimen cross-section used in the test conformed to the ASTM Designation: E23-47T, latest revision, February 1948.

The dimensions of the specimens used were 0.394 x 0.394 x 2 1/4 inches. The velocity of impact was five feet per second, and the maximum kinetic energy given the striker was 8 inch-pounds.

Graphite (type CS) impact specimens were used both to calibrate this equipment and for comparison of the results obtained with results from other methods of measuring impact resistance. The results from this comparison are given in Table IX. These results show that the impact strength of graphite falls within a fairly narrow range, regardless of the test method. The somewhat higher strengths obtained with the Sonntag machine may be due to the higher impact velocity which was inherent with the machine used. In essence, the method used for the beryllides and silicides was a scaled-down Sonntag method, yet more sensitive than the Sonntag method.

In the test, the specimen was mounted on the specimen support and, for the elevated temperature measurements, an oxyacetylene flame was used to bring the specimen to the temperature of the test. In order to obtain the desired temperatures and at the same time avoid breaking the samples due to thermal shock, a broad flame which enveloped the sample and the support was used initially. As the specimen and surroundings absorbed heat, the flame was enriched with oxygen, narrowing the envelope and necessitating a back-and-forth motion of the flame over the sample and support to achieve temperature. An optical pyrometer was used to measure the temperature. The pyrometer was oriented 180° from the torch so that the point at which the temperature

TABLE IX

ROOM TEMPERATURE IMPACT TESTS ON GRAPHITE SPECIMENS

Type of Test	Impact Radius (inches)	Velocity of Impact (ft/sec)	Impact Energy (in. -lb)
Ball (Simple Pendulum)	~1/2	3.6	0.60-0.65
Drop-Impact	1/8	5.5	0.60-1.40
Sonntag (Pendulum)	ASTM Striker	11	1.2-1.8
Pendulum: Brush Machine (Repeated Blow)	ASTM Striker	2	0.50-1.0
Pendulum: Brush Machine (Strike-Thru Method)	ASTM Striker	2	0.90-1.45
Pendulum: Brush Machine (Strike-Thru Method)	ASTM Striker	5	0.85-1.03

was measured was actually the cold edge of the gradient across the specimen. Temperature control is at present the most serious problem in this measurement, and other methods of obtaining temperature are being investigated.

The specimen was raised to a temperature 100°F above the test temperature to allow for cooling of the specimen in the interim between removal of the flame and impact. The flame was removed, the specimen impacted, and the impact energy read on the dial. The results obtained are given in Table X.

The impact resistance of Ta_2Be_{17} increases slightly with temperature. The specimen which gave the high value at 2500°F did not break on the first or second attempts, but broke on the third attempt. There is an indication here that considerable impact resistance is possible for this material; studies are necessary to determine the factors which affect this property. For $TaSi_2$, the impact energy was the same at 2500° and 2750°F and was slightly higher at these temperatures than at room temperature. The results obtained for WSi_2 remained fairly constant throughout the temperature range used. The highest value at 2750°F is probably not representative, since the pendulum was seen to waver after impact.

Comparison of the values in Tables IX and X shows that the impact resistance of the intermetallic compounds tested is somewhat greater than the impact resistance of graphite (grade CS) at room temperature.

3. Thermal Shock

Semiquantitative thermal-shock data have been obtained for $TaBe_{12}$, Ta_2Be_{17}, Hf_2Be_{21}, $MoSi_2$, $TaSi_2$, and WSi_2. It was originally planned to carry out the thermal-shock tests using an oxygen-gas or oxygen-acetylene flame to heat the samples to 2750°F, followed by forced-air cooling to approximately 400° - 500°F. An oxygen-gas torch was used in the preliminary tests. In order to reach a temperature of 2500° to 2750°F, an oxygen-rich flame was required. This heated a very narrow section of the test sample, the really hot portion of the flame being essentially a point. This method proved too stringent, since most of the specimens tested failed during the heating part of the cycle, in many instances during the first heat-up; therefore, this method of testing was discontinued. A modification of this method which would allow a larger section of the specimen to be uniformly heated may prove to be satisfactory for making thermal shock measurements.

TABLE X

IMPACT TESTS ON INTERMETALLIC COMPOUNDS

Specimen	% of Absolute Density	Temperature (°F)	Impact Energy (in.-lb)
Ta_2Be_{17} - H. P. 426	99.8	Room	1.65
	99.4	Room	1.55
	100.	2500	6.1
	100.	2500	2.65
	96.6	2750	4.0
$TaSi_2$ - H. P. 376	100.	Room	0.85
	100.	Room	1.8
	100.	2500	2.3
	100.	2750	2.35
	100.	2750	2.5
WSi_2 - H. P. 306	100.	Room	2.5
H. P. 306	100.	Room	2.55
H. P. 306	100.	2500	2.5
H. P. 300	100.	2500	2.6
H. P. 300	100.	2750	2.22
H. P. 306	100.	2750	4.25

In view of the above experience, a bottom-loading muffle furnace was used to heat the specimens for this test. BeO supports were arranged so that the ends of the specimens rested on these supports. A specimen was brought to temperature (2500°F) within the furnace, the furnace bottom was lowered, and the center of the sample was cooled by a compressed-air jet to below red heat.

The specimen designs which have been used in these tests are shown in Figure 14. Samples of $TaBe_{12}$, Ta_2Be_{17}, and $MoSi_2$ of both designs have successfully withstood 50 cycles with no failures. Only round specimens of $TaSi_2$, WSi_2, and Hf_2Be_{21} were tested; these materials also passed the 50-cycle test. A cycle consisted of 2 1/2 to 3 minutes for heating and 30 seconds for cooling. When round samples were cooled, a section about 1/2 inch long in the center of the sample was brought below red heat in approximately 15 seconds (indicated cooling rate of 120°F/sec.); after 30 seconds, about two-thirds of the sample (all but the ends resting on the BeO supports) was below red heat. For the flat samples, a section about 3/4 inch long was below red heat in about 5 seconds (indicated cooling rate of 300°F/sec.). After 10 to 15 seconds, the entire reduced center section was below red heat; after 30 seconds, portions of the end sections were below red heat.

Before the tests, samples of $TaBe_{12}$, Ta_2Be_{17}, and $TaSi_2$ were annealed at 2700°F for 3 hours in vacuum so that a comparison could be made between annealed and unannealed samples. Since all the samples passed the 50-cycle test, effects of annealing, if any, were not observed. The samples were dye-checked after 50 cycles, with no evidence of cracking, spalling, or other deteriorating effects being noted in any case. These results, coupled with observations from other high-temperature measurements where thermal shock conditions were present (oxidation, transverse-rupture, etc.) indicate that the compounds tested are resistant to thermal shock when large temperature gradients are involved.

In some of the related high-temperature measurements performed in this laboratory, it has been observed that some of the intermetallics fail, probably due to thermal shock, when the temperature of these intermetallics is raised to approximately 1600°F and cooled. Specimens of $TaBe_{12}$, Ta_2Be_{17}, $MoSi_2$, $TaSi_2$, and WSi_2 which had passed the 50-cycle test (2500°F to below red heat) were checked in this 1600°F-to-below-red-heat range, using the same procedure as for the 2500°F tests. These compounds successfully withstood 25 cycles of testing in this low-temperature range with no evidence of deleterious effects.

Fig. 14 - Typical Thermal Shock Specimens

C. Thermal Properties

1. Thermal Expansion

a. Equipment and Method

The apparatus for the measurement of thermal expansion is illustrated in Figure 15, and a diagram is shown in Figure 16. It utilizes tandem-mounted Gaertner telemicroscopes which allow the dimensional changes of the sample with temperature to be read directly. The furnace is heated by means of six silicon carbide heating elements, which are spaced radially about the specimen chamber. The specimen is situated in the stabilized zirconia chamber such that each squared end can be viewed through the 1/2-inch holes in the sides of the chamber. These holes are aligned with similar holes through the insulation and furnace walls on the other side so that a light outside the furnace on one side illuminates the specimen for viewing with the telemicroscopes at low temperatures. The sight holes are covered with pyrex sight glasses which are sealed with rubber O-rings, making vacuum-tight seals. The temperature of the specimen is obtained with three platinum-platinum, 10% rhodium thermocouples which pass through appropriate holes in the zirconia chamber and are situated approximately 1/4 inch above the specimen. Two are located at opposite ends of the specimen and one at the center. The thermocouple leads pass through Conax fittings at the furnace wall to provide vacuum seals. The test specimens are bars 3 1/4 inches long by 1/2 by 1/4 inch.

The technique used in a determination included an initial outgassing period, with argon being admitted at about 200°F. Each time the temperature and dimensional changes were measured, the temperatures of the three thermocouples were recorded first, followed by a set of three readings with the telemicroscopes, immediately after which the temperatures of the three thermocouples were again recorded. A specimen temperature was taken as the average of the six readings. In general, the six readings varied randomly, and it is thought that the average temperature taken was accurate to within 5°F since the entire range of six readings was seldom greater than 20°F.

The telemicroscopes were read to the nearest 0.0001 inch, this division being read directly with the aid of a vernier scale. The average deviation within a set of three readings was approximately 0.0003 inch at temperatures below 2000°F. The precision was temperature-dependent to the extent that at higher temperatures the specimen emitted light, which decreased the contrast between specimen and background. The measurements taken above 2200°F were made in air to avoid difficulties previously encountered in attempts to reach 2750°F

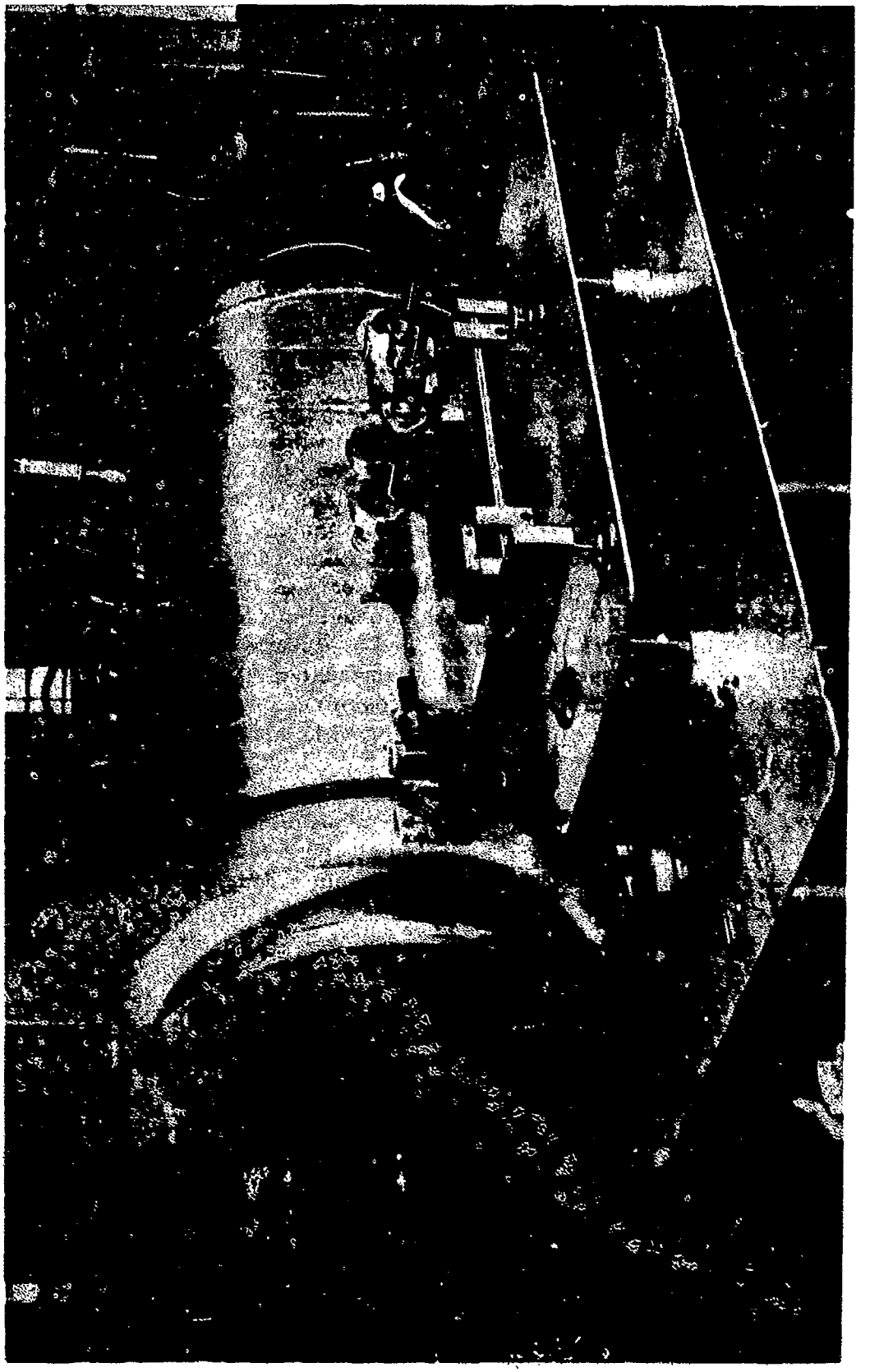

Fig. 15 - Thermal Expansion Furnace

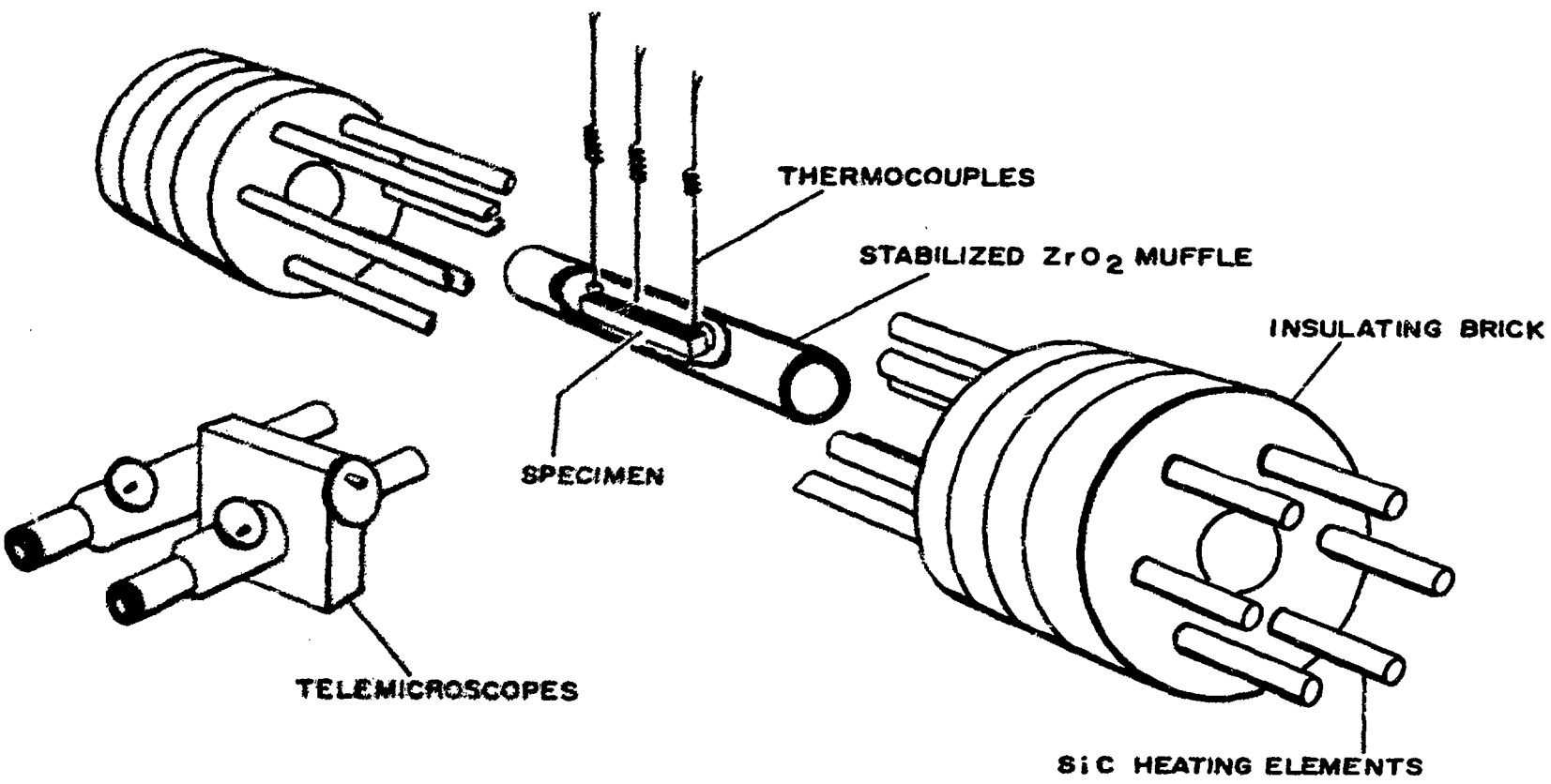

Fig. 16 - Thermal Expansion Furnace (Schematic)

in an inert atmosphere, using silicon carbide heating elements. At the higher temperatures in air, the formation of oxide scale interfered with the measurements, but once an adherent scale formed, the error introduced by further oxidation was minimized. For this reason, the samples were pre-oxidized at 2700°F.

Most of the data reported here were obtained during the heating cycle. When the temperature of a specimen reached the measurement temperature, adequate time was allowed for the attainment of thermal equilibrium in the specimen before measurements were taken. In addition, several datum points were obtained on each specimen during the cooling cycle.

b. Experimental Data and Discussion

To check the validity of the method, the thermal expansion of electrolytic tough pitch copper had been determined to 1800°F.[1]

The data obtained in these measurements agreed well with published values for copper, the average variation being about 3%.

The thermal expansions of Hf_2Be_{21}, Ta_2Be_{17}, $TaBe_{12}$, $MoSi_2$, $TaSi_2$, and WSi_2 are plotted in Figures 17 to 22. The data reported here for Ta_2Be_{17} and $TaBe_{12}$ were determined for a previous program. The mean linear thermal expansion coefficients for these compounds are given in Table XI.

In the case of $TaSi_2$ (Figure 21), when the experiment was made in argon with the sample not preoxidized, the formation of an oxide scale began to affect the expansion measurements at about 1800°F. When the sample was preoxidized, a temperature of 2400°F was reached before oxidation of the sample began to affect the expansion measurements. It will be observed that the curve drawn through the cooling points is parallel to the heating curve, which indicates that the oxide scale is adherent and that it is valid to extrapolate the heating curve to the higher temperatures.

2. Specific Heat

a. Equipment and Procedure

The specific heat of the compounds under investigation has been determined by the adiabatic calorimeter method. In this

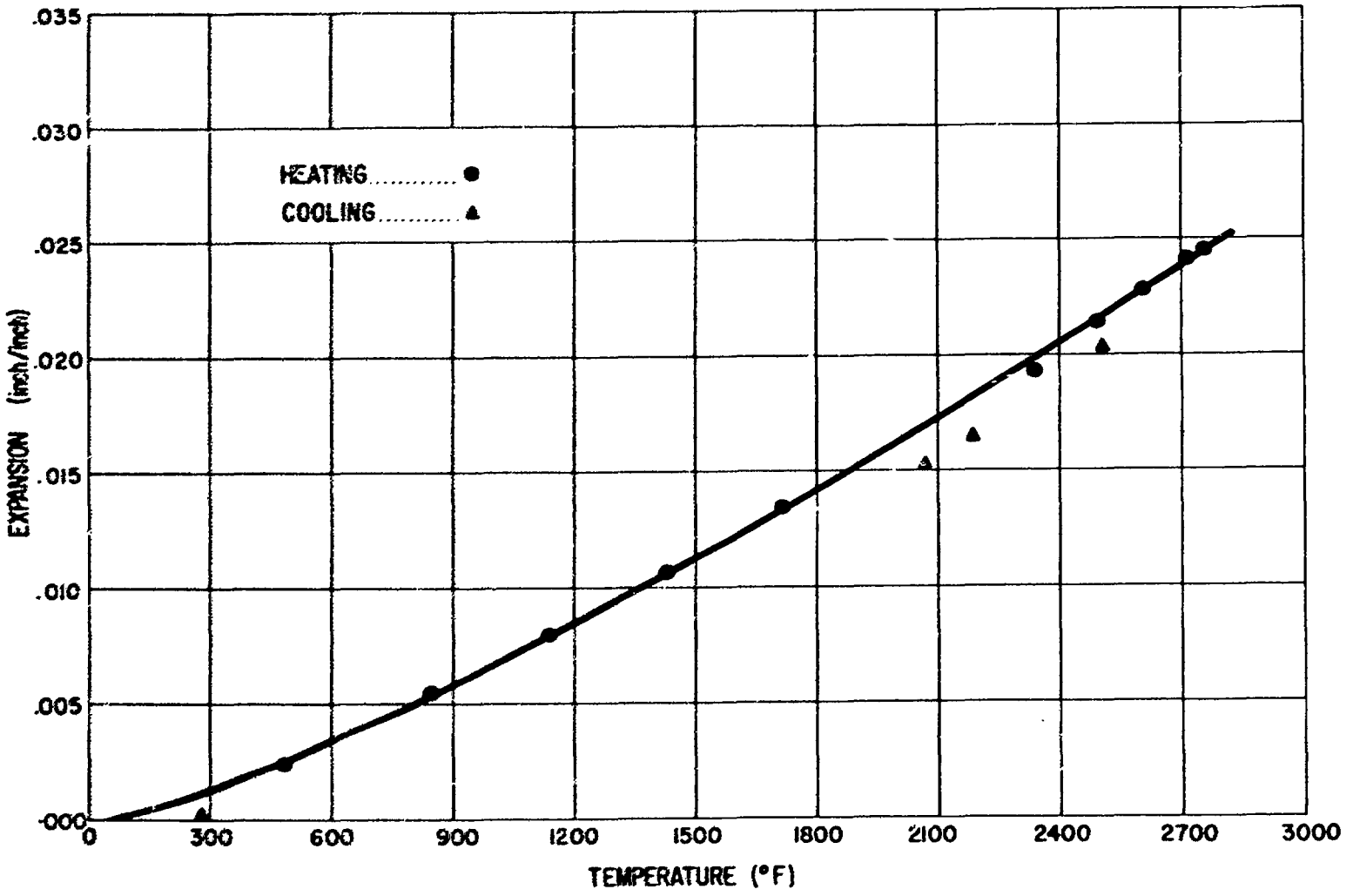

Fig. 17 - Thermal Expansion of Hf_2Be_{21} - H. P. 322

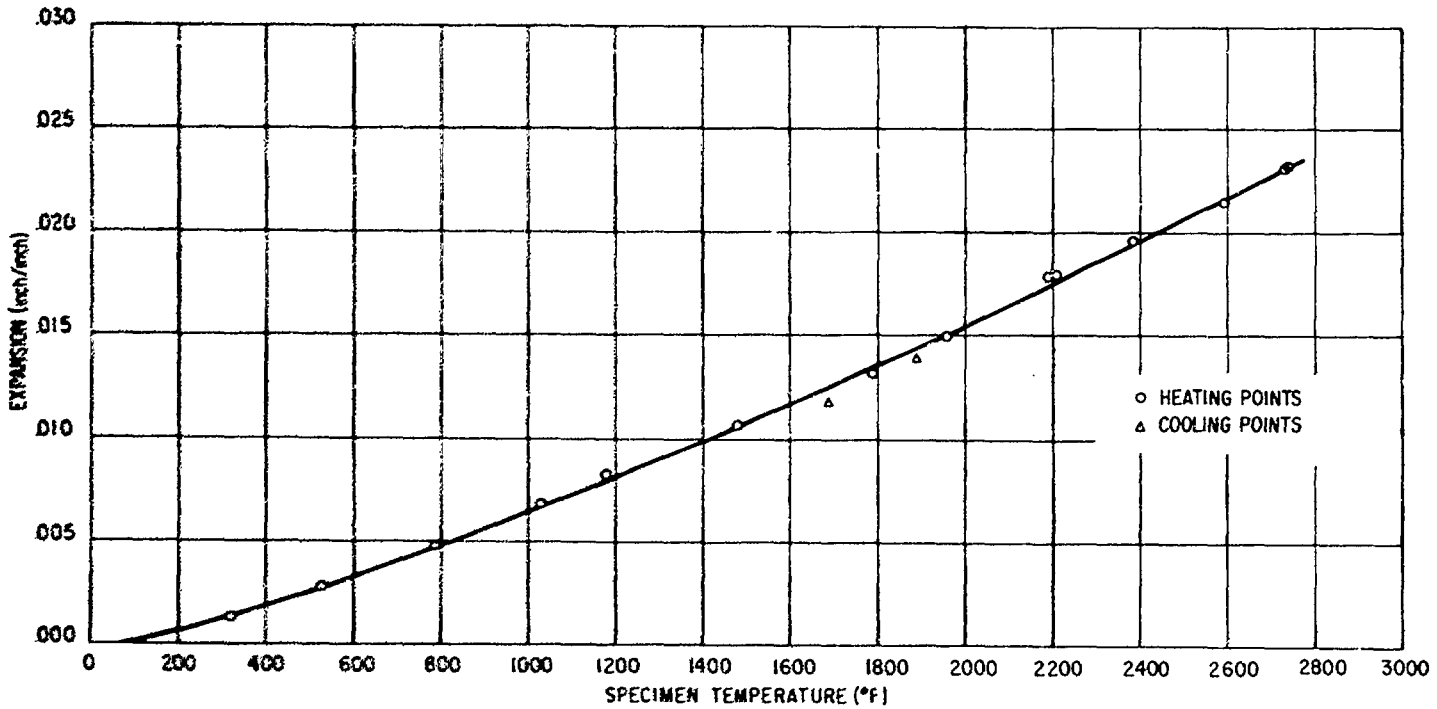

Fig. 18 - Thermal Expansion of Ta_2Be_{17} - H. P. 227

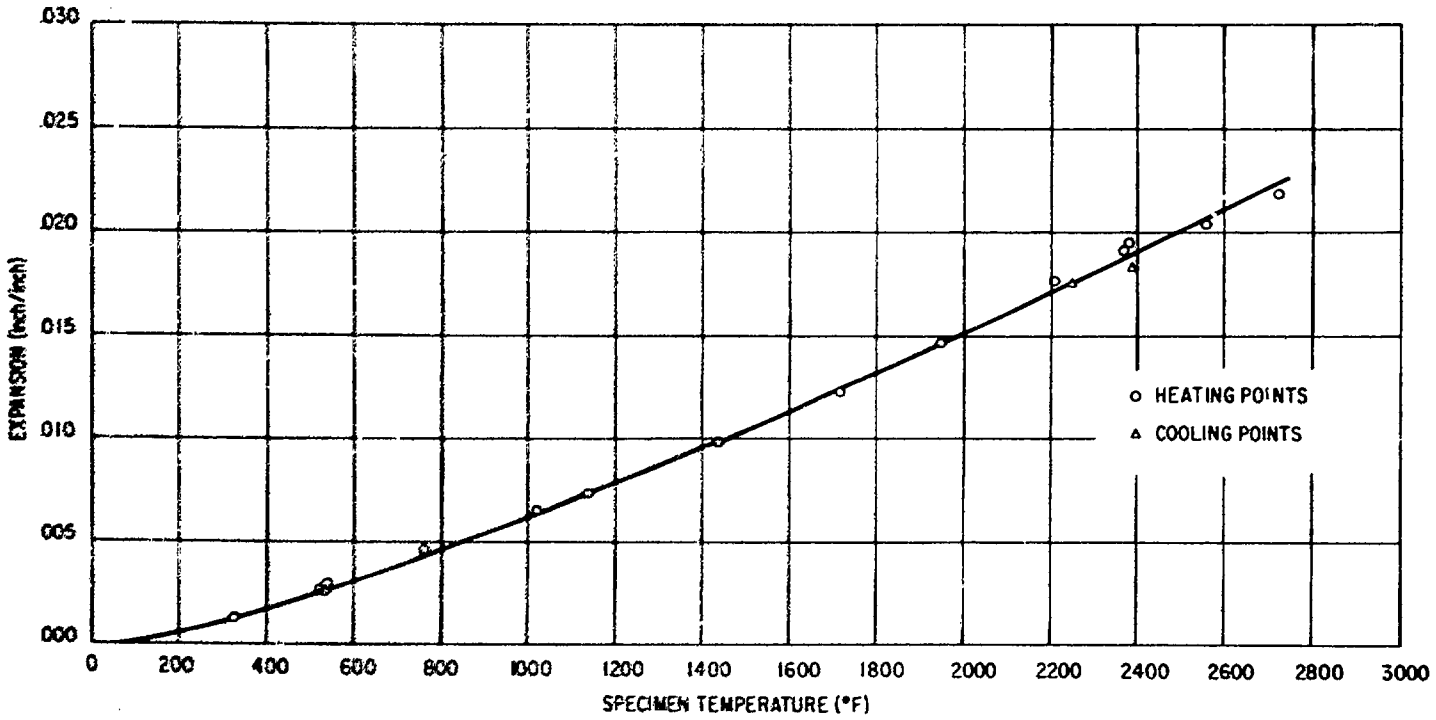

Fig. 19 - Thermal Expansion of $TaBe_{12}$ - H. P. 222

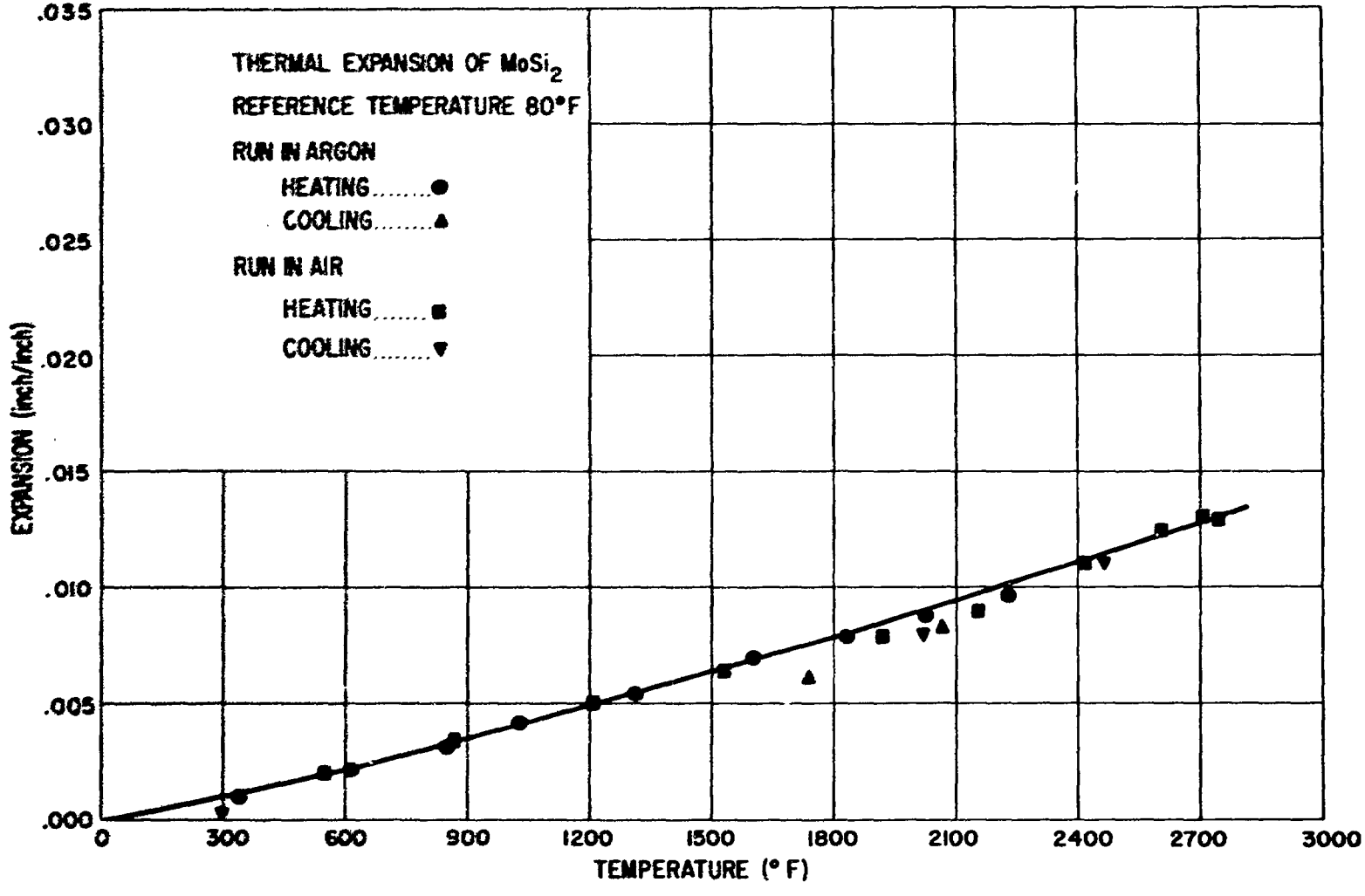

Fig. 20 - Thermal Expansion of $MoSi_2$ - H. P. 305

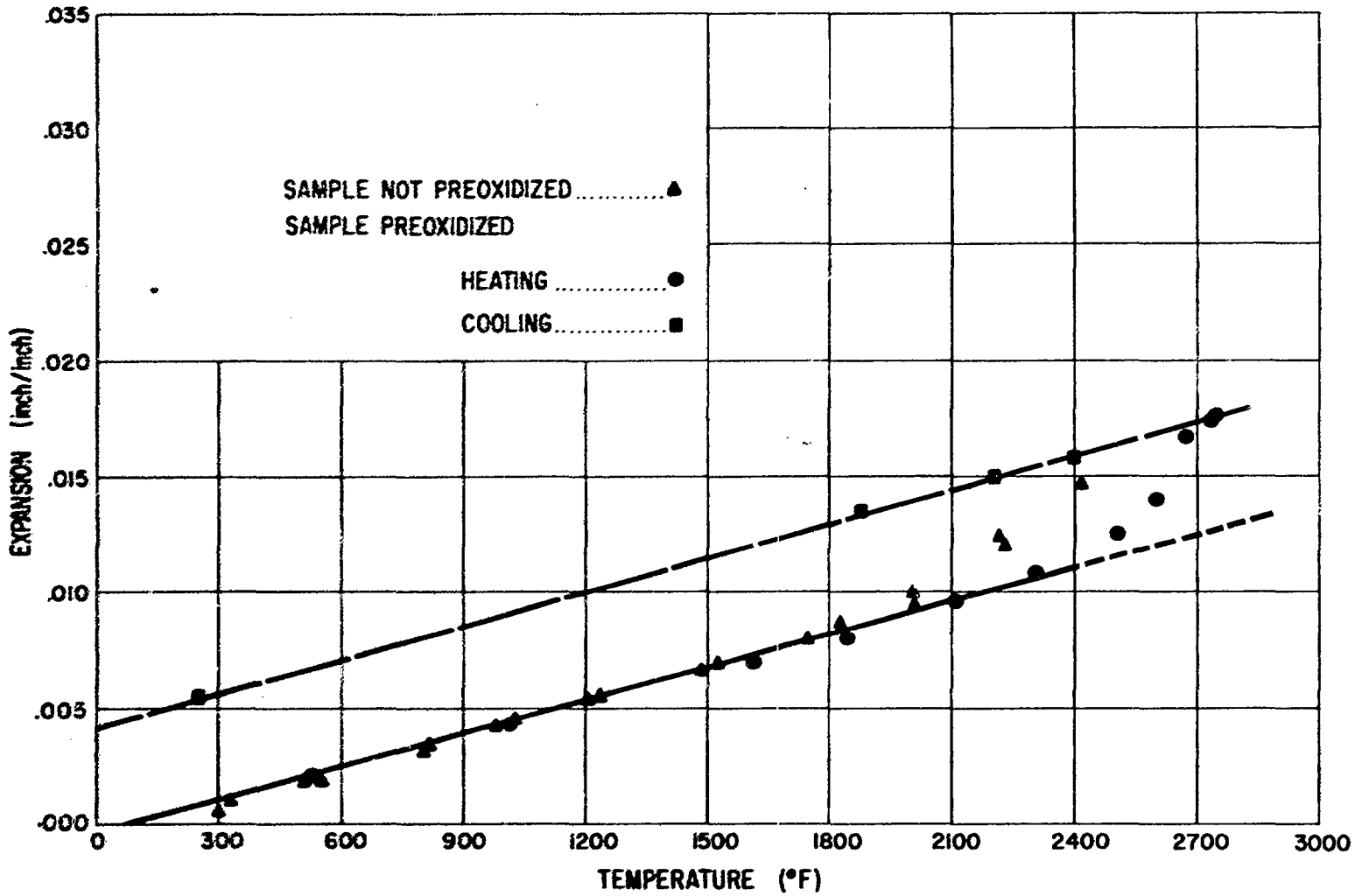

Fig. 21 - Thermal Expansion of $TaSi_2$ - H. P. 301

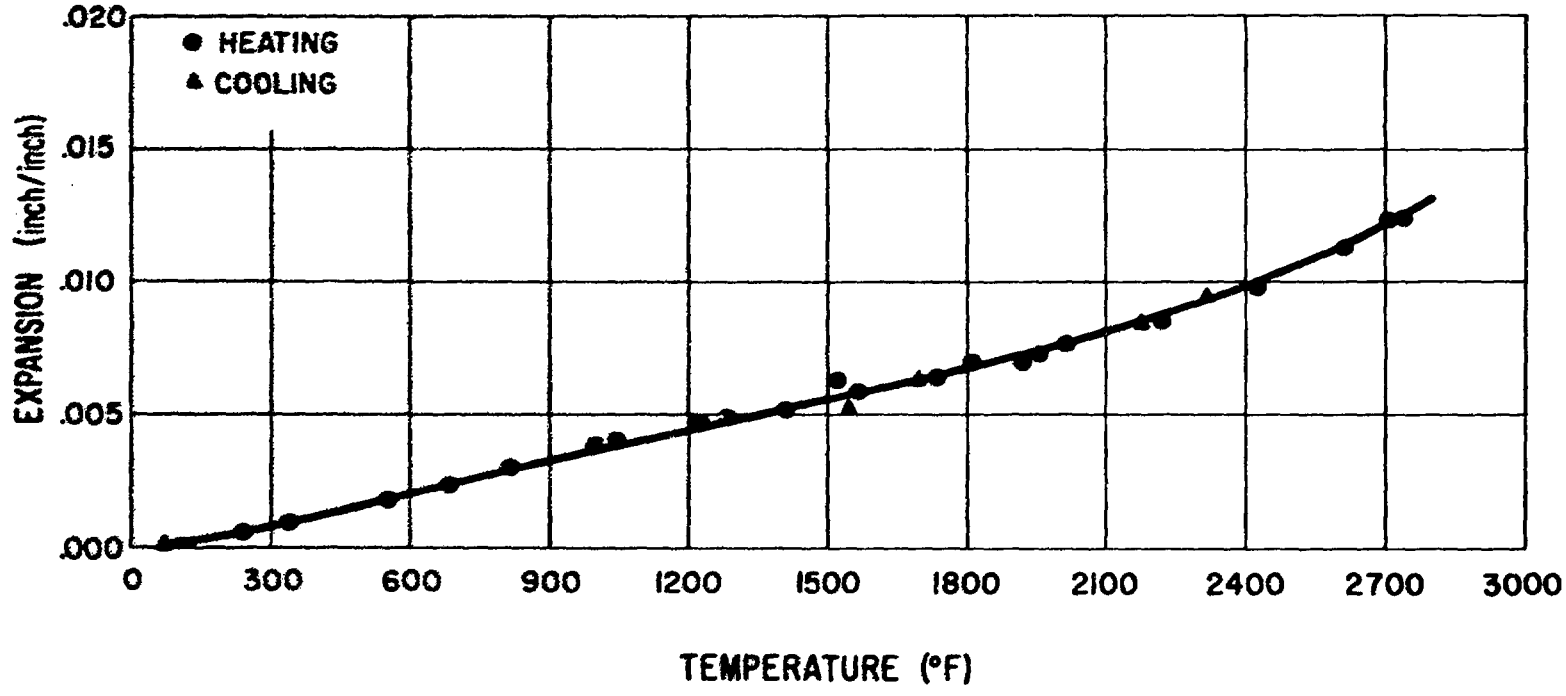

Fig. 22 - Thermal Expansion of WSi_2 - H. P. 347

TABLE XI

MEAN LINEAR THERMAL EXPANSION COEFFICIENTS

Temp Range (°F)	Mean Linear Expansion Coefficients, (10^{-6} in./in./°F)					
	Hf_2Be_{21}	Ta_2Be_{17}	$TaBe_{12}$	$TaSi_2$	$MoSi_2$	WSi_2
80-200	5	6	5	5	4	4
80-400	5.6	5.9	5.3	4.7	3.8	4.0
80-600	6.5	6.2	5.8	4.7	4.0	4.0
80-800	7.1	6.7	6.4	4.7	4.2	4.0
80-1000	7.4	6.8	6.6	4.7	4.3	4.0
80-1200	7.7	7.1	6.9	4.7	4.3	4.0
80-1400	7.9	7.4	7.1	4.7	4.4	4.0
80-1600	8.03	7.56	7.36	4.67	4.41	3.98
80-1800	8.20	7.79	7.61	4.67	4.42	3.98
80 2000	8.39	8.02	7.81	4.67	4.48	3.98
80-2200	8.58	8.20	7.97	4.67	4.58	4.06
80-2400	8.84	8.40	8.14	4.67[a]	4.70	4.20
80-2600	9.05	8.57	8.29	4.67[a]	4.80	4.44
80-2750	9.18	8.72	8.42	4.67[a]	4.91	4.68

[a]Values calculated from extrapolated portion of curve.

method, the change in heat content (enthalpy) of the material is measured and the specific heat is obtained by processing the enthalpy data. The apparatus used is shown in Figure 23 and is schematically represented in Figure 24. The design is basically the same as that used by the Armour Research Foundation.[4]

The apparatus consisted of a furnace and a calorimeter connected by means of a stainless steel tube, with the calorimeter located below the furnace. The furnace was heated by two hairpin-shaped Super-Kanthal elements. These heating elements were symmetrically arranged about a 1 1/2-inch-I. D. aluminum oxide tube, which served as the heating chamber. The furnace was insulated as shown in the schematic diagram. A drop tube was attached to the top of the furnace and aligned with the heating chamber. The calorimeter used was a double-jacketed adiabatic calorimeter made by the Parr Instrument Co., which was modified to meet our requirements. The calorimeter proper was made of stainless steel. Gate valves in the stainless steel connecting tube and on the calorimeter were provided to isolate the calorimeter from the furnace.

The inner chamber of the calorimeter was filled with a measured amount of water. A Beckman thermometer measured the temperature change of the water in this chamber. Adiabatic conditions were effected by maintaining the water in the inner and outer chambers at the same temperature. A second Beckman thermometer was used to control the water temperature in the outer chamber. The temperature of the inlet water to the outer chamber was controlled by means of an adjustable water heater. Stirrers were provided to circulate the water in both chambers.

The sample was suspended from a length of platinum wire, the other end of which extended up into the drop tube where it was attached to an aluminum plug. This plug, in conjunction with an air-valve outlet at the bottom of the drop tube, controlled the drop rate of the sample.

For a measurement of enthalpy, the sample was suspended in the furnace at the measurement temperature and allowed to attain thermal equilibrium. Specimen temperature was determined by comparing the readings from three platinum-platinum, 10% rhodium thermocouples located such that the temperature of a 2 1/2-inch longitudinal zone in which the specimen was suspended could be

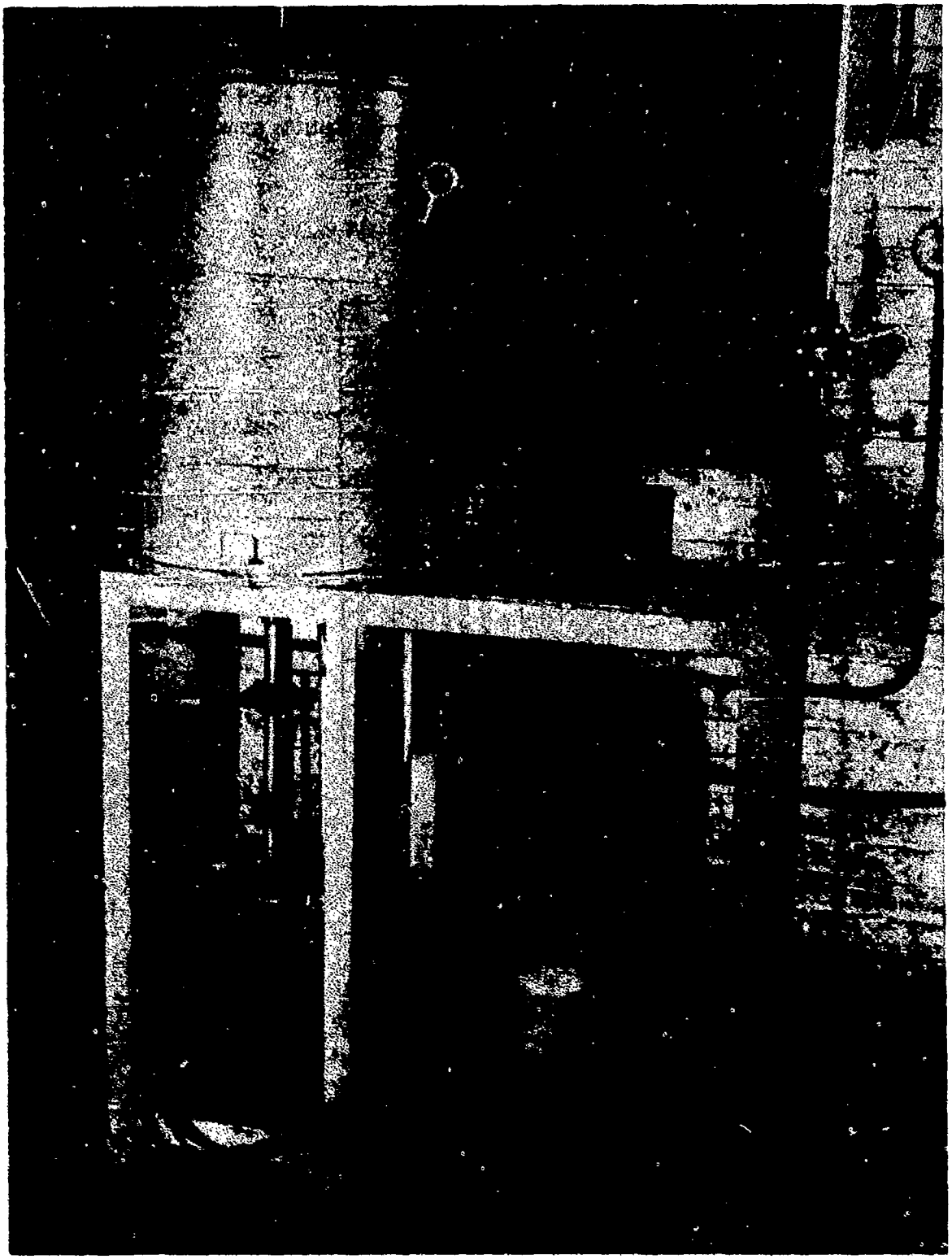

Fig. 23 - Specific Heat Apparatus

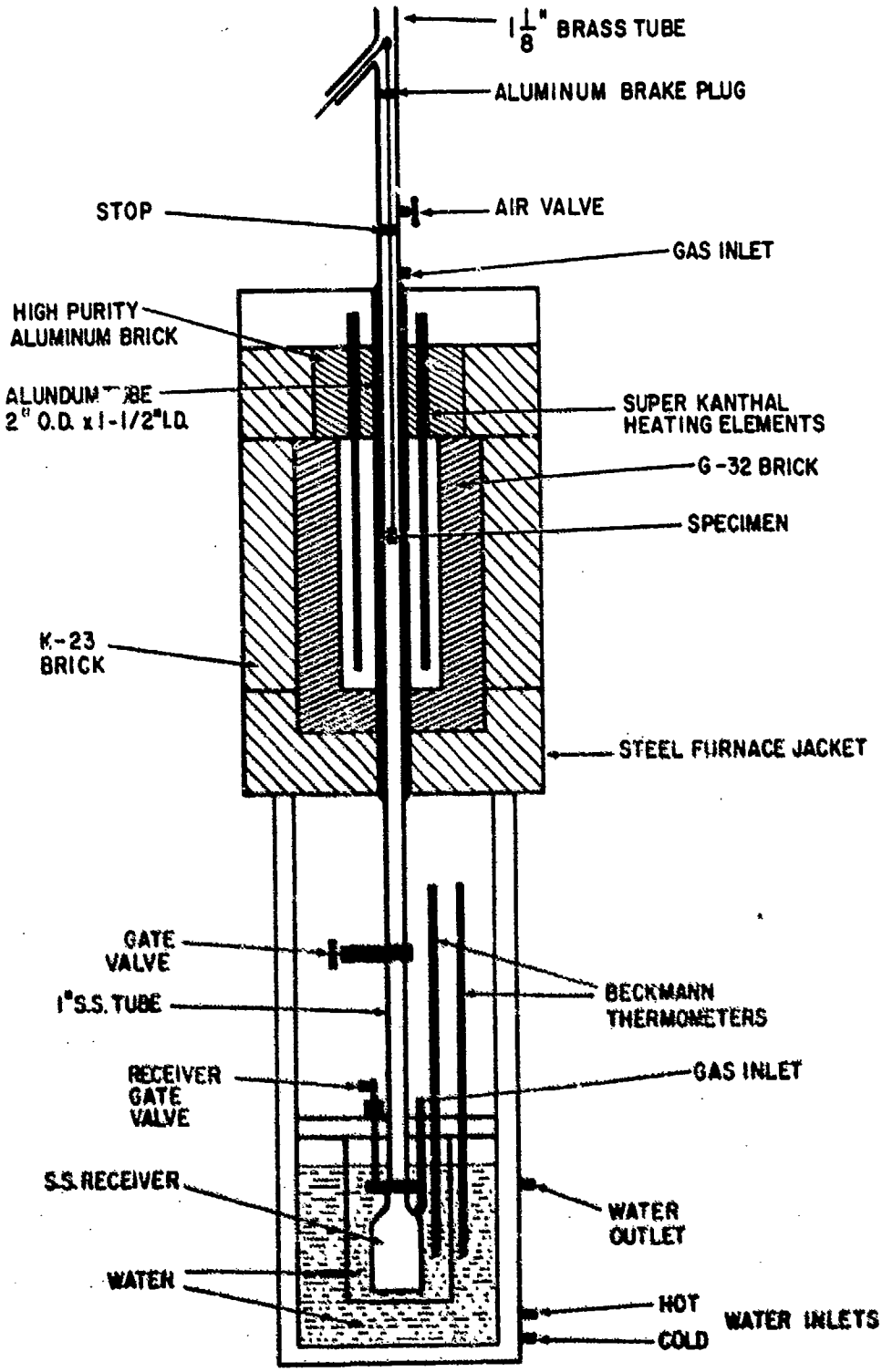

Fig. 24 - Specific Heat Apparatus (Schematic)

accurately controlled. When thermal equilibrium was attained, the gate valves isolating the calorimeter from the furnace were opened, the sample dropped into the stainless steel receiver, and the gate valves closed. The temperature rise in the inner chamber was measured.

The change in heat content (ΔH) of the material was calculated from the known sample weight, the heat capacity of the calorimeter, and the observed temperature rise in the calorimeter.

b. Experimental Data and Discussion

The equipment was checked by measurements of the enthalpy of copper from 830° to 1724°F and the enthalpy of nickel from 379° to 2392°F. Selected values of the enthalpy data obtained are compared in Table XII with the values obtained for these metals by Fieldhouse et al.[4] The agreement in the enthalpy values from the separate determinations is excellent.

Enthalpy as a function of temperature was determined for Hf_2Be_{21}, Ta_2Be_{17}, $MoSi_2$, $TaSi_2$, and WSi_2. The data obtained from these measurements, along with data for $TaBe_{12}$ and $ZrBe_{13}$ previously obtained for another project, are plotted in Figure 25. The values in Table XIII were taken from these plots to allow comparisons of enthalpy values at the same temperature. The equation which expresses the enthalpy change as a function of temperature as observed in these measurements was found to be

$$\Delta H = a + bT + cT^2 \qquad (1)$$

The values for the constants, a, b, and c, for the intermetallic compounds and for copper and nickel are given in Table XIV. T is in degrees Fahrenheit.

The relationship between enthalpy and heat capacity is given by

$$C_p = \left(\frac{\partial(\Delta H)}{\partial T}\right)_p \qquad (2)$$

Substituting equation (1) and differentiating gives

$$C_p = b + 2cT \qquad (3)$$
$$= b + c'T$$

TABLE XII

ENTHALPIES OF COPPER AND NICKEL -
COMPARISON OF BRUSH AND ARMOUR VALUES

Specimen Temp. (°F)	ΔH^a (Btu/lb)			
	Copper		Nickel	
	Armour[4]	Brush	Armour[4]	Brush
900	--	78.0	--	98.0
1100	98.0	99.0	126.0	124.0
1300	120.5	121.0	152.0	150.0
1500	143.5	143.0	178.0	176.0
1700	167.5	167.0	206.0	204.0
1900	193.0	--	234.0	232.0
2100			264.0	261.0
2300			296.0	290.0
2500			329.0	--

[a]These data were interpolated from enthalpy plots and are rounded off to 0.5 Btu/lb.

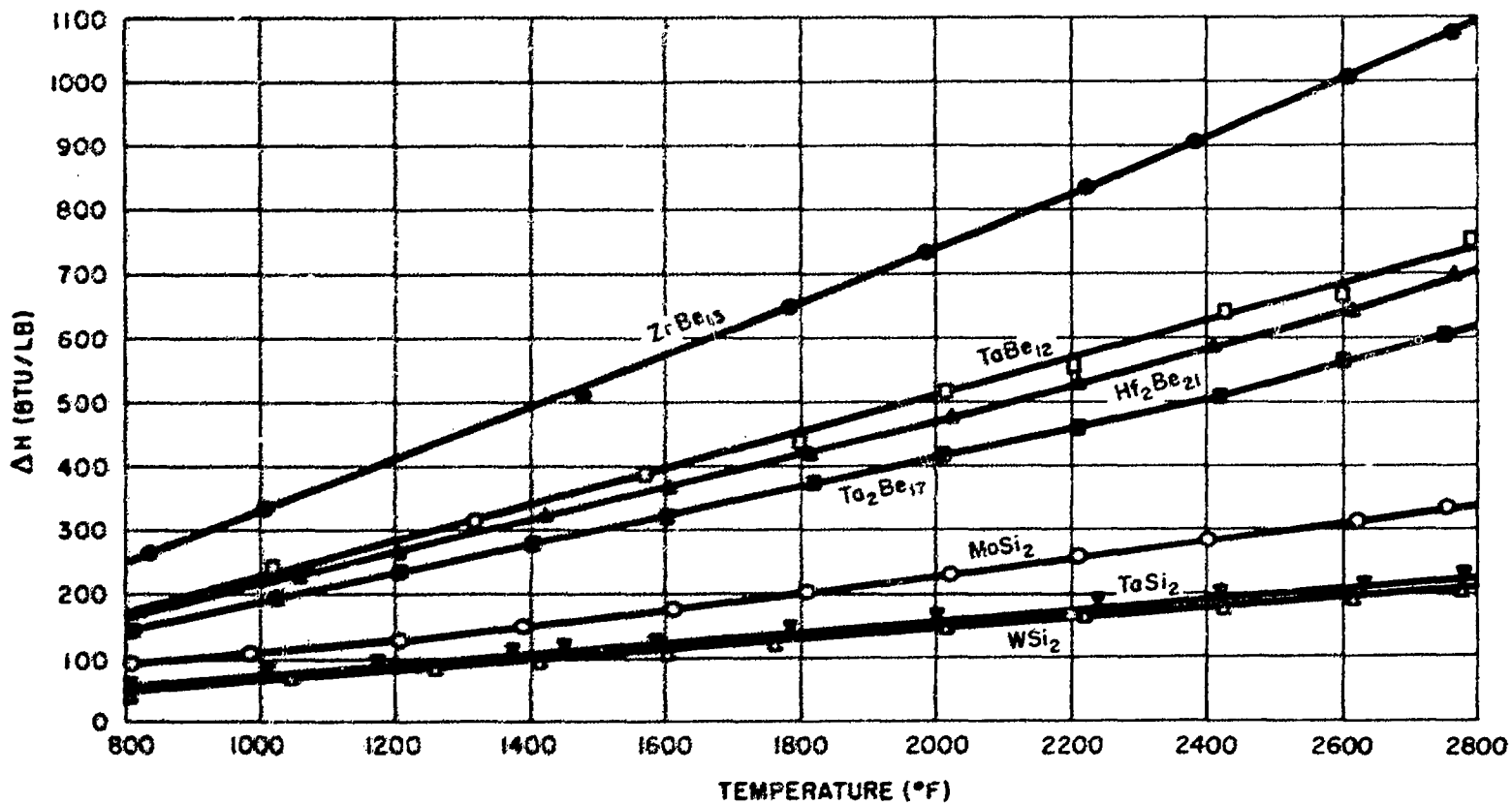

Fig. 25 - Enthalpy Values for Various Intermetallic Compounds

TABLE XIII

SUMMARY OF ENTHALPY DATA

Temp. (°F)	ΔH (Btu/lb)						
	$TaBe_{12}$	Ta_2Be_{17}	Hf_2Be_{21}	$ZrBe_{13}$	$MoSi_2$	$TaSi_2$	WSi_2
850	177	155	173	265	90	56	53
1000	220	182	210	326	106	68	64.5
1200	278	230	260	407	128.5	84.5	81
1400	334	273	312	488	152	101.5	96
1600	390	320	362	570	175.5	118	113
1800	448	360	410	647	201	135	129
2000	507	408	463	730	228	152	145.5
2200	562	456	518	825	257	169	151.5
2400	620	503	575	905	284	186	178
2600	680	559	638	998	310.5	203.5	195
2750	723	600	688	1074	330	216	207

TABLE XIV

ENTHALPY TEMPERATURE COEFFICIENTS

$\Delta H = a + bT + cT^2$

Material	Temperature Range (°F)	a	b	c x 10^5
Copper	783-1724	-3.509	0.08097	1.118
Nickel	379-2392	-9.382	0.1153	0.6401
Hf_2Be_{21}	827-2769	-7.795	0.20658	1.621
Ta_2Be_{17}	825-2750	-16.980	0.18660	1.3351
$TaBe_{12}$	788-2797	-39.01	0.2537	0.8448
$TaSi_2$	812-2782	-9.582	0.07592	0.2488
$MoSi_2$	795-2757	-1.758	0.09920	0.8008
WSi_2	809-2769	-13.962	0.07807	0.094826

Thus, the specific heat is a linear function of temperature at the temperatures measured, as expected. The values for b and $c' = 2c$ are listed in Table XV. The curves expressing the variation of specific heat with temperature as calculated from equation (3) are shown in Figures 26 - 31, and are reproduced in Figure 32 to facilitate comparisons.

3. Thermal Conductivity

a. Equipment and Procedure

The apparatus used for the thermal conductivity measurements employed the radial heat flow method developed by R. W. Powell. The method consisted of measuring the radial flow of heat in a hollow cylindrical specimen by determination of the relationship between the heat equivalent of the electrical energy input and the radial temperature drop across the specimen. The design is basically the same as that used by the Armour Research Foundation.[5]

The apparatus, pictured in Figure 33 and diagramed in Figure 34, consisted of a 4-inch-I.D. molybdenum-wound core surrounded by insulating brick and contained in a steel jacket with provisions for vacuum or inert atmosphere. This core surrounded the specimen assembly and was used for heating and maintaining the specimen at the desired temperature for the determination.

A specimen assembly consisted of five vertically stacked hollow cylinders, each 2 5/8 inches O.D. and 1 inch high and having a 1/4-inch bore concentric with the axis. The 1/4-inch bore was to accommodate a small heater by means of which a temperature drop was imposed across the radius of the specimen. Each disc contained eight longitudinal holes of 3/32-inch diameter. Four of these holes were located 90 degrees apart on a 1/2-inch-diameter circle concentric with the specimen axis. The remaining four holes were located 90 degrees apart on a 2 1/4-inch-diameter circle. These eight holes were for the accommodation of thermocouples. Four of the holes which lay 180 degrees apart were used for measuring the radial temperature drop in the center disc, or test section. Of the four remaining holes (which lay 90 degrees with respect to those holes containing the test-section thermocouples), one pair was used for measuring the temperature gradient in the top disc, while the other pair was employed for measuring the temperature gradient in the bottom disc. These latter two pairs of thermocouples provided a means of measuring the longitudinal heat flow. In order to minimize any tendency toward longitudinal heat flow,

TABLE XV

SPECIFIC-HEAT TEMPERATURE COEFFICIENTS

$C_p = bT\ c'T$

(where C_p = Btu/lb °F and T = °F)

Material	Temperature Range (°F)	b	$c' \times 10^5$
Copper	783-1724	0.08097	2.236
Nickel	379-2392	0.1153	1.280
Hf_2Be_{21}	827-2769	0.20658	3.242
Ta_2Be_{17}	825-2750	0.18660	2.6702
$TaBe_{12}$	788-2797	0.2537	1.6896
$TaSi_2$	812-2782	0.07592	0.4976
$MoSi_2$	795-2757	0.09920	1.6016
WSi_2	809-2769	0.07807	0.1895

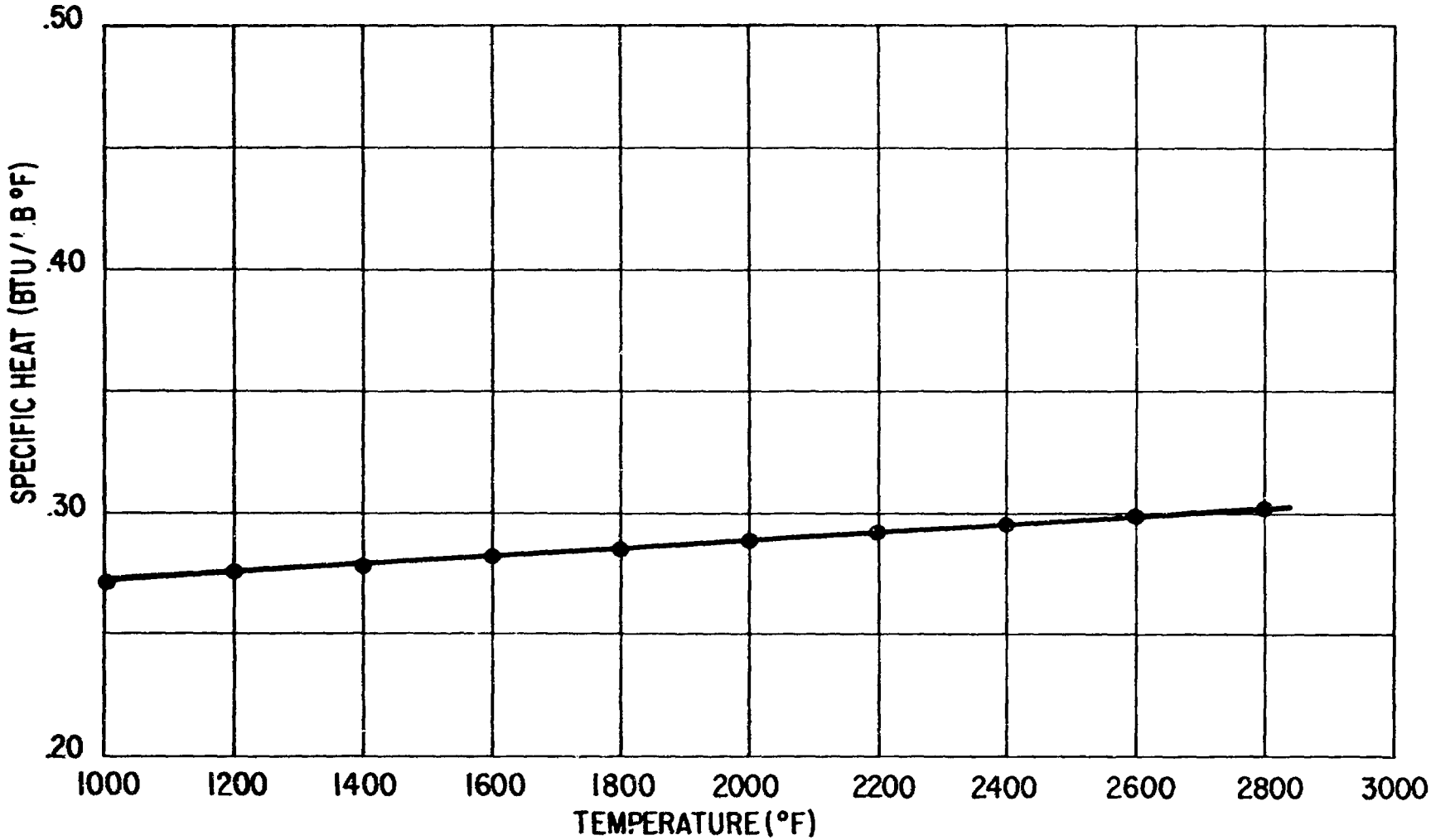

Fig. 26 - Specific Heat of $TaBe_{12}$

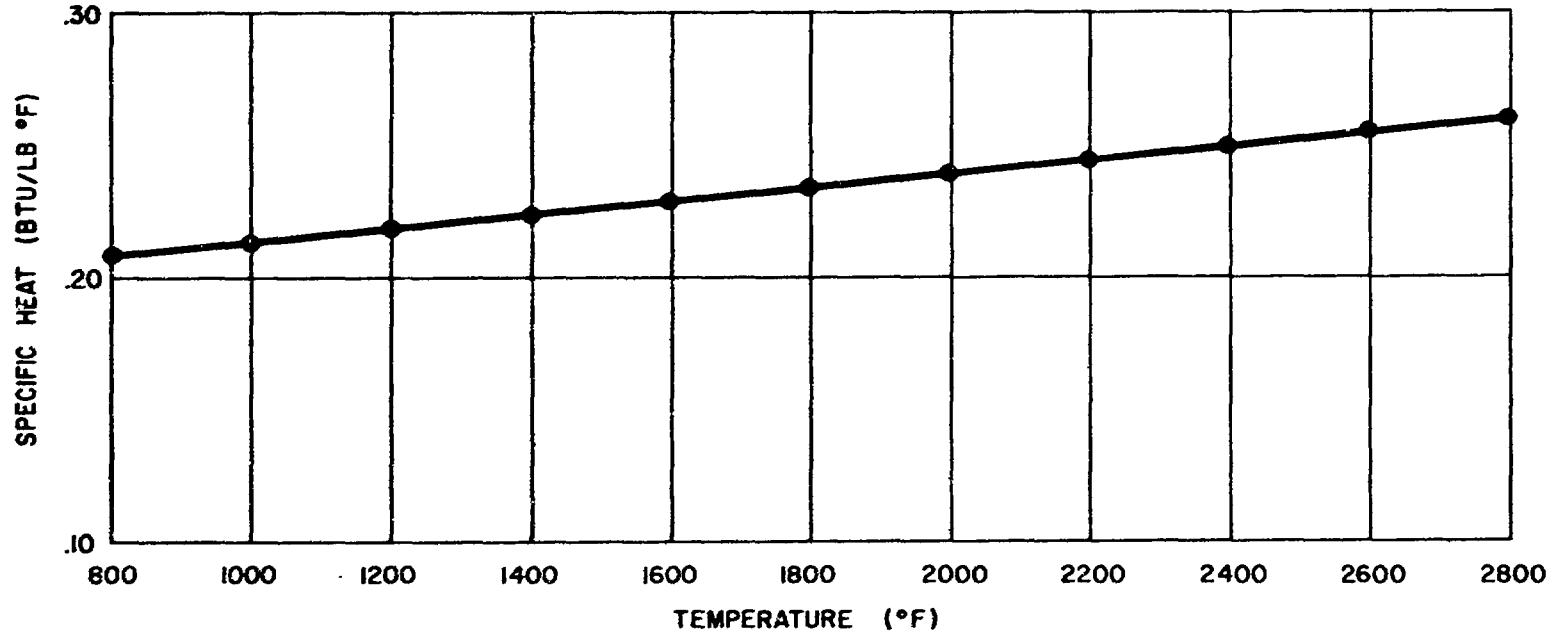

Fig. 27 - Specific Heat of Ta_2Be_{17}

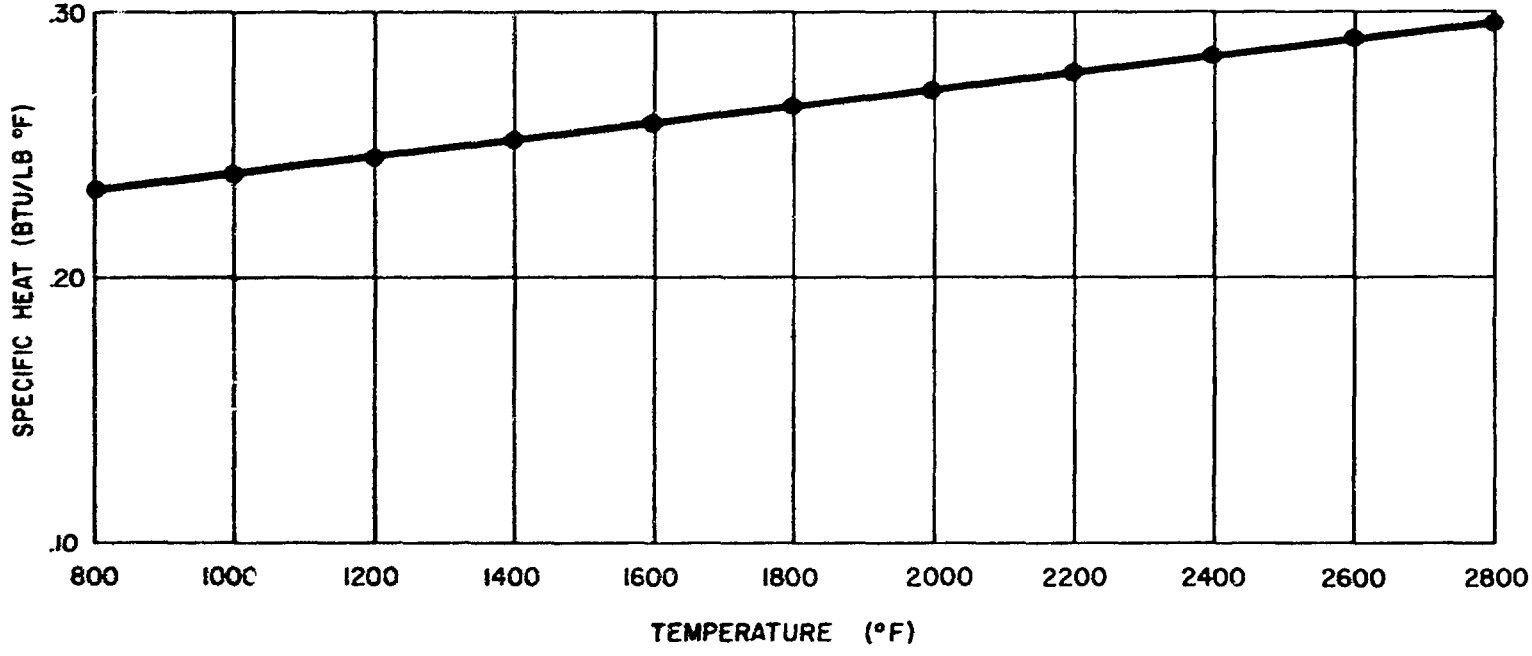

Fig. 28 - Specific Heat of Hf_2Be_{21}

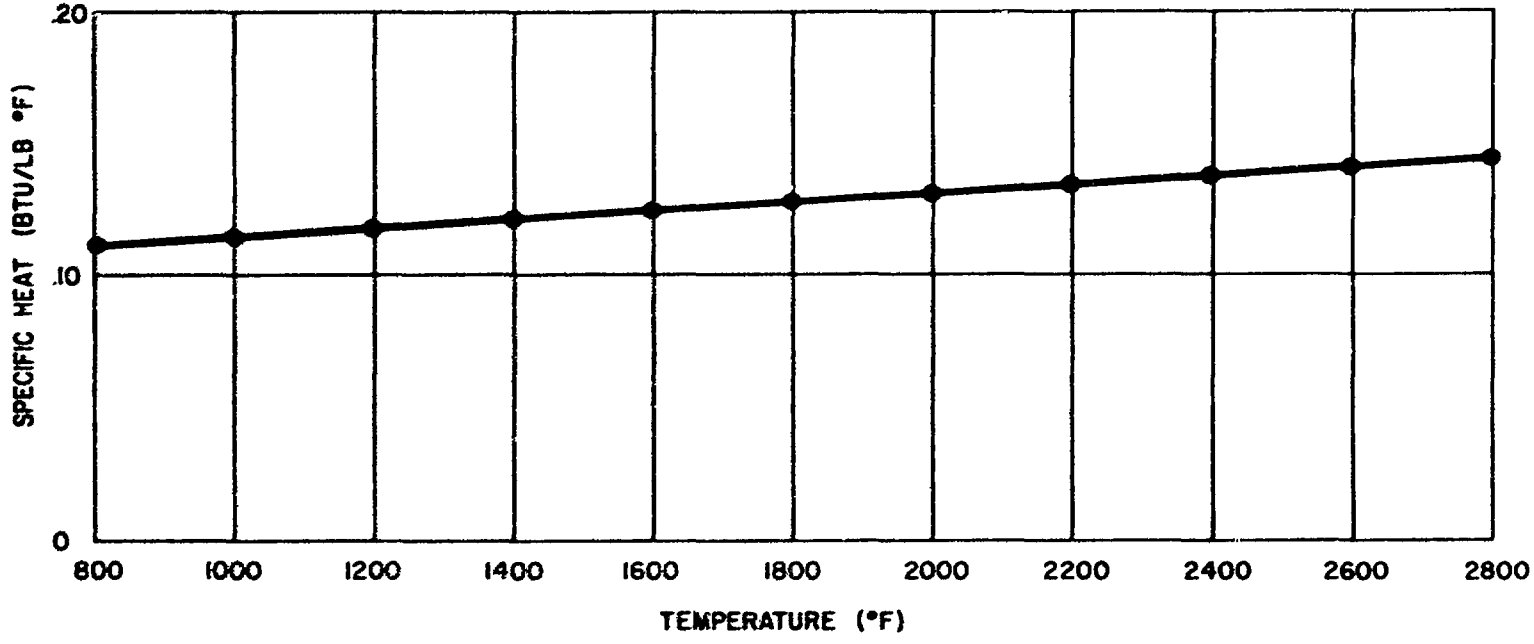

Fig. 29 - Specific Heat of $MoSi_2$

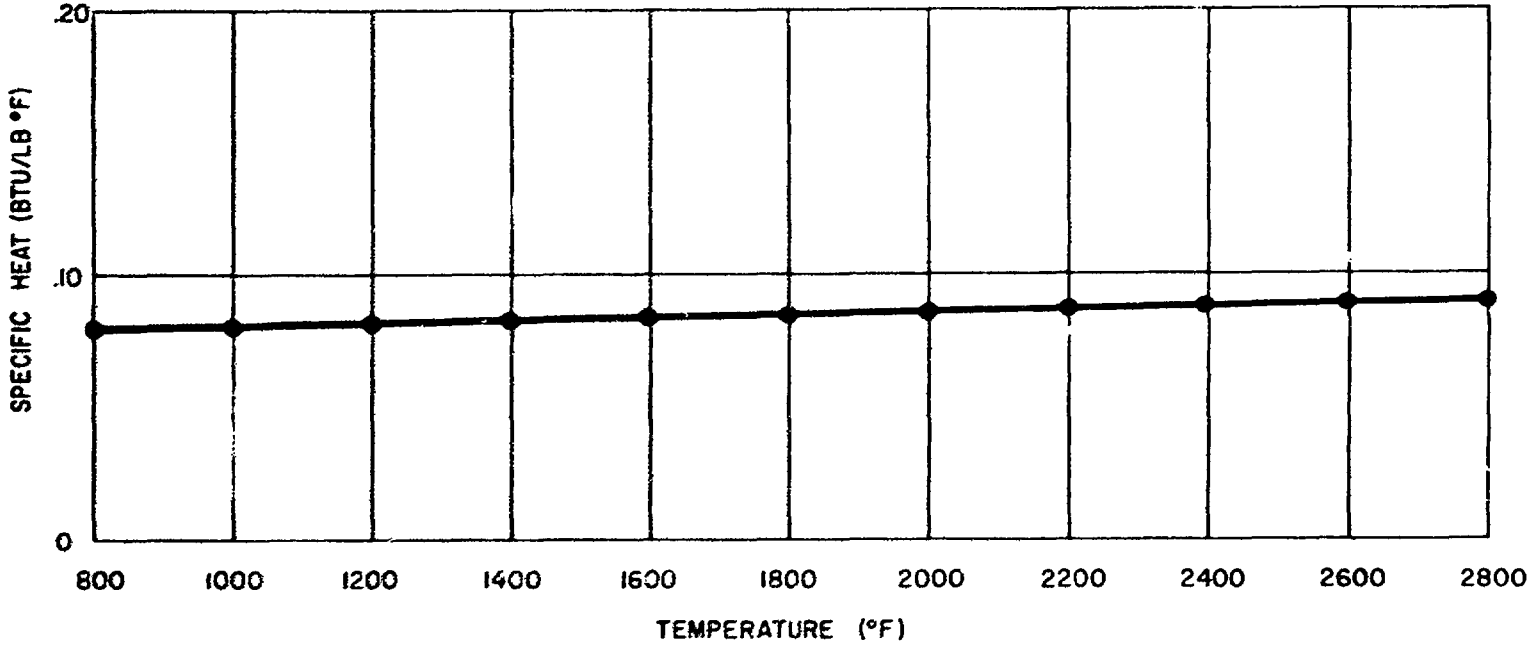

Fig. 30 - Specific Heat of $TaSi_2$

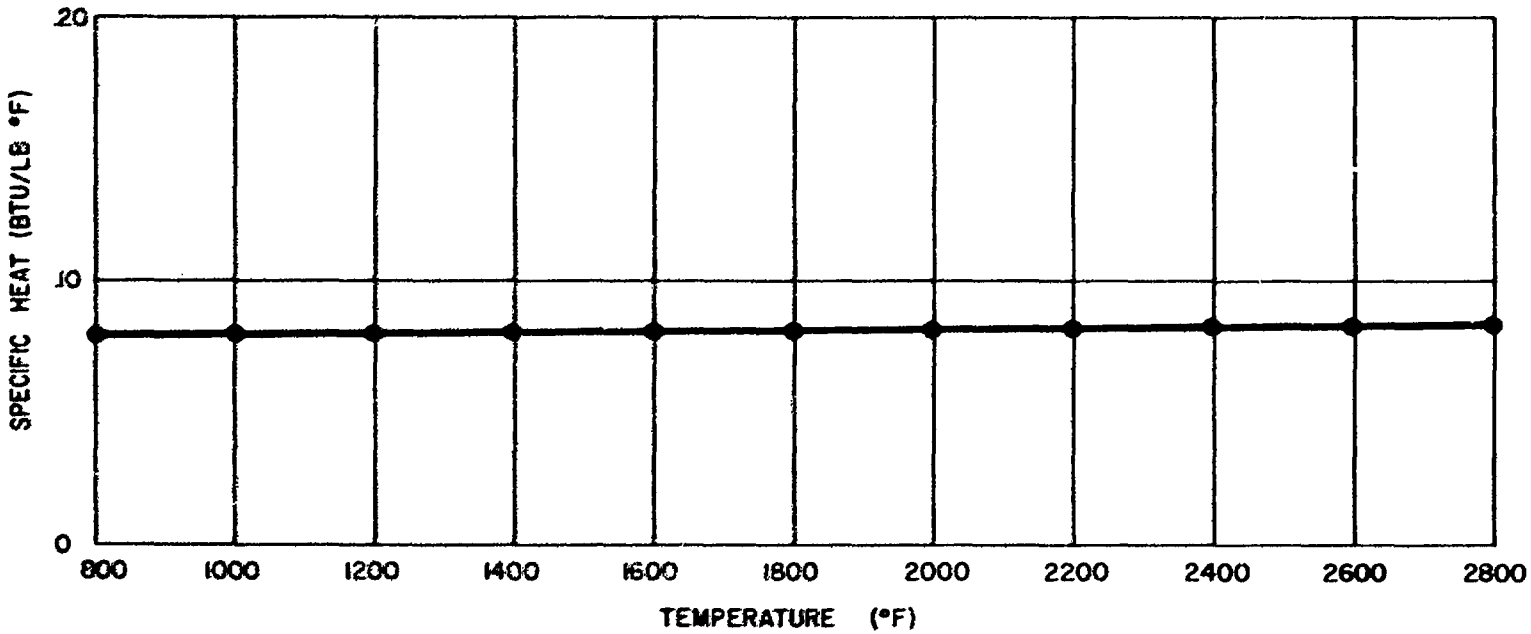

Fig. 31 - Specific Heat of WSi_2

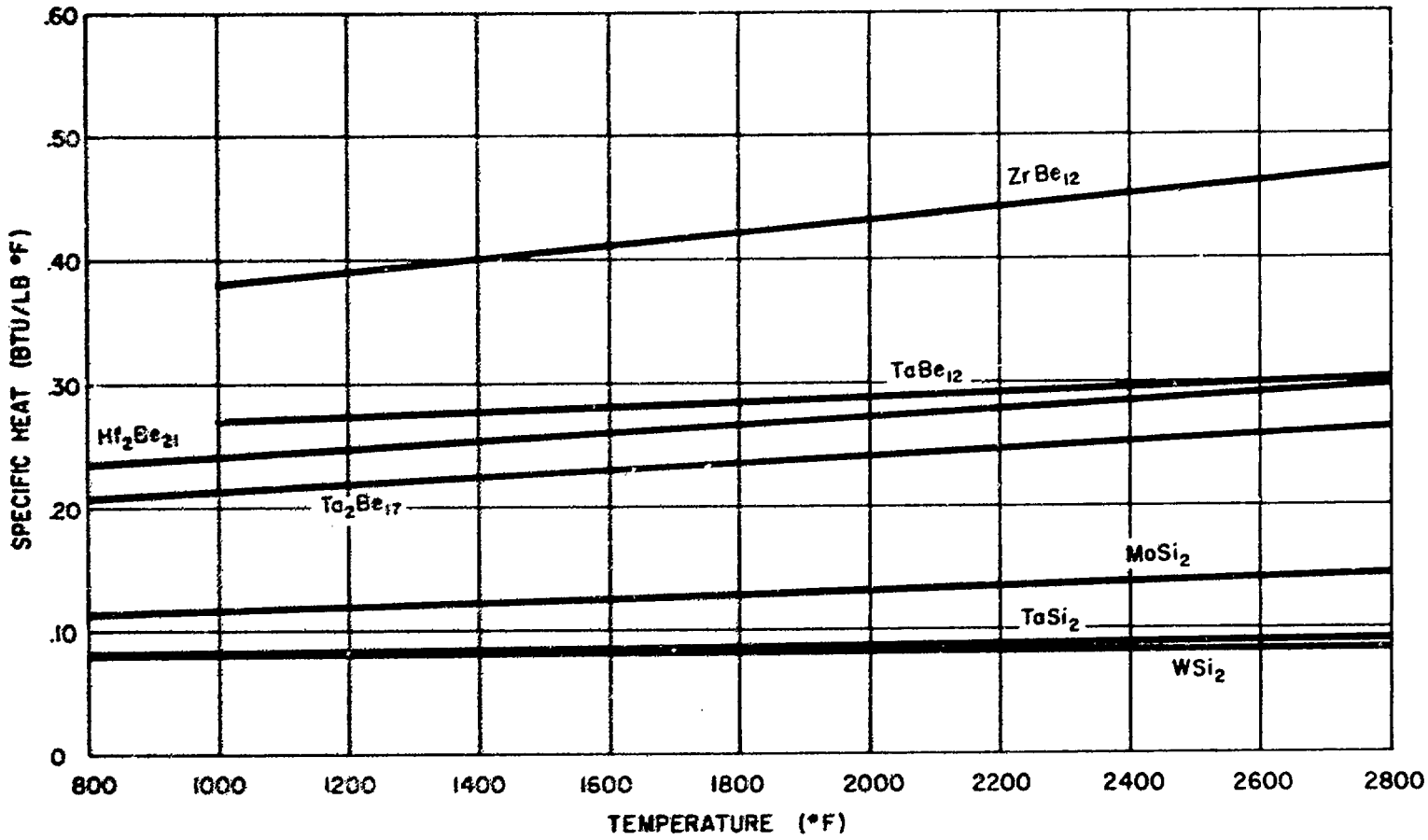

Fig. 32 - Comparison of Specific Heat Data for Various Intermetallic Compounds

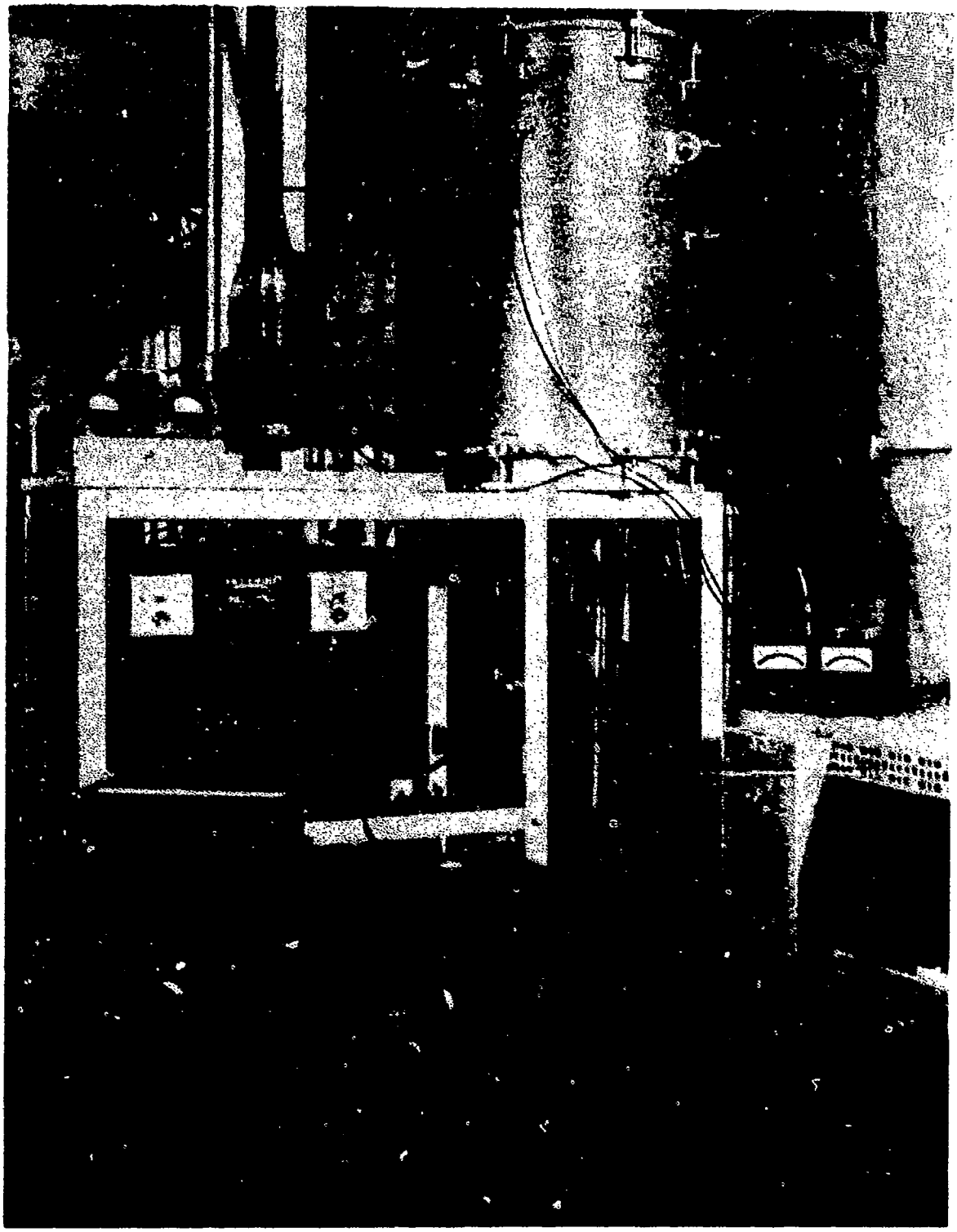

Fig. 33 - Thermal Conductivity Apparatus

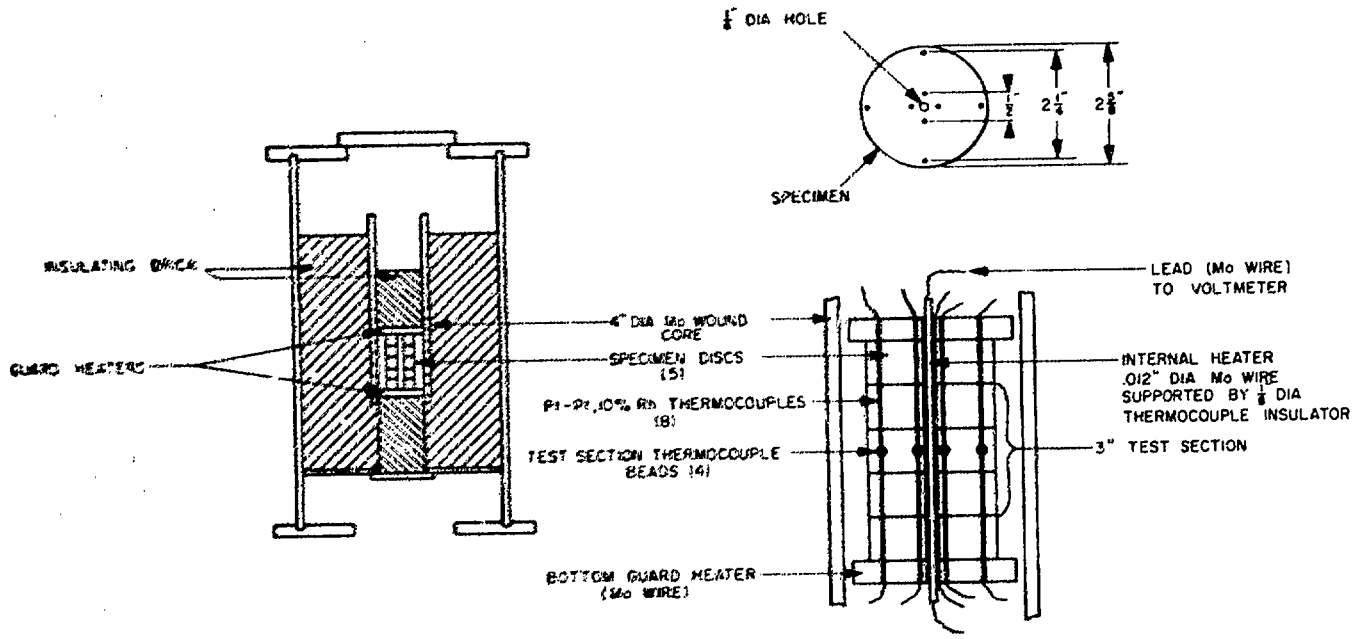

Fig. 34 - Thermal Conductivity Apparatus (Schematic)

guard heaters were employed on the top and bottom of the specimen. The fact that the specimens were composed of discs reduced the longitudinal heat flow, since the flow of heat was restricted at the interfaces.

Figure 35 shows one of the intermetallic discs used in this determination.

The thermal conductivity, k, was calculated using the following relationship:

$$k = \frac{q \ln r_2/r_1}{(\Delta T)\ 2\pi L}$$

where:

k = thermal conductivity (Btu hr^{-1} ft^{-2} ft $°F^{-1}$)
q = radial heat flow (Btu hr^{-1})
ΔT = radial temperature drop (°F)
$\frac{\ln r_2/r_1}{2\pi L}$ = body factor for a cylinder

where:

r_1 = radius of inner thermocouple (ft)
r_2 = radius of outer thermocouple (ft)
L = length of test section (ft)

The radial heat flow, q, was taken to be that quantity of heat generated inside the hollow cylindrical specimen and was measured as a function of the electrical energy output of the internal heater. This was accomplished by measuring the IR drop of the heating element across 3 inches of its length including the test section and the current flowing through the element. The radial temperature drop, ΔT, was measured by means of platinum-platinum, 10% rhodium thermocouples located in the longitudinal holes in the specimen.

The two major probable sources of error arise from longitudinal heat flow and an unbalanced radial temperature drop throughout the specimen. In practice, the radial temperature drop was measured in two directions 180 degrees apart. The average temperature difference measured was assumed to be the average radial drop for the specimen in all directions. Since the two values measured for the radial temperature drop were generally in close agreement, it was assumed that the average value obtained was representitive of the average radial drop over 360 degrees. With regard to longitudinal heat flow, guard heaters were employed on both ends of the specimen in conjunction with

Fig. 35 - Single Thermal Conductivity Specimen (As Machined)

thermocouples, which permitted regulation of the temperature of the top and bottom specimens. In addition, the radial temperature drop in the end specimens could be regulated to some extent so that these values would be essentially the same as those which occurred in the test section. Excellent control of longitudinal heat flow was obtained in the 800° - 2000°F range for the materials reported here; however, the control became progressively more difficult at temperatures above 2000°F. The ability to control longitudinal heat flow was also a function of the thermal conductivity of the specimen since more heat was lost for the specimens having high thermal conductivity. Although the magnitude of the two errors mentioned above was not determined, the observed data indicate that the precision of measurement was within 5%. The data also indicate that in general, the values obtained below 2300°F were more accurate than those obtained above this temperature.

b. Experimental Data and Discussion

As a means of checking the apparatus, the thermal conductivities of "L" nickel and beryllium oxide were determined and were compared with literature values. Comparisons of the Brush data with the literature data are given in Tables XVI and XVII. Comparative data are plotted in Figures 36 and 37.

For nickel, it will be observed that the slopes of the three curves plotted in the figure are essentially the same; however, the actual thermal conductivity values differ. Brush data are of the order of 10% higher than the data reported by Armour. The values reported by ANL[6] lie midway between those of Armour and Brush. Note that the data obtained by Armour are for "A" nickel, while the data obtained by Brush are for "L" nickel. One would expect that the thermal conductivity for "L" nickel would be somewhat higher, since this grade of nickel has a lower carbon content. Spectrographic analysis of the material used by Brush showed a higher overall purity than that listed for commercial grade "L" nickel.

A comparison of the four beryllium oxide curves shows similar slopes with discrepancies in the actual values. The points on the graph representing data taken from The Reactor Handbook reported by ANL[6] were obtained from a smooth curve, while the points representing Brush data are observed values. The greatest discrepancies occur among the values at the low temperatures, while agreement at high temperatures is quite good. Note that the data shown here for Brush includes measurements obtained during an earlier

TABLE XVI

THERMAL CONDUCTIVITY OF NICKEL -
COMPARISON OF BRUSH AND LITERATURE VALUES

Mean Specimen Temperature (°F)	Thermal Conductivity (Btu hr^{-1} ft^{-2} ft $°F^{-1}$)		
	ANL[a]	Armour[4]	Brush
940	30.5	28.2	32.8
1007	31.1	29.2	33.3
1057	31.6	29.1	33.8
1196	32.7	31.81	34.9
1467	35.1	34.40	37.2
1490	35.4	31.0	37.4
1507	35.5	33.2	37.5
1530	35.7	36.0	37.7
1710		34.67	39.2
2025		37.6	41.8
2171		39.85	43.0
2449		41.56	

[a]Data obtained from curve drawn by ANL[6] for various literature values.

TABLE XVII

THERMAL CONDUCTIVITY OF BERYLLIUM OXIDE - COMPARISON OF BRUSH AND LITERATURE VALUES

Mean Specimen Temperature (°F)	Thermal Conductivity (Btu hr^{-1} ft^{-2} ft $°F^{-1}$)			
	ANL[a]	ANL[b]	Brush[c]	Brush[d]
800	48	30	41	--
1000	33	24	32	--
1200	24	20	26	29
1400	18	16	21	23
1600	15	13	18	19
1800	12	11	15	17
2000	11	10	13	15
2200	10	10	12	13
2400	--	--	10	12
2600	--	--	10	11

[a]Data reported by ANL[6] which was taken from NYO-3647.

[b]Data reported by ANL[6] which was taken from Reactor Handbook.

[c]Present data.

[d]Previous data obtained by a different method.

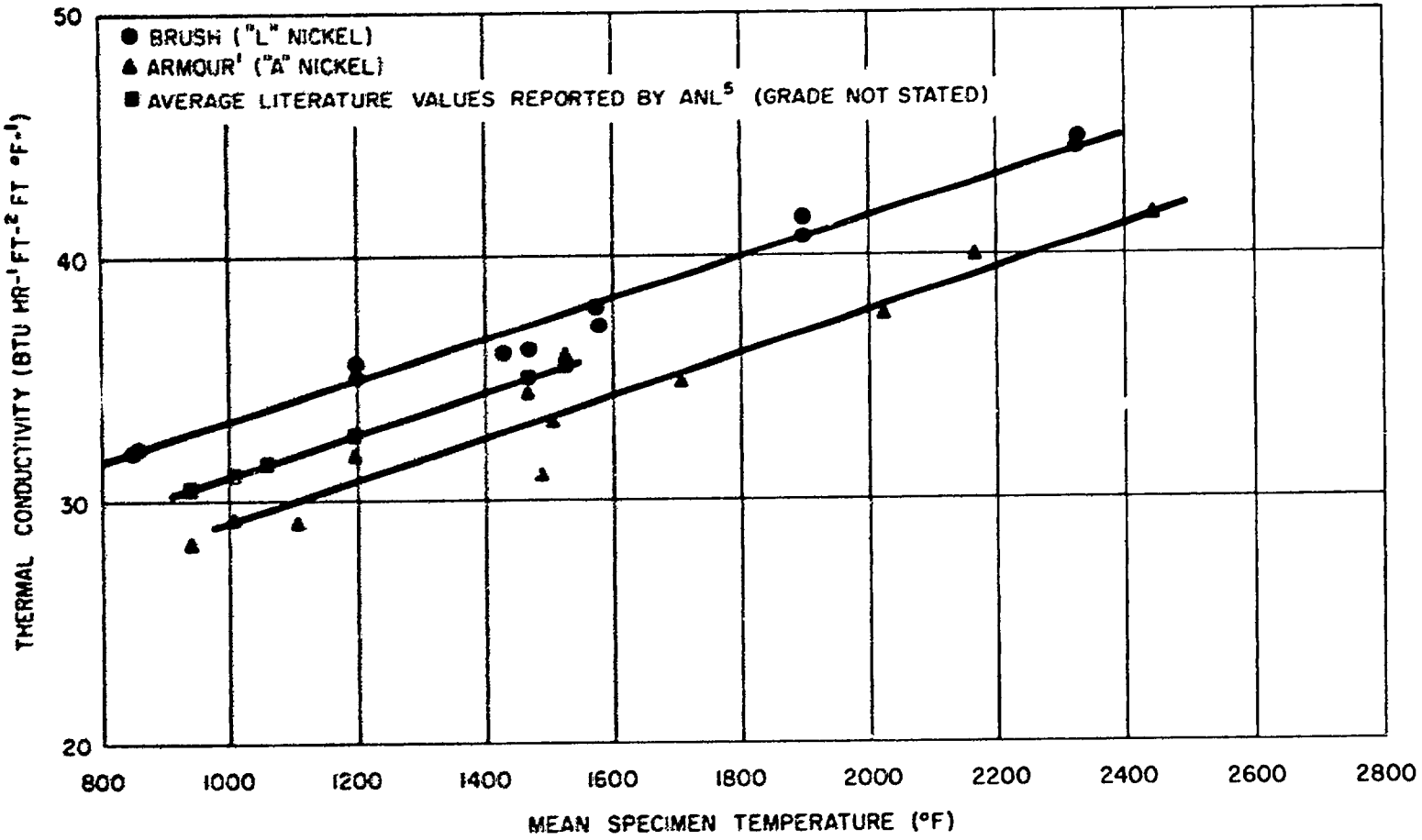

Fig. 36 - Thermal Conductivity of Nickel - Comparison of Brush and Literature Values

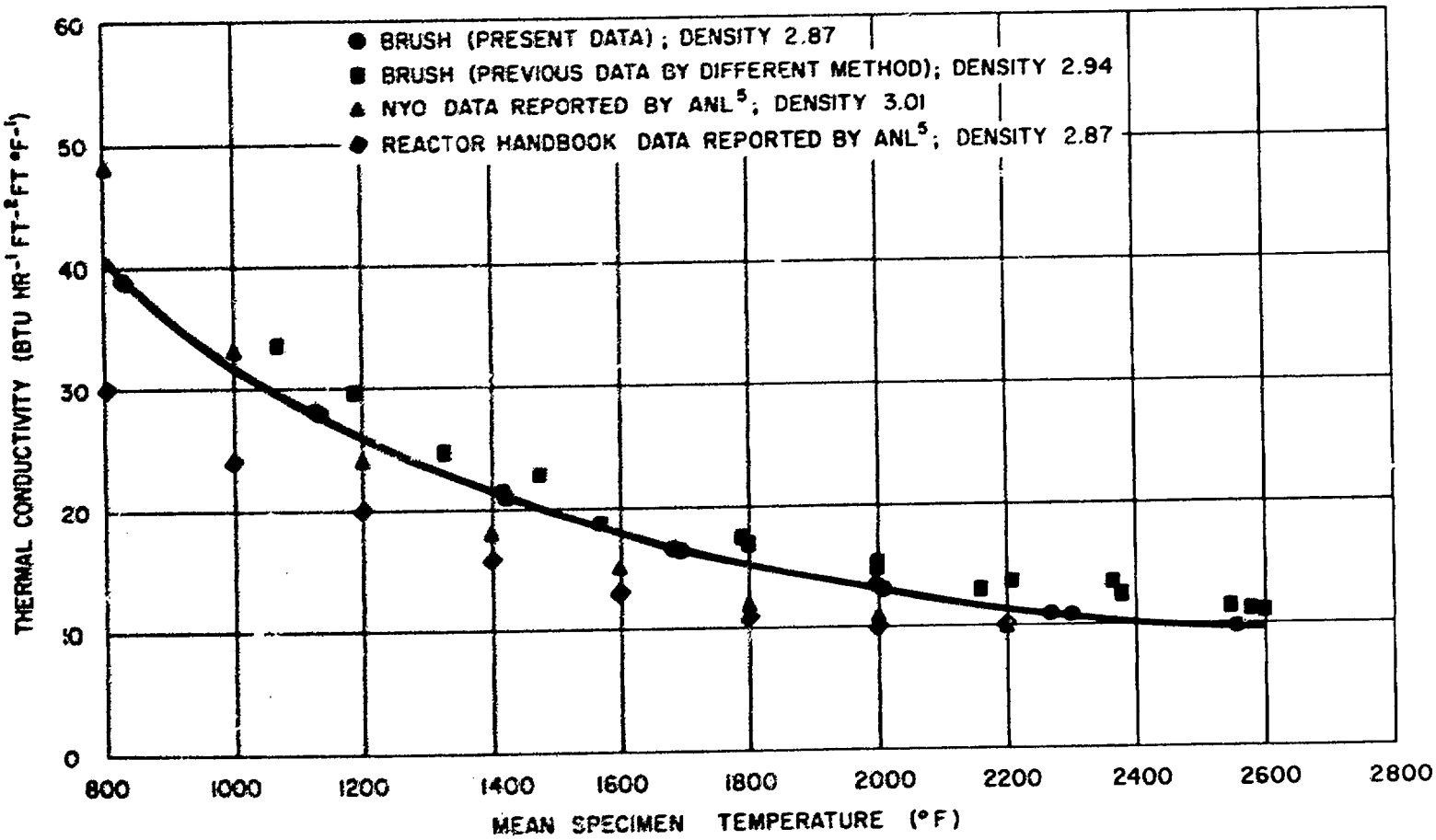

Fig. 37 - Thermal Conductivity of Beryllium Oxide - Comparison of Brush and Literature Values

program using a different apparatus, as well as those obtained during the present program. The values for the latter measurements are slightly lower than those reported earlier. Much of this difference is attributed to differences in specimen densities, the earlier specimen having a density of 2.94 g/cc, while the density for the present specimen is 2.87 g/cc.

The thermal conductivity of $TaBe_{12}$ from approximately 850° to 2600°F was determined. Failure of a thermocouple precluded further measurements above this temperature. The thermal conductivity of WSi_2 was determined from approximately 850° to 2750°F. The observed data are given in Tables XVIII and XIX and are plotted in Figures 38 and 39. The data show the thermal conductivity of $TaBe_{12}$ to be linear throughout the temperature range, whereas for WSi_2 there is an initial decrease in conductivity between 800° and 1400°F, a range of relatively constant conductivity, and finally a sharp increase in conductivity at about 2600°F.

TABLE XVIII

THERMAL CONDUCTIVITY OF $TaBe_{12}$

Mean Specimen Temperature (°F)	Thermal Conductivity (Btu hr^{-1} ft^{-2} ft $°F^{-1}$)
838	16.1
845	16.1
1084	16.6
1093	16.6
1397	16.9
1400	16.9
1632	18.4
1640	18.2
1800	19.0
1804	18.8
2035	19.8
2055	19.5
2055	19.8
2300	20.3
2320	20.6
2596	22.3

TABLE XIX

THERMAL CONDUCTIVITY OF WSi_2

Mean Specimen Temperature (°F)	Thermal Conductivity (Btu hr^{-1} ft^{-2} ft $°F^{-1}$)
860	22.7
864	22.7
890	22.0
896	21.6
1115	19.6
1130	19.8
1130	20.1
1152	19.5
1152	19.4
1410	17.9
1415	18.0
1720	17.2
1721	17.3
2004	17.6
2012	17.3
2192	18.4
2207	18.6
2307	17.1
2308	17.8
2502	18.8
2518	18.9
2632	18.1
2637	18.2
2720	21.2
2761	22.6
2764	22.3
2767	23.1

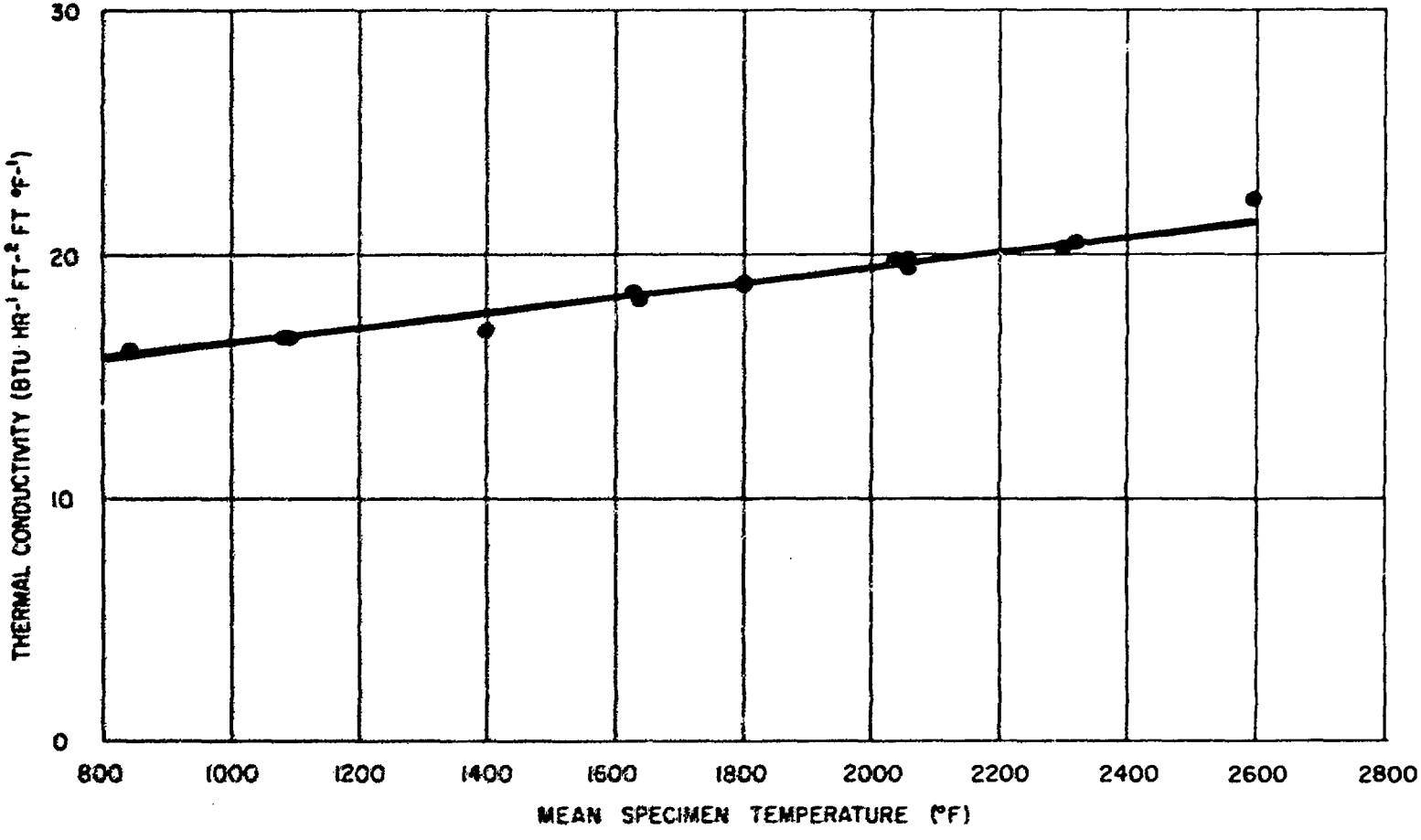

Fig. 38 - Thermal Conductivity of $TaBe_{12}$

Fig. 39 - Thermal Conductivity of WSi_2

IV. FUNDAMENTAL STUDY OF OXIDATION MECHANISM

A. Oxidation Rates

The oxidation resistance of certain intermetallic compounds has been discussed in Section III-A of this report. It was concluded in that section that the beryllides studied possessed satisfactory oxidation resistance to be serviceable for short times at 3000°F. Some of the beryllide compounds have melting points considerably higher than 3000°F, e.g., Ta_2Be_{17} (3610°F), and it is conceivable that this upper limit of serviceability may be extended. It would be possible to alter the resistance to oxidative attack more effectively if the mechanism by which oxidation takes place were known. Consequently, determination of the mechanism of oxidation of the beryllides has been undertaken, and progress in this work is discussed below.

Before a mechanism of oxidation can be assigned, the rate of oxidation must be known. In addition, the products of the oxidation reaction must be identified, and the activation energy necessary for continuation of the process should be available. The first step in the mechanism study is determination of the oxidation rate.

1. Determination of Oxidation Rates

The determination of the rates of oxidation of the beryllides, $TaBe_{12}$, Ta_2Be_{17}, Hf_2Be_{21}, and $ZrBe_{13}$, has been initiated, using the method of measuring the weight change as a function of time. For this measurement, an Ainsworth semi-micro, automatic recording, analytical balance was used to record the weight change versus time at a given temperature. Each of the intermetallic oxidation specimens was 1/2 x 1/2 x 1/4 inch with a 0.133-inch hole drilled through the center. These specimens were suspended from the balance into the oxidation chamber by means of a length of 60/40 platinum-rhodium alloy wire. A BeO insert prevented the suspension wire from contacting the intermetallic. A one-inch-ID Morganite Triangle RR tube served as the oxidation chamber. The middle 5 1/2 inches of this tube was heated by means of a 60/40 platinum-rhodium alloy wire winding. Oxygen gas dried by bubbling through concentrated sulfuric acid or Ascarite was used as oxidant. The samples were suspended into the middle of the hot zone. Temperature was measured with a platinum-platinum, 10% rhodium thermocouple. The apparatus is shown in Figure 40. During the measurement, a plastic shield (not shown in the picture) was used to shield the suspension wire from air currents.

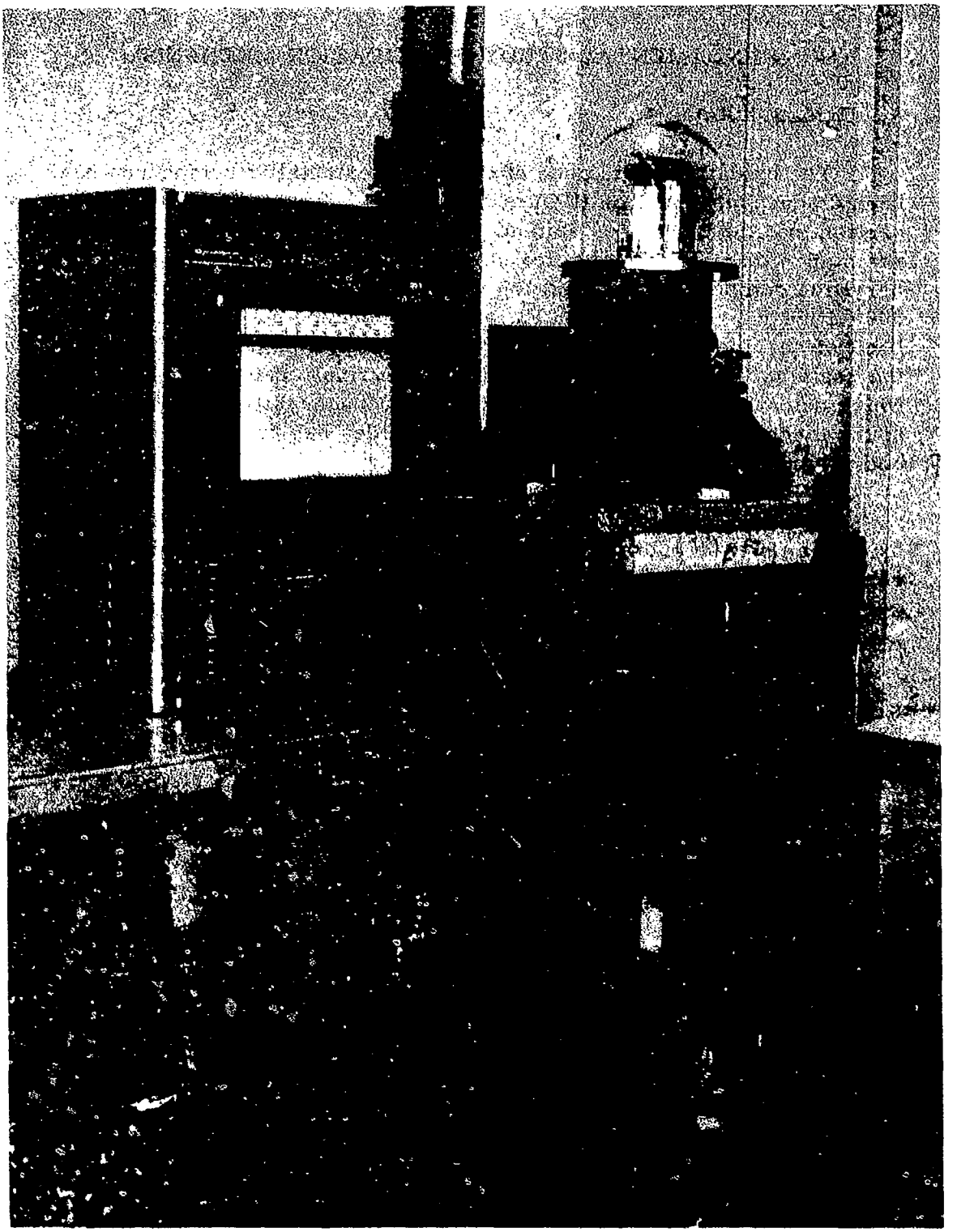

Fig. 40 - Oxidation Apparatus

Data have been obtained at 2300°, 2500°, and 2750°F for $TaBe_{12}$, Ta_2Be_{17}, and Hf_2Be_{21}, and at 2300° and 2500°F for $ZrBe_{13}$. No 2750°F data for $ZrBe_{13}$ were obtained due to equipment difficulties (failure of the platinum furnace winding). In each case, the shape of the weight change vs. time curve indicated a decrease in the initial rate of oxidation. This, in turn, indicated that protection against linear oxidation was afforded by the products of oxidation, which remained on the surface of the sample.

From the shape of the weight change curves, and by comparison of the sample weight changes as recorded by the automatic equipment with the sample weights before and after oxidation (Table XX), it was determined that the sample suspension assembly was not maintaining a constant weight over the long time period of these runs. It is apparent from the tabulation that differences between the recorded weights and the weight actually gained by the samples occurred at all temperatures, but were greatest at 2750°F.

A typical analysis of the weight changes encountered in the BeO and 60 % platinum-rhodium alloy suspension system is given below for the 75-hour oxidation of Hf_2Be_{21} at 2750°F:

Weight of Suspension Wire (mg)	Before	7550.3		
	After	7554.6		
	Net change		+4.3 mg	
Weight of Sample Holder (mg)	Before	673.6		
	After	661.2		
	Net change		-12.4 mg	
Net change in Weight of Suspension				-8.1 mg
Sample Weight (mg)	Before	3684.7		
	After	3718.2		
	Net change			+33.5 mg
Net change in weight of sample and suspension				+25.4 mg
Recorded weight change				+26.25 mg

The greatest weight change in the suspension system was found to be in the sample holder portion, which was expected, since this portion is exposed to maximum heating. The weight loss here is believed to be primarily due to the volatilization of the platinum-

TABLE XX

COMPARISON OF WEIGHT CHANGE DATA

Temp. (°F)	Material	Sample Weight (mg) Before	After	Change	Recorded Weight Change (mg)
2300	$ZrBe_{13}$	1882.0	1895.2	+13.2	+12.90
	$TaBe_{12}$	3073.0	3082.6	+ 9.6	+ 7.98
	Ta_2Be_{17}	3764.1	3774.5	+10.4	+ 9.00
	Hf_2Be_{21}	3814.1	3830.5	+16.4	+13.26
2500	$ZrBe_{13}$	1947.0	1988.2	+31.2	+34.70
	$TaBe_{12}$	3778.0	3792.3	+14.3	+10.78
	Ta_2Be_{17}	4163.0	4175.7	+11.27	+11.25
	Hf_2Be_{21}	3654.0	3671.5	+12.5	+11.75
2750	$TaBe_{12}$	3676.9	3703.3	+26.4	+12.85
	Ta_2Be_{17}	3642.8	3669.5	+16.7	+12.72
	Hf_2Be_{21}	3684.7	3718.2	+33.5	+26.25

rhodium alloy. While this has not yet been experimentally proven, the evidence of the weight gain of the suspension wire due to condensation of a black material on the cool portion of this wire, the extreme volatilization of the 60/40 platinum-rhodium winding of the furnace itself (outside the oxidation chamber), and the continuation of the weight loss throughout the various runs despite the repeated use of the same BeO sample holder pieces strongly support this position. Thus, while the 60/40 platinum-rhodium alloy was originally chosen because of its high melting point and reported low evaporation rate,[7] it is apparent that this particular suspension system is not serviceable at high temperature without correction for weight loss. Typical weight change versus time curves obtained without correction for weight change in the suspension system are illustrated in Figure 41, which plots the results for $TaBe_{12}$ at 2300°, 2500°, and 2700° F.

A corrected curve may be obtained by assuming a constant rate of mass loss from the suspension system. When this is done, the slopes of the curves are compatible with expected results. Figs. 42, 43, 44, and 45 are weight gain versus time curves for the oxidation of $TaBe_{12}$, Ta_2Be_{17}, Hf_2Be_{21}, and $ZrBe_{13}$, respectively, with the correction applied at those temperatures where significant deviation from the true weight change was indicated by the raw data.

If the general rate expression, $W^n = kt$, is applicable to the oxidation of these beryllides the plot of log of weight change per unit area versus the log of time should give a straight line with a slope of $1/n$, where n denotes the rate law which the oxidation process obeys, and W is the weight change with time, t. Plots of the log of the weight change per square centimeter versus the log of time for $TaBe_{12}$, Ta_2Be_{17}, Hf_2Be_{21}, and $ZrBe_{13}$ are shown in Figs. 46, 47, 48, and 49, respectively. In some cases, more than one straight line results, which indicates a change in the oxidation process with time.

For $TaBe_{12}$ at 2300° F, two straight lines are obtained, with the slope change occurring at 15 hours. The slopes of these lines are 0.37 and 0.32, corresponding to n values of 2.8 and 3.1 in the expression, $W^n = kt$. Thus, both lines indicate that the oxidation proceeds according to the cubic rate law at 2300° F. At 2500° F, a single straight line is obtained with n = 3.8. Finally, at 2750° F, the slope of the straight line plot yields a value for n of 3.3. Thus, it seems reasonable to conclude that the oxidation of $TaBe_{12}$ in the temperature range from 2300° to 2750° F is governed by the cubic rate law.

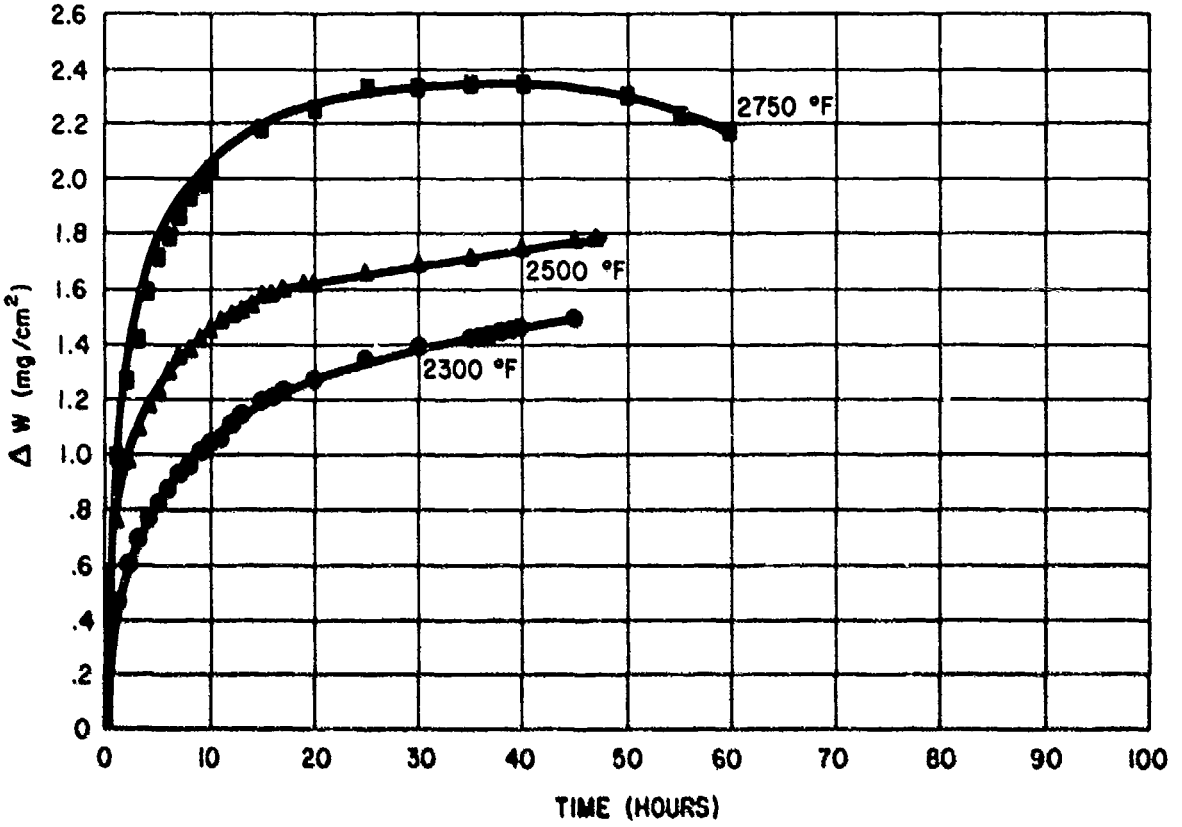

Fig. 41 - Oxidation of $TaFe_{12}$

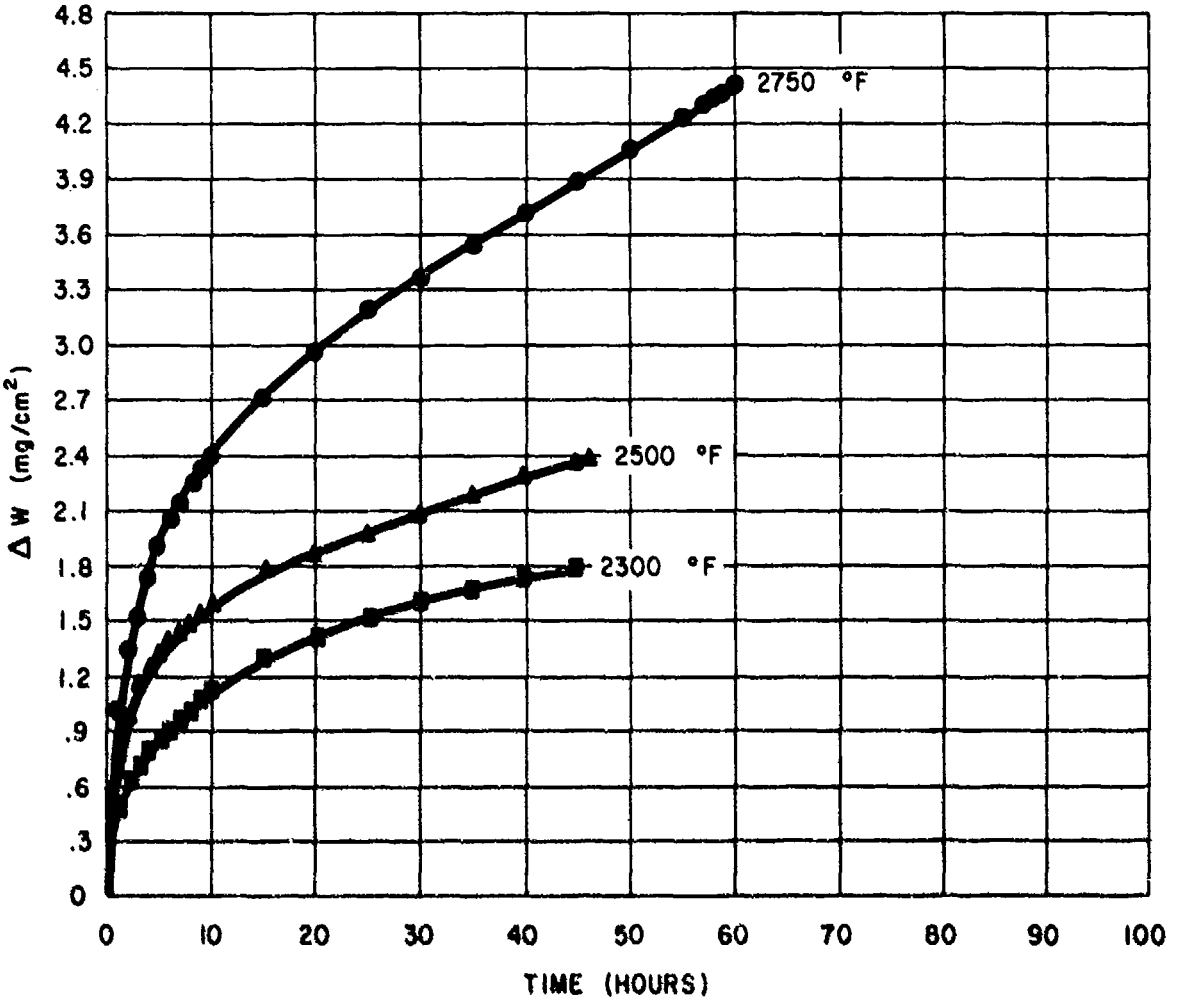

Fig. 42 - Oxidation of $TaBe_{12}$

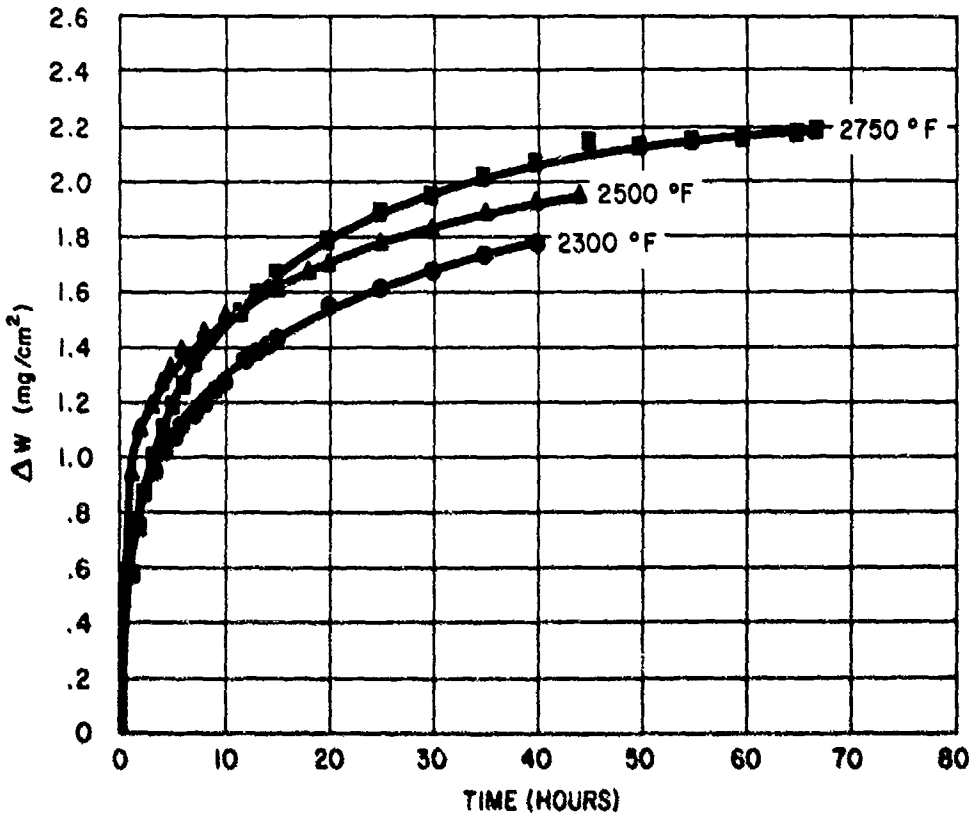

Fig. 43 - Oxidation of Ta_2Be_{17}

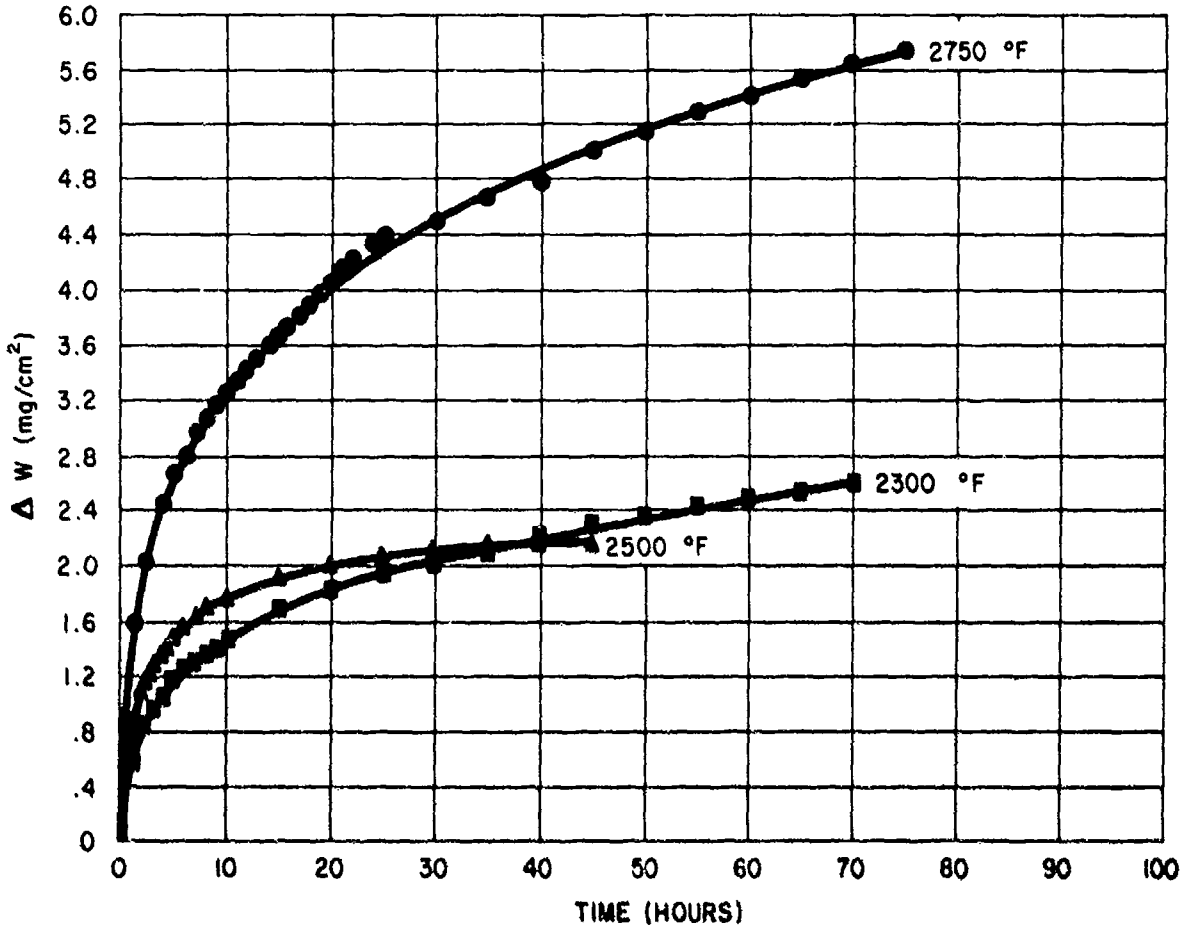

Fig. 44 - Oxidation of Hf_2Be_{21}

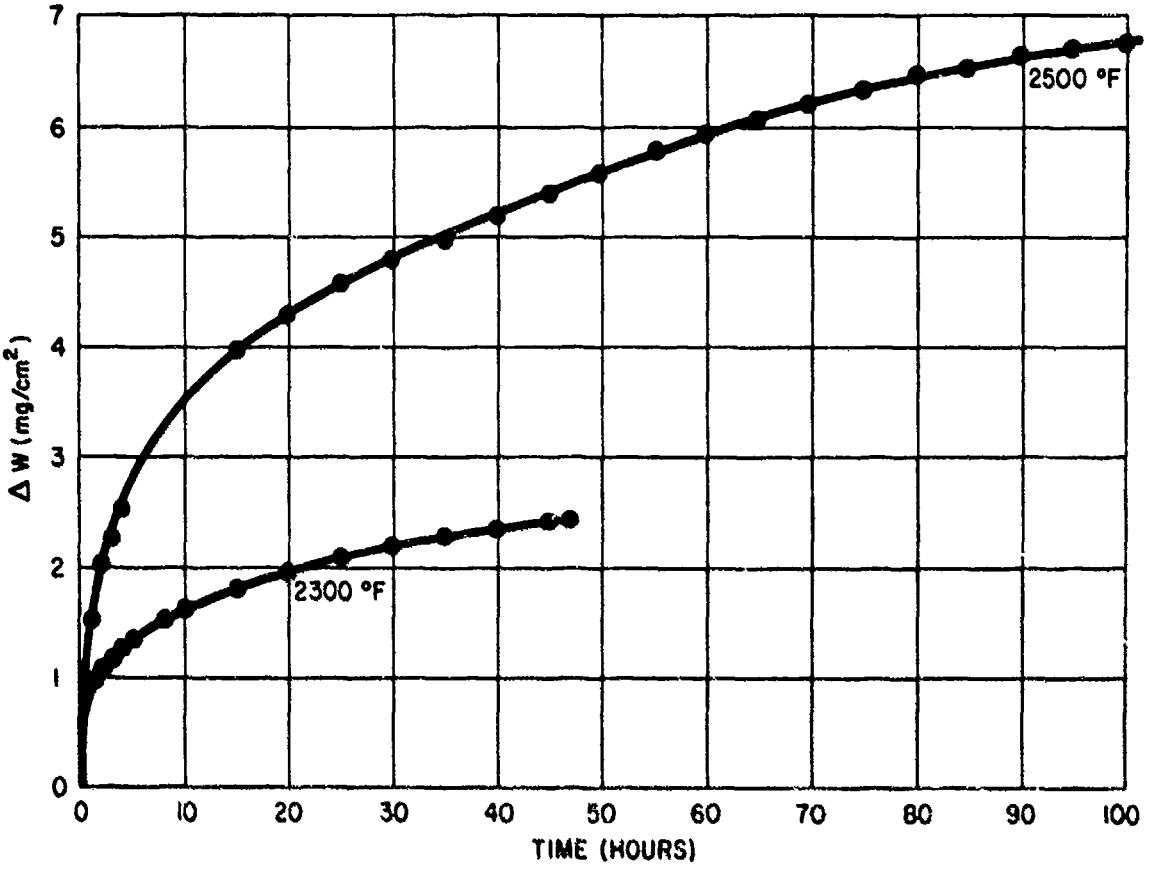

Fig. 45 - Oxidation of $ZrBe_{13}$

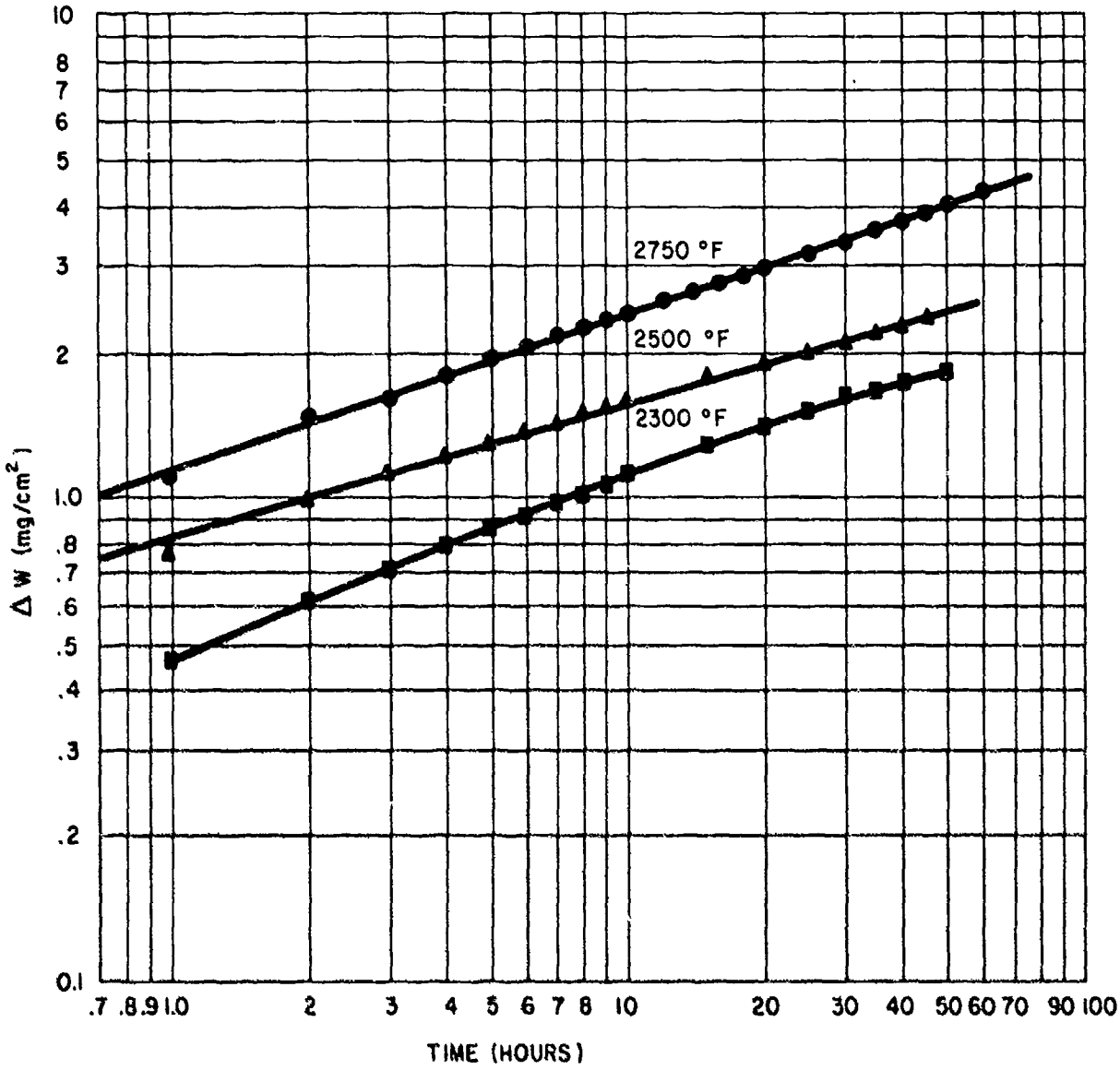

Fig. 46 - Oxidation of $TaBe_{12}$ (Graph)

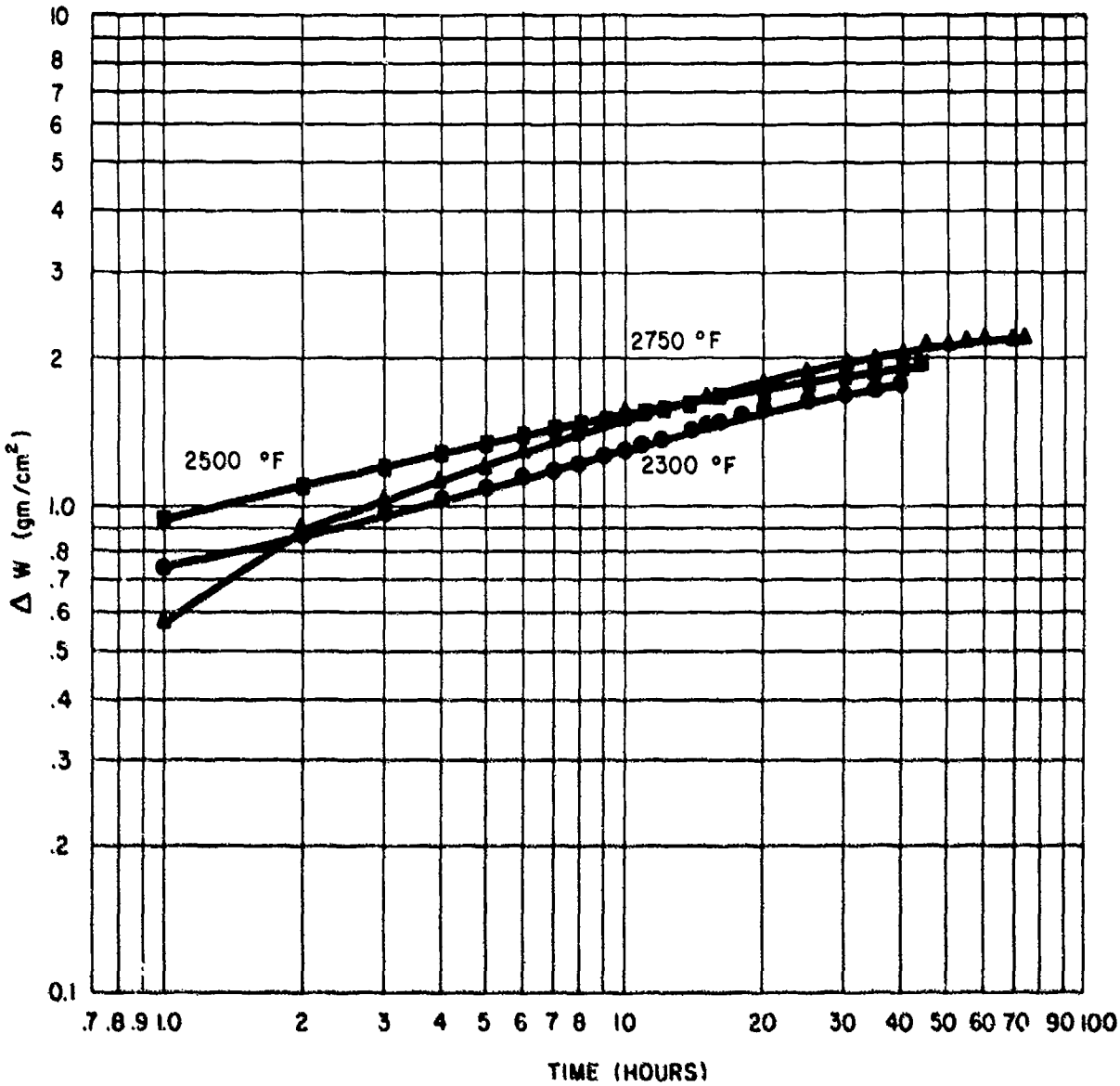

Fig. 47 - Oxidation of Ta_2Be_{17}

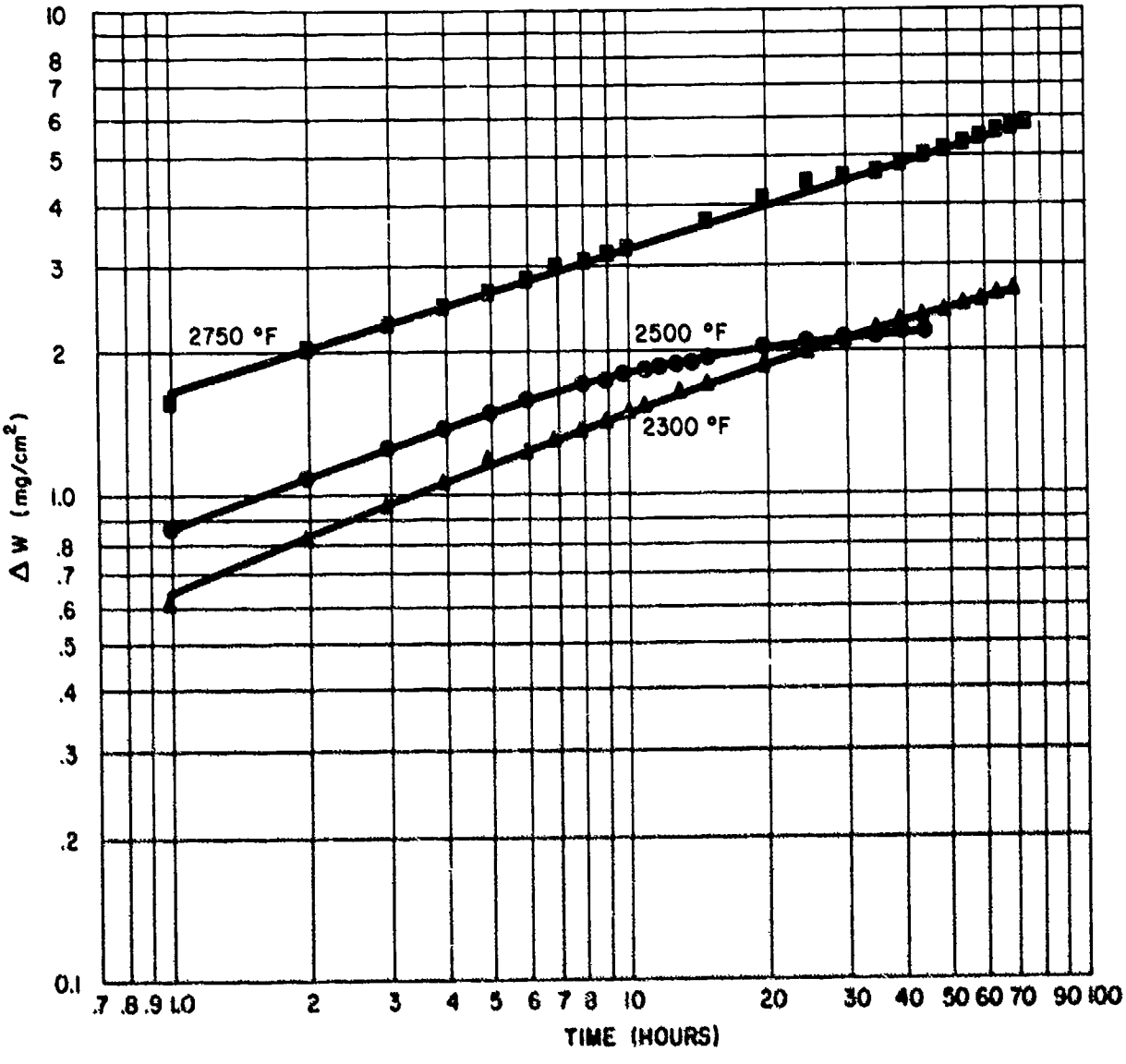

Fig. 48 - Oxidation of Hf_2Be_{21}

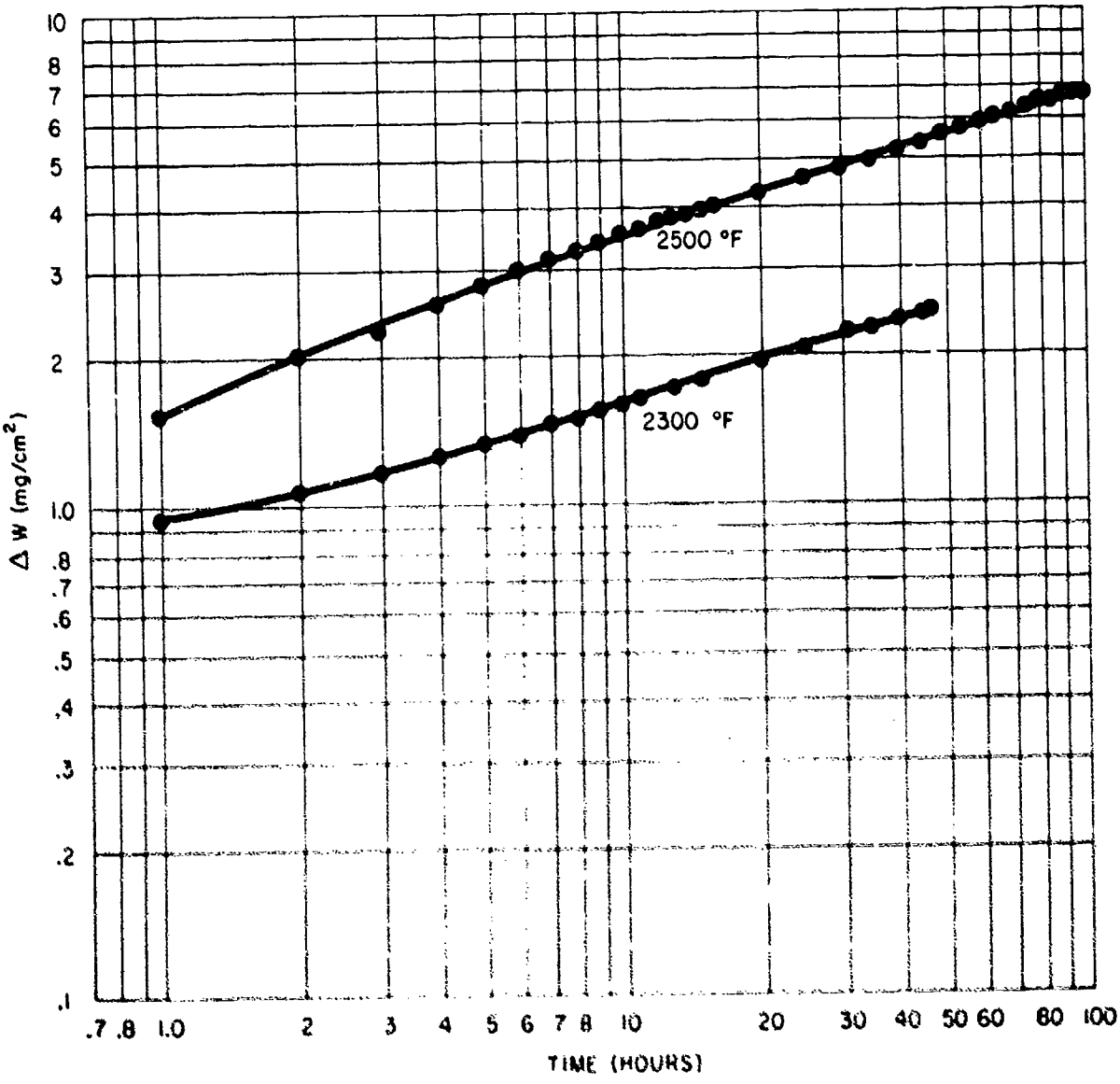

Fig. 49 - Oxidation of $ZrBe_{13}$

By plotting W^3 versus t, the rate constants were calculated to be 0.128 $(mg/cm^2)^3$/hr at 2300° F, 0.255 $(mg/cm^2)^3$/hr at 2500° F, and 1.32 $(mg/cm^2)^3$/hr at 2750° F. The activation energy calculated from an Arrhenius plot of the log of the rate constant versus 1/T is 35.9 k cal/mole.

In the case of Ta_2Be_{17}, there was no difference between the recorded and measured weight gains at 2500° F and only small differences at 2300° and 2750° F. The log-log plot of the data at 2300° F gives three lines with slopes of 0.23, 0.29, and 0.18, respectively. A single straight line with a slope of 0.23 may be drawn; however, deviations from this line occur in the 10 to 25 hour region, with the greatest deviation occurring at about 19 hours. In general, deviations occur in the 10 to 20 hour range of the corrected curves. It will be observed that it is in this time range that the slowdown in oxidation occurs. The overall oxidation of Ta_2Be_{17} at 2300° F is probably exponential as expressed by the n value of 4.3 (1/n = 0.23). The exponential oxidation is also present at 2500° F as indicated by the 1/n values of 0.22 and 0.21 and an average n value of 4.65 of the two slightly different straight lines. The change in 1/n begins at 10 hours. At 2750° F, four straight lines were obtained, with the value of 1/n decreasing with time. The significance of these four straight-line portions of the log-log plot of the oxidation test data for Ta_2Be_{17} at 2750° F is not capable of analysis without further study.

Attempts to fit the Ta_2Be_{17} data to a logarithmic rate were unsuccessful. Also, equally good straight lines could be drawn when the weight change was plotted versus $t^{1/4}$ or $t^{1/5}$ for the 2300° F data. In view of the wide variations of 1/n values which are attributed to lower power rate laws (cubic and parabolic), it is not surprising that the 1/n values of Ta_2Be_{17} are difficult to interpret. A theoretical foundation upon which an explanation of oxidation behavior of the type exhibited by Ta_2Be_{17} can be based is not yet available. The possibility of a volatible component in the oxidation products must not be overlooked. The oxidation products must be identified before definite conclusions concerning the rate of oxidation of Ta_2Be_{17} are drawn.

When log-log plots were made for Hf_2Be_{21}, straight lines with slopes of 0.36 and 0.28 (n = 2.8 and 3.6) were obtained at 2300° F, with the change in slope observed at 13 hours. Both of these 1/n values are considered to indicate the cubic rate law; however, different processes may be involved in the oxidation reaction. At 2500° F, three straight lines are obtained with 1/n values of 0.33, 0.23, and 0.1, respectively (n = 3.0, 4.3, and 10), with changes at 7 and 20 hours. The initial cubic rate changes with time to higher power rates. In this respect, Hf_2Be_{21} at this

temperature exhibits behavior similar to that of Ta_2Be_{17} at 2750°F. The data for Hf_2Be_{21} at 2750°F gives a straight line with a slope of 0.29 (n = 3.4). Thus, with the cubic rate law operative at 2300°F, 2750°F, and for the first 7 hours at 2500°F, it would appear probable that Hf_2Be_{21} follows the cubic law at these three temperatures. The deviation from the cubic law after seven hours at 2500°F seems to be the result of experimental factors with this particular run and should be accepted only upon confirmation. The calculated cubic rate constants are 0.32 $(mg/cm^2)^3/hr$ at 2300°F; 0.63 $(mg/cm^2)^3/hr$ at 2500°F; and 3.33 $(mg/cm^2)^3/hr$ at 2750°F. A tentative activation energy was calculated to be 50 k cal.

The plots for $ZrBe_{13}$ in Figure 49 were made from the observed data. At 2300°F, two straight lines are obtained with slopes of 0.21 and 0.28 (n = 4.8 and 3.6), with the slope change occurring at 3 hours. The 0.28 slope can be considered to indicate a cubic rate. At 2500°F, a straight line with a slope of 0.29 (n = 3.4) can be drawn if some of the short-time (<5 hr) points are neglected. When the 0- to 5-hour weight gain is included, as was done in the figure, three straight lines with slopes of 0.16, 0.35, and 0.29 are obtained. It seems reasonable to conclude that the cubic rate law is operative when $ZrBe_{13}$ is oxidized at this temperature.

The oxidation rate of $ZrBe_{13}$ at 2500°F has also been approached in another manner. Tests were made on 1/2- x 1/2- x 1/4-inch specimens in a five-tube Globar furnace. Samples were oxidized for 1, 3, 5, 7, 10, 20, 25, 40, and 100 hours at temperature. A given sample was oxidized for the entire time without cycling. Two separate runs were made. The results are summarized in Table XXI, and a plot of weight gain versus time is shown in Figure 50. The log of the weight change versus the log of time is plotted in Figure 51. The straight line drawn is the line obtained when the method of least squares is applied to the datum points from both runs. The straight line indicates agreement with the general rate expression, $W^n = kt$. The slope of the line (1/n) equals 0.35 in this case, and the value of n is 2.9. This indicates that the overall rate of oxidation of $ZrBe_{13}$ at 2500°F is best expressed by the cubic rate law.

Both methods of determination indicate a cubic rate law for the oxidation of $ZrBe_{13}$ at 2500°F. The calculated rate constants are 4.18×10^{-2} $(mg/cm^2)^3/min$ from the automatically recorded data and 6.03×10^{-3} $(mg/cm^2)^3/min$ from the Globar furnace data. The differences in the two methods included: (1) use of oxygen at one atmosphere versus compressed air as oxidant and (2) the significant difference in total weight gain per square centimeter for the samples

TABLE XXI

SUMMARY OF OXIDATION DATA FOR $ZrBe_{13}$
OBTAINED BY PERIODIC WEIGHING
AT 2500°F

Time (hr)	Density (g/cc)	% of Absolute Density	Weight Gain (mg/cm^2)
		Run 1	
1	2.73	99.6	0.52
3	2.71	98.9	0.84
5	2.72	99.3	0.84
7	2.72	99.3	1.06
10	2.73	99.6	1.16
20	2.72	99.3	1.43
25	2.72	99.3	1.94
40	2.72	99.3	2.41
100	2.73	99.6	2.68
		Run 2	
1	2.72	99.3	0.57
3	2.72	99.3	0.70
5	2.72	99.3	1.24
7	2.72	99.3	1.28
10	2.71	98.9	1.24
20	2.71	98.9	2.21
25	2.71	98.9	1.43
40	2.73	99.6	2.36
100	2.71	98.9	3.17

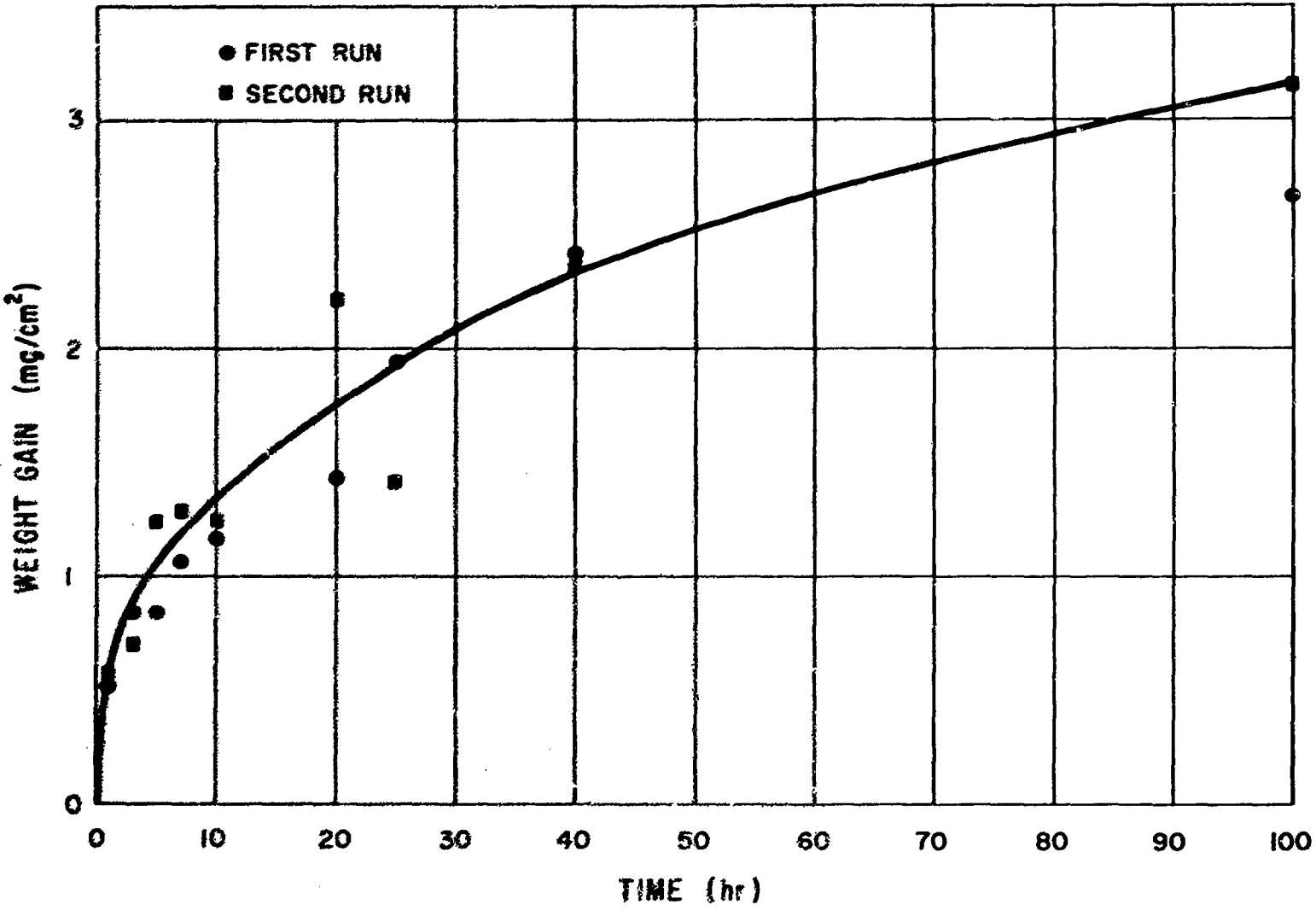

Fig. 50 - Oxidation of $ZrBe_{13}$ at 2500°F in Globar Furnace

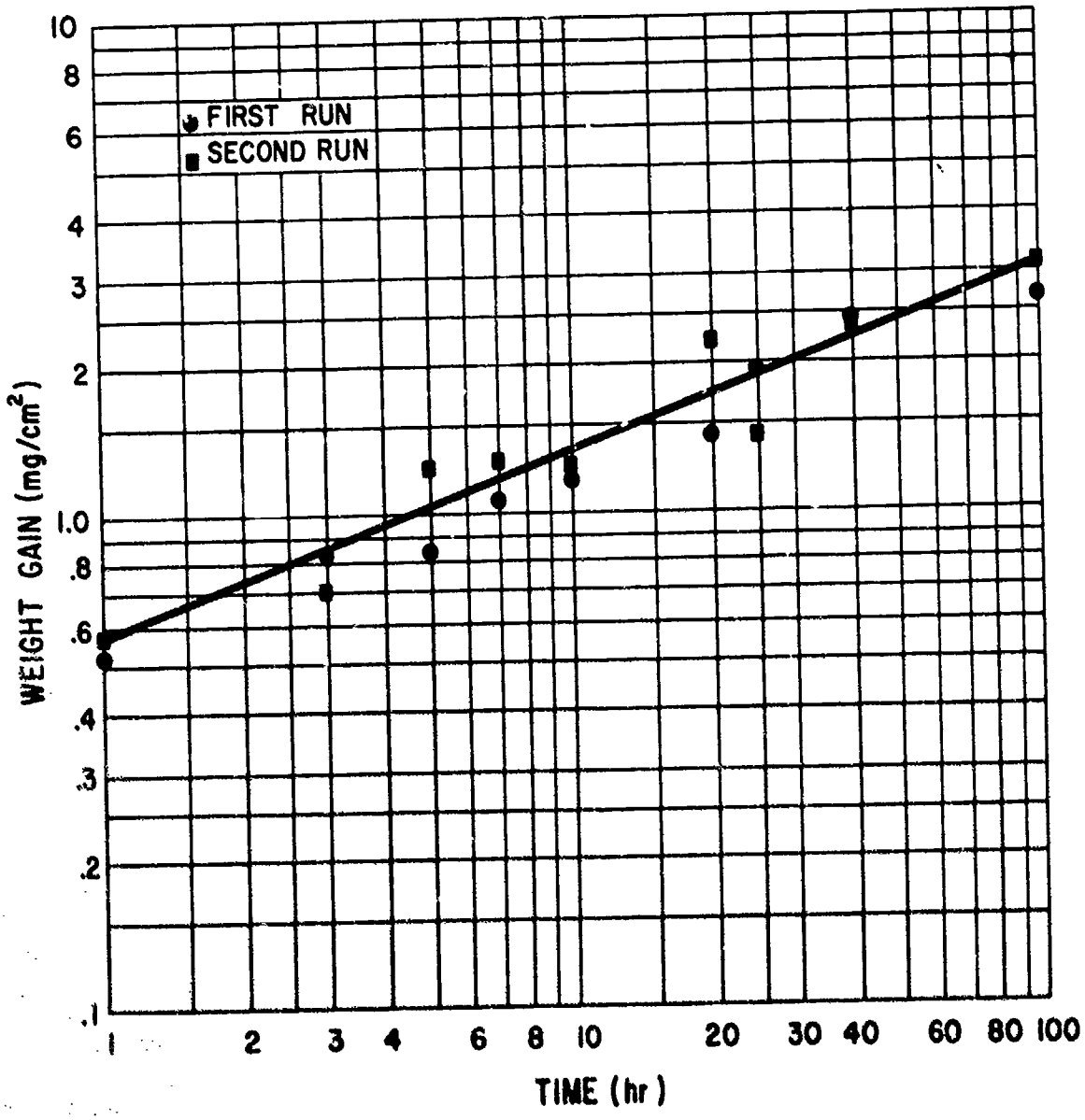

Fig. 51 - Log Weight Gain Versus Log Time for $ZrBe_{13}$ at 2500°F

measured (6.71 versus 3.14 mg/cm^2). When these differences are considered, the agreement of the rate constants is surprisingly good.

2. Identification of Oxidation Products

In view of the relatively large number of materials, $ZrBe_{13}$ was chosen as a prototype for initial studies on the mechanism of oxidation operative in the case of the beryllides. Thus, work on the identification of oxidation products has been limited to this compound in the studies carried out thus far.

$ZrBe_{13}$ samples which were oxidized in the Globar furnace at 2500° F have been examined using the techniques of X-ray diffraction and electron microscopy for the purpose of identifying the reaction products. Upon cooling, the outer scale flaked from all of the samples except for the one-hour runs. Also, a small amount of this outer scale remained on the samples oxidized for three hours. The flaked scales were analyzed by X-ray diffraction. The results are tabulated below:

Time of Test (hr)	Analysis of Scale
3	BeO
10	BeO + Zr_2Be_{17}
40	BeO + Zr_2Be_{17}
100	BeO + Zr_2Be_{17} + $ZrBe_{13}$

The intermetallic content of the scales is estimated to be only a few per cent.

The 100 hour sample had several chips missing from the edges as a result of flaking of the scale. The $ZrBe_{13}$ in the scale of this sample evidently resulted from spalling of small amounts of this intermetallic with the scale. The amount of Zr_2Be_{17} in the scale increased with time of oxidation. Zr_2Be_{17} covered the surface of all the samples from which the scale had flaked. The Zr_2Be_{17} remaining on the sample surfaces after flaking of the scale was highly oriented as was the BeO remaining on the surface of the one-hour sample. The Zr_2Be_{17} and the BeO have the same crystal habit. Figure 52 is an electron micrograph of the surface of the 10-hour sample in which is shown the orientation of the Zr_2Be_{17}. Figure 53 shows $ZrBe_{13}$ (top) and Zr_2Be_{17} (bottom) surfaces which were prepared in the same manner as the $ZrBe_{13}$ samples which were oxidized. It is clear from this figure that the $ZrBe_{13}$ surface is changed in the oxidation process and that the orientation of the Zr_2Be_{17} produced as a result of the oxidation of $ZrBe_{13}$ is different from the orientation of Zr_2Be_{17} as machined and slightly polished.

Fig. 52 - Electron Micrograph of Surface of $ZrBe_{13}$ Specimen After Oxidation, Showing Oriented Zr_2Be_{17} Grains. 600X Before Reproduction

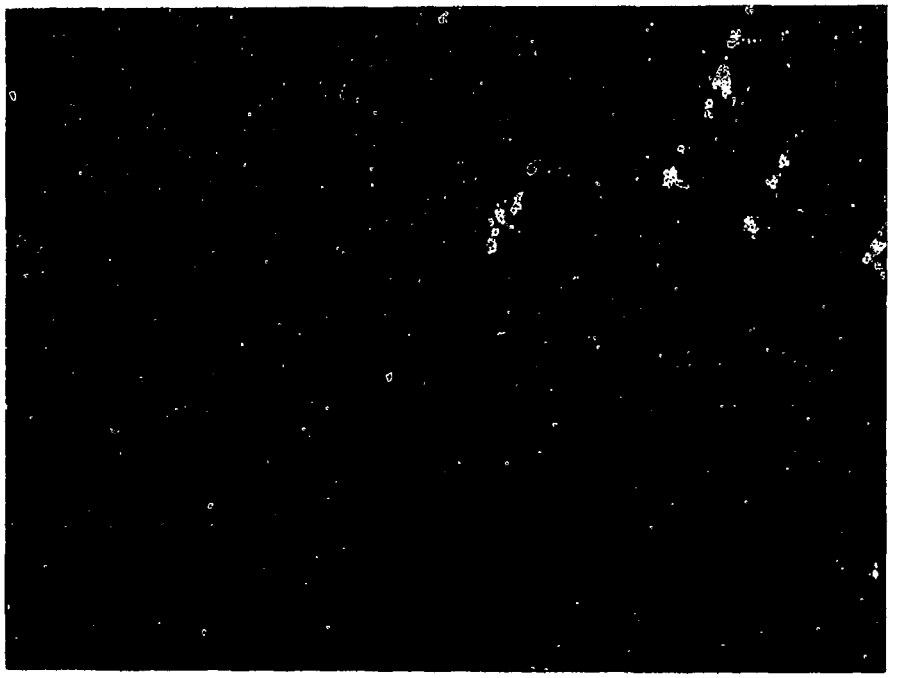

Fig. 53 (Top) - Electron Micrograph of $ZrBe_{13}$ Surface As-Machined and Slightly Polished, 2000X Before Reproduction

(Bottom) - Electron Micrograph of Zr_2Be_{17} Surface As-Machined and Slightly Polished, 2000X Before Reproduction

The thickness of the Zr_2Be_{17} on the surface of the samples was measured by comparing the relative intensities of the Zr_2Be_{17} and $ZrBe_{13}$ diffraction peaks. X-ray diffraction patterns of the surface were obtained after removal of thin sections from the surface. The thickness data obtained are plotted in Figure 54. The thickness of the Zr_2Be_{17} layer remaining on the surface does not change between about 25 and 100 hours. The total Zr_2Be_{17} layer does continue to increase in thickness, however, since the amount of Zr_2Be_{17} present in the scale increases with time.

From these analyses of the scale and the surface of the oxidized $ZrBe_{13}$ samples, it appears that the equation for the oxidation of $ZrBe_{13}$ should be written

$$4\ ZrBe_{13} + 9\ O_2 \rightarrow 2\ Zr_2Be_{17} + 18\ BeO$$

The equation is balanced on the basis of the products positively identified. The possibility that unoxidized Be or other products are present still exists, since small amounts or noncrystalline forms would not be detected by X-ray diffraction.

Since the Zr_2Be_{17} formed on the surface could be an important factor in deciding the course of oxidation of $ZrBe_{13}$, an attempt was made to determine the time at which Zr_2Be_{17} first appeared. An increase in surface Zr_2Be_{17} over the amount present on an untreated surface was observed when samples of $ZrBe_{13}$ were exposed to 2500°F for 10, 5, and even 2 minutes. It has also been observed that Zr_2Be_{17} forms on the surface when $ZrBe_{13}$ is heated under vacuum at temperatures as low as 2000°F.

3. Discussion of Results

An exponential rate law appears to be operative during the oxidation of the intermetallic compounds, $TaBe_{12}$, Ta_2Be_{17}, Hf_2Be_{21}, and $ZrBe_{13}$, in the temperature range of 2300° to 2750°F. Furthermore, the rate laws appear to be cubic or slower. The cubic rate law is operative over the entire temperature range for $TaBe_{12}$. Also the cubic rate law appears to be operative for $ZrBe_{13}$ at 2500°F and in the later stages at 2300°F; for Hf_2Be_{21} at 2300°F, 2750°F, and probably at 2500°F; and probably for one stage of the oxidation of Ta_2Be_{17} at 2750°F. These conclusions are based on the performance of single samples at each of the indicated temperatures, since time was not available for repeat runs. Future work in this area is expected to

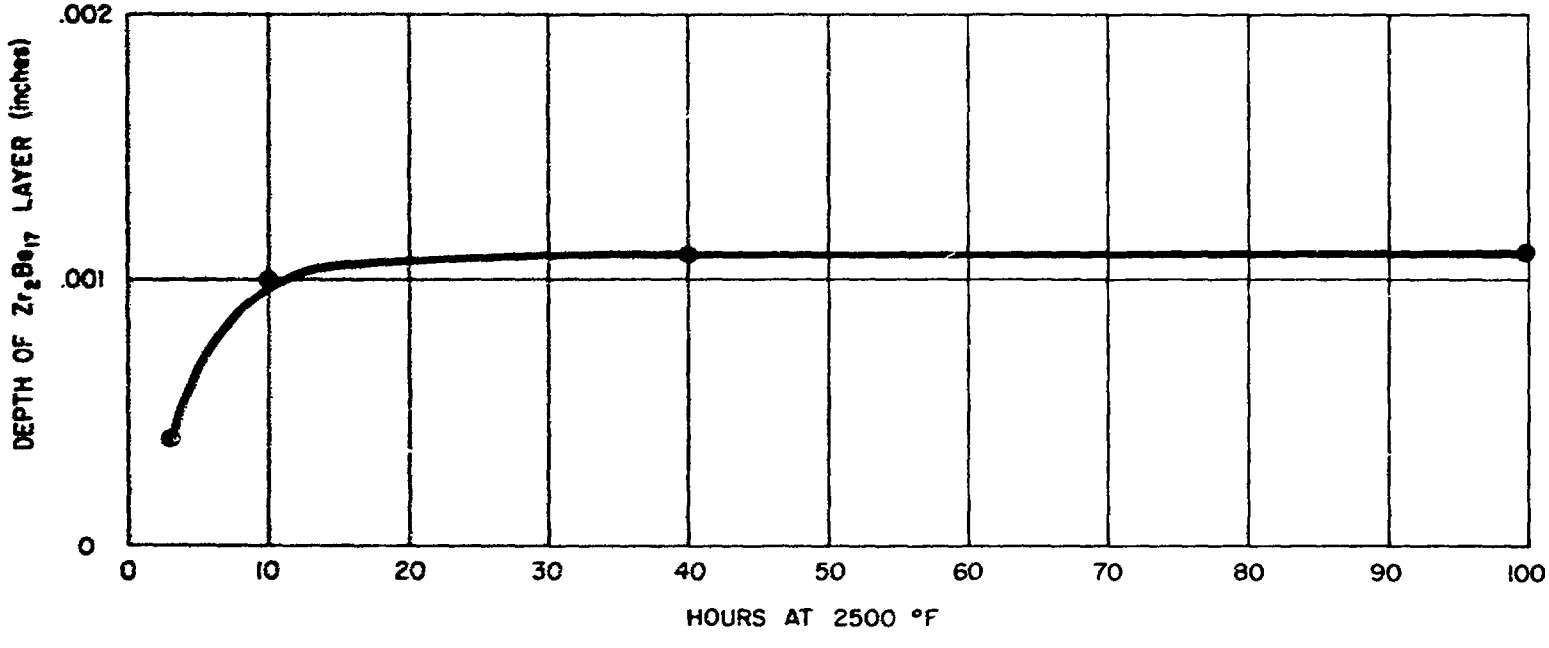

Fig. 54 - Depth of Zr_2Be_{17} Layer Versus Hours at 2500°F

remove the areas of uncertainty and further clarify the rate laws operative in the several cases which are presently not capable of interpretation.

No generally accepted theory is available for explaining the mechanism of oxidation which obeys the cubic rate law, although some attempts have been made to provide a theoretical basis for the cubic rate equation.[8-11] It has been observed experimentally[12] that the oxidation takes place by anion migration through the oxide film toward the metal-metal oxide boundary. Thus, oxidation of those intermetallic beryllides which obey the cubic rate law may proceed by anion migration through the oxide scale.

$ZrBe_{13}$ was chosen to serve as a prototype in the mechanism studies. The products of oxidation at 2500°F have been identified for this compound, but the activation energy of the process is not yet available. In the process of oxidation, the $ZrBe_{13}$ is decomposed into Zr_2Be_{17} and beryllium, the beryllium (at least in part, if not all) is oxidized into BeO, and continued oxidation takes place across a protective oxide film. According to some experimental evidence, the cubic rate law predicts that the oxidation continues by anion migration through the oxide layer. Alternatively, the oxidation of beryllium is reported to obey the parabolic rate law up to 1785°F.[13, 14] Several equally plausible routes can be envisioned which would lead to the observed end products. Until experimental evidence is available to definitely indicate which route is favored, no attempt will be made to propose a mechanism. Meanwhile, data which will aid in the interpretation of the proper mechanism should continue to be assembled.

B. Vapor Pressure

Determination of the dissociation or decomposition pressures of some of the beryllides was initiated in the later stages of this contract. $ZrBe_{13}$ was chosen as the compound for which the initial measurements would be made. (This coincides with its choice as a model for oxidation mechanism studies.) $ZrBe_{13}$ is known to decompose at high temperature. The only decomposition product which has definitely been identified is Zr_2Be_{17}. Beryllium is assumed to be the other product. Since the vapor pressures of the beryllides in general were expected to be low, the Knudsen cell technique was chosen as the method to be used in their determination. Construction of the equipment for this determination was completed during the contract term, but special tooling required to prepare the small orifice in the Knudsen cell was not received in time for experimental work to be carried out. Since this is a continuing program, the vapor pressure work with this equipment will be initiated in the near future. A discussion of the planned method and the equipment constructed is presented here.

In the Knudsen method, the sample whose vapor pressure is to be measured is placed in a container which is closed except for a small orifice. Those vapor molecules so oriented may escape through this orifice into a region which has a lower pressure than the pressure in the container. If the pressures on both sides of the orifice are sufficiently low, the mean free path of the effusing vapor molecules will be such that a given molecule will suffer no collisions with other molecules as it travels across the cell and through the orifice. The relationship between the rate of mass loss, m, and the vapor pressure, P, of the material is

$$m = P\left(\frac{M}{2\pi RT}\right)^{1/2}$$

Rearranging and adding a correction for the channeling effect of the orifice (The Clausing factor W_o)

$$P_K = m\left(\frac{2\pi RT}{M}\right)^{1/2} = \frac{Z\,(MT)^{1/2}}{44.33\,W_o\,at}$$

where M = molecular weight of the vapor; Z = the total moles of material lost in an effusion run lasting for time, t, from a cell of

orifice with area a; P_K is the Knudsen cell pressure, and W_o the Clausing factor.

A more detailed analysis of the system used in laboratory experiments for vapor pressure measurements by the Knudsen method takes into consideration the channel effect exerted by the Knudsen Cell itself, as well as the fact that the pressure outside the cell is not zero, and relates the pressure measured to the true equilibrium pressure. For normal Knudsen cells when the length approximates the diameter, the relationship is

$$P_{eq} = \left(1 + \frac{W_o a}{A\alpha}\right) P_K$$

where A is the surface area of the sample from which evaporation occurs and α is the condensation coefficient.

The vapor pressure may also be obtained from continuous weighings of a Knudsen cell. The apparent weight of the cell will be increased as material effuses from the cell by an amount dependent on the momentum of the effusing species. The pressure is given directly in terms of the increase in weight of the cell caused by effusion through the equation

$$P = 2F/\pi r^2 = 2\Delta W g/\pi r^2$$

where F is the force exerted by the effusing molecules, and r is the radius of the effusion hole.

Both approaches for obtaining vapor pressure data from Knudsen cell measurements were incorporated in the equipment assembled for the determination of the vapor pressure of the beryllides. The weights of the cell and sample before and after the run are easily obtained. The cell and sample will be suspended from one arm of an Ainsworth, automatic recording, semi-micro, analytical balance, which can be used in high vacuum applications, to make the direct weighings. The suspension system is made of BeO and tungsten.

The Knudsen cell is of BeO. The cell has a one square centimeter cross section and is one centimeter deep. A delay in the delivery of the diamond tooling required to machine the orifice prevented completion of the cell in time for measurements to be made before the termination of experimental work for this contract. However, the vapor pressure of $ZrBe_{13}$ will be determined and reported

at a later date. The cell will be heated by means of a cylindrical, tungsten wire filament 1 3/4 inches in diameter and 5 1/2 inches long. This tungsten filament is contained in a stainless steel jacket having the dimensions, 10 3/4 inches O.D. by 18 inches long and a 1/4-inch wall. A vacuum seal is effected by locating a rubber O-ring in the flanged top of the stainless steel jacket. Tantalum and stainless steel heat shields are used in the area of the tungsten filament. Temperature is measured by a tungsten-rhenium thermocouple. A variable autotransformer controls the power input to the filament.

A pressure of 8×10^{-5} mm of Hg (10^{-7} atm) was obtained when the entire system was evacuated. This pressure should be sufficient for measurement for vapor pressures of the order of 10^{-5} atm. Since the vapor pressure of the beryllides may be somewhat lower than 10^{-5} atm at the low end of the temperature range of interest, alterations in the pumping system are planned which should allow a higher vacuum to be obtained.

The products resulting from the decomposition of the beryllide will be identified. The free energy, enthalpy, and entropy of formation of the decomposing species can be calculated from the measured vapor pressure. The energy of decomposition can be obtained from the variation of the vapor pressure with temperature. Correlating these data with energies obtained from oxidation studies will aid in establishing the mechanism of oxidation of the beryllides and will provide data on the thermal stability of the materials.

V. SUMMARY

Intermetallic beryllides from the systems, tantalum-beryllium, hafnium-beryllium, and tungsten-beryllium, and the compounds, $MoSi_2$, $TaSi_2$, and WSi_2, have been investigated for the purpose of evaluating the potential of compounds from this grouping to serve as structural materials at temperatures in excess of 2500°F for relatively short periods of time. After an initial screening, compounds with demonstrated potential were examined from the aspects of (1) preparation and fabrication, (2) oxidation resistance, and (3) certain mechanical and thermal properties.

In general, preparation of the desired intermetallic compounds was accomplished in a routine manner. On the other hand, original attempts to fabricate some of the compounds were not always straightforward. WSi_2 and $MoSi_2$ presented the greatest difficulties, especially for rectangular shapes, in that severe reaction with the graphite tooling was encountered when these materials were hot pressed. The use of molybdenum foil to isolate the silicides from the graphite proved to be a satisfactory solution to the problem. Also, instability of $HfBe_{13}$ at the temperature of fabrication was first observed in attempts to fabricate this compound. $HfBe_{13}$ lost beryllium, forming the new and more stable compound, Hf_2Be_{21}. The dissociation of MBe_{13} or MBe_{12} compounds into lower beryllides probably occurs generally, but the ease with which this occurs varies, depending upon the thermal stability of the higher beryllide. In this respect $HfBe_{13}$ appears to be considerably less stable than most of the other MBe_{13} or MBe_{12} compounds investigated. The stability of the MBe_{13} and MBe_{12} compounds at high temperatures should be examined more closely.

The silicides have shown better oxidation resistance than the beryllides at temperatures above 2900°F for 6 to 10-hour periods; however, the silicides have also shown poor oxidation resistance at lower temperatures (below 2000°F for $MoSi_2$ and between 2000° and 2300°F for $TaSi_2$ and WSi_2). WSi_2 and $TaSi_2$ have shown good oxidation resistance to 3200°F.

The transverse-rupture strengths of these materials vary, with WSi_2, Ta_2Be_{17}, and $TaBe_{12}$ showing higher strengths than Hf_2Be_{21}, $TaSi_2$, and $MoSi_2$. Density, grain size, and composition are among the factors which influence the strengths of these materials, and since it is difficult to isolate these variables singly, it is also difficult to properly evaluate the effect of a single variable. The values given in Table VIII support the view that a high density, small-grained material should exhibit excellent transverse-rupture strengths in the temperature range of these measurements.

A brief summary of the properties of the materials under study is given in Table XXII.

In general, the beryllides have higher coefficients of expansion and greater specific heats than do the silicides. The higher expansion coefficients may not be an asset, however, since the thermal shock resistance is inversely proportional to the coefficient of expansion. The thermal shock resistance tests performed in this work have not shown the higher expansion coefficients of the beryllides to be detrimental, since both groups of intermetallics were equal in withstanding the thermal shocks induced.

Both $TaBe_{12}$ and WSi_2 are good conductors of heat. WSi_2 has a somewhat higher overall thermal conductivity than does $TaBe_{12}$ in the same temperature range. The curves which express the thermal conductivity as a function of temperature assume different shapes for the two materials. The curve for $TaBe_{12}$ is a gently sloping linear function, while the curve for WSi_2 shows positive deviations at the low and high ends of the temperature range covered with an almost constant value in between. The choice of material based on thermal conductivity data would depend on the specific end use, with the lighter weight of the beryllides a contributory factor. On the basis of these data, WSi_2 would be the preferred silicide for use as a high temperature material, while Ta_2Be_{17} and $TaBe_{12}$ appear equally advantageous at this time.

In addition to the preparation and property evaluation phases, determination of the mechanism of oxidation of the beryllides has been considered. An exponential rate law which is cubic or a higher power is operative when $TaBe_{12}$, Ta_2Be_{17}, Hf_2Be_{21}, and $ZrBe_{13}$ are oxidized between 2300° and 2750°F. In most cases, a cubic rate law is applicable. In some cases, there appears to be a change in the cubic rate process with time. The activation energy of the cubic rate process for $TaBe_{12}$ was calculated as 36 kcal and for Hf_2Be_{21} as 50 kcal. Much more data, such as product identification and vapor pressures, will be required before the exact mechanisms may be assigned.

The products of oxidation for $ZrBe_{13}$ at 2500°F have been identified as Zr_2Be_{17} and BeO. The equation for the oxidation of $ZrBe_{13}$ based on these products is:

$$4\ ZrBe_{13} + 9\ O_2 \longrightarrow 2\ Zr_2Be_{17} + 18\ BeO$$

TABLE XXII

SUMMARY OF PROPERTIES OF INTERMETALLIC COMPOUNDS UNDER STUDY

	Ta_2Be_{17}	$TaBe_{12}$	Hf_2Be_{21}	$TaSi_2$	WSi_2
X-Ray Density, g/cc	5.05	4.18	4.26	9.10	9.87
Melting Point, °F	3610	3360	--	4350	3960
Modulus of Rupture, psi					
2300°F	66,800	53,200	21,800	29.600	57,500
2500°F	53,400	43,000	24,000	13,000	70,000
2750°F	30,600	26,000	17,000	16,000	51,100
Oxidation Resistance Maximum temperature of resistance to oxidation for short-time use					
5 hours	3000°F	3000°F	3000°F	~3200°F	3200°F
10 hours	2900°	2900°	2900°	>3000°	>3000°
Thermal Properties					
Linear Coefficient of Expansion 80° - 2750°F in./in./°F x 10^{-6}	8.7	8.4	9.2	4.7	4.7
Specific Heat Btu/lb °F					
1000°F	0.21	0.27	0.23	0.08	0.08
2800°F	0.26	0.30	0.30	0.09	0.08
Thermal Conductivity Btu hr^{-1} ft^{-2} ft °F^{-1}					
1100°F	--	16.6	--	--	19.6
2600°F	--	22.3	--	--	18.1

VI. CONCLUSIONS

1. The compound $HfBe_{13}$ is unstable above approximately 2600°F and decomposes to the more stable compound, Hf_2Be_{21}. The latter compound was identified and characterized for the first time in this work.

2. In addition to WBe_2 and WBe_{12}, the compound, WBe_{22}, is present in the tungsten-beryllium system. The compound $MoBe_{22}$ also exists.

3. The oxidation resistance of the silicides is excellent at 3000°F for a ten-hour period. WSi_2 has shown satisfactory oxidation resistance at 3200°F for 6 hours. However, the silicides evidence poor oxidation resistance at certain temperatures below 2300°F.

4. The maximum temperature of service for the beryllides, based on oxidation resistance equivalent to two mils penetration, is 3000°F for times less than 10 hours.

5. The transverse-rupture strength of WSi_2 is very good at 2750°F with values of 54,500 and 47,600 psi observed. Values of 32,500 and 26,500 psi have been observed for Ta_2Be_{17} and $TaBe_{12}$ respectively, at 2750°F. The transverse-rupture strength of Ta_2Be_{17} and $TaBe_{12}$ decreased with increasing temperature. A maximum in the strength versus temperature curve occurred at 2500°F in the case of WSi_2. The strengths of Hf_2Be_{21}, $TaSi_2$ and $MoSi_2$, although individually different, were about the same at 2300° and 2500°F and decreased at 2750°F for a particular compound.

6. The compounds are resistant to thermal shock under the conditions induced in this investigation; however, there appears to be some dependence upon the method of applying heat.

7. The mean-linear coefficients of thermal expansion between 80° and 2750°F range between 9.18 and 8.42 μ in./in./°F for the beryllides and from 4.91 to 4.67 μ in./in./°F for the silicides.

8. The specific heats of the beryllides and silicides tested are a linear function of temperature in the temperature range, 800° to 2750°F, obeying an equation of the type

$$C_p = a + bT$$

The beryllides have higher specific heat capabilities than do the silicides.

9. The thermal conductivity of $TaBe_{12}$ is a gently sloping linear function of temperature in the range, 850° to 2600°F, whereas in the case of WSi_2 positive deviations from an almost constant value occur at the low and high ends of the temperature range from 800° to 2800°F.

10. The beryllides oxidize in conformance with an exponential rate law which is cubic or a higher power in the temperature range, 2300° to 2750°F. The activation energy of the cubic rate process was calculated to be 36 kcal for $TaBe_{12}$ and 50 kcal for Hf_2Be_{21}.

11. The products from the oxidation of $ZrBe_{13}$ at 2500°F have been identified as Zr_2Be_{17} and BeO. The equation for the reaction between $ZrBe_{13}$ and O_2 is:

$$4\ ZrBe_{13} + 9\ O_2 \longrightarrow 2\ Zr_2Be_{17} + 18\ BeO$$

12. The results of this investigation indicate that service temperatures above 3200°F are not obtainable with compounds thus far studied from binary metallic systems, despite the relatively high melting points of the materials. WSi_2, with an indicated potential of 3200°F, is the most promising silicide studied from the combined standpoint of oxidation resistance and high temperature strength. Ta_2Be_{17} and $TaBe_{12}$ appear of equal advantage to temperatures in the 2900 to 3000°F range and compare favorably with the tungsten silicide at these temperatures in view of their specific gravity, which is approximately 50% that of WSi_2.

VII. BIBLIOGRAPHY

1. WADC TR 59-29, Parts I and II.
2. Private communication from UCRL.
3. S. D. Mark, Jr., Am. Ceramic Soc. Bul., 24, 203 (1955).
4. I. B. Fieldhouse et al. (Armour Research Foundation), "Measurement of Thermal Properties," WADC TR 55-495, Part I, September, 1956.
5. I. B. Fieldhouse et al. (Armour Research Foundation), "Measurement of Thermal Properties," WADC TR 58-274, November, 1958.
6. F. J. Tebo (Argonne National Laboratory), "Selected Values of the Physical Properties of Various Materials," ANL-5914, September, 1958.
7. P. St. Pierre, Ceramic Bulletin, 39, 264 (1960).
8. N. Mott, Trans. Faraday Soc., 36, 472 (1940).
9. N. Cabrera and N. F. Mott, Rept. Prog. Phys., 12, 162 (1949).
10. H. Engell, K. Hauffe, and B. Ilschner, Z. Electrochem., 58, 478 (1954).
11. H. H. Uhlig, Acta Met., 4, 541 (1956).
12. M. W. Mallett and W. M. Albrecht, J. Electrochem. Soc., 102, 407 (1955).
13. E. A. Gulbransen and K. F. Andrew, J. Electrochem. Soc., 97, 383 (1950).
14. D. Cubicciotti, J. Am. Chem. Soc., 72, 2084 (1950).
15. R. Kieffer, F. Benesovsky, and H. Schmid, "Formation of the Systems Niobium-Silicon and Vanadium-Silicon", Plansee Proc., 1955, 154-65 (1956); Chem. Abstracts 50, 11917a (1956).

APPENDIX I

X-RAY DIFFRACTION POWDER PATTERN OF Hf_2Be_{21}

Cu K_α Radiation
Diffractometer Pattern, 8-75° 2θ

d, Å	Intensity	hkl[a]
6.42	5	110
4.84	85	203
3.715	100	206
3.693	35	301
3.20	5	220, 221
2.954	30	224
2.618	85	316
2.315	35	414, 411, 412
2.295	20	229
2.151	30	330, 331, 310
2.03	5	418, 506
1.955	15	513, 419
1.859	60	338, 332, 311
1.843	10	602, 509
1.740	10	606, 633, 610
1.732	20	524
1.664	10	608
1.653	15	614
1.576	5	617
1.451	10	627
1.447	10	5, 2, 12
1.409	10	5, 2, 13
1.400	10	6, 1, 12
1.349	5	7, 0, 12

APPENDIX I (Continued)

X-RAY DIFFRACTION POWDER PATTERN OF Hf_2Be_{21}

Cu K_α Radiation
Diffractometer Pattern, 8-75° 2θ

d, Å	Intensity	hkl[a]
1.341	5	6, 2, 11
1.315	20	4, 4, 13
1.310	15	6, 2, 12
1.268	5	7, 1, 12

[a]Based on a hexagonal lattice:

a = 12.84 Å

c = 29.79 Å

c/a = 2.32

M = 20

Px = 4.26 g/cc

APPENDIX I (Continued)

X-RAY DIFFRACTION POWDER PATTERN OF WBe_{22}

Cu K_α Radiation
Diffractometer Pattern, 8-75° 2θ

d, Å	Intensity	hkl[a]
6.707	95	111
4.105	100	220
3.506	85	311
2.908	30	400
2.667	40	331
2.374	50	422
2.238	35	511, 333
2.056	25	440
1.967	50	531
1.838	35	620
1.773	30	533
1.752	5	622
1.678	5	444
1.627	15	711, 551
1.553	20	642
1.514	25	731,553
1.454	5	800
1.420	5	733
1.370	20	822, 660
1.343	10	751, 555
1.300	5	840
1.276	10	911, 753

[a]Based on a cubic lattice: a = 11.64 Å; O_h^9 or T_h^4 type.

THE BRUSH BERYLLIUM COMPANY, Cleveland, Ohio
INVESTIGATION OF INTERMETALLIC COMPOUNDS FOR VERY HIGH TEMPERATURE APPLICATIONS, by Jonathan Booker, Robert M. Paine, and A. James Stonehouse, April 1961. 143p. incl. figs. and tables. (Project 7350; Task 73500) (WADD TR 60-689) (Contract AF 33(616)-6540)
Unclassified report

Intermetallic beryllides from the systems tantalum-beryllium, tungsten-beryllium, and hafnium-beryllium along with the disilicides of tungsten, tantalum, and molybdenum, were screened for compounds capable of serving as structural materials at temperatures above 2500°F. The compounds studied were $TaBe_{12}$, Ta_2Be_{17}, Hf_2Be_{21}, $MoSi_2$, $TaSi_2$, and WSi_2. The preparation, fabrication, oxidation

(over)

UNCLASSIFIED

UNCLASSIFIED

THE BRUSH BERYLLIUM COMPANY, Cleveland, Ohio
INVESTIGATION OF INTERMETALLIC COMPOUNDS FOR VERY HIGH TEMPERATURE APPLICATIONS, by Jonathan Booker, Robert M. Paine, and A. James Stonehouse, April 1961. 143p. incl. figs. and tables. (Project 7350; Task 73500) (WADD TR 60-689) (Contract AF 33(616)-6540)
Unclassified report

Intermetallic beryllides from the systems tantalum-beryllium, tungsten-beryllium, and hafnium-beryllium along with the disilicides of tungsten, tantalum, and molybdenum, were screened for compounds capable of serving as structural materials at temperatures above 2500°F. The compounds studied were $TaBe_{12}$, Ta_2Be_{17}, Hf_2Be_{21}, $MoSi_2$, $TaSi_2$, and WSi_2. The preparation, fabrication, oxidation

(over)

UNCLASSIFIED

resistance, and thermal-shock resistance are discussed. Values are given for the transverse-rupture strengths, impact resistance, mean-linear coefficients of thermal expansion, enthalpy, specific heat, and thermal conductivity.

An investigation of the rates of oxidation of intermetallic beryllides was initiated. The oxidation of $TaBe_{12}$, Hf_2Be_{21}, $ZrBe_{13}$, and Ta_2Be_{17} in the range 2300° to 2750°F was found to obey an exponential rate law which was cubic or a higher power rate law. In most cases, the cubic rate law applied. The products of the oxidation of $ZrBe_{13}$ at 2500°F were identified as Zr_2Be_{17} and BeO. Tentative activation energies for a cubic rate process were calculated for $TaBe_{12}$ and Hf_2Be_{21}.

UNCLASSIFIED

UNCLASSIFIED

resistance, and thermal-shock resistance are discussed. Values are given for the transverse-rupture strengths, impact resistance, mean-linear coefficients of thermal expansion, enthalpy, specific heat, and thermal conductivity.

An investigation of the rates of oxidation of intermetallic beryllides was initiated. The oxidation of $TaBe_{12}$, Hf_2Be_{21}, $ZrBe_{13}$, and Ta_2Be_{17} in the range 2300° to 2750°F was found to obey an exponential rate law which was cubic or a higher power rate law. In most cases, the cubic rate law applied. The products of the oxidation of $ZrBe_{13}$ at 2500°F were identified as Zr_2Be_{17} and BeO. Tentative activation energies for a cubic rate process were calculated for $TaBe_{12}$ and Hf_2Be_{21}.

UNCLASSIFIED